

For Reference

NOT TO BE TAKEN FROM THIS ROOM

For Reference

NOT TO BE TAKEN FROM THIS ROOM

Ex LIBRIS
UNIVERSITATIS
ALBERTAENSIS





Digitized by the Internet Archive
in 2018 with funding from
University of Alberta Libraries

<https://archive.org/details/Watkins1961>

DIRECTION OF THE GEOMAGNETIC FIELD DURING THE TRIASSIC PERIOD IN SIBERIA

By

Dr. E. R. DEUTSCH

and

N. D. WATKINS

*Reprinted from Nature, Vol. 189, No. 4764, pp. 543-545,
February 18, 1961*

DIRECTION OF THE GEO- MAGNETIC FIELD DURING THE TRIASSIC PERIOD IN SIBERIA

By DR. E. R. DEUTSCH

Imperial Oil Research Laboratory, Calgary, Alberta
AND

N. D. WATKINS

Shell Oil Co. of Canada, Edmonton, Alberta

AN earlier detailed study of the Deccan Trap formation^{1,2} revealed, wherever samples were taken, the existence of a stable remanent magnetization making large angles with the ambient field. One explanation has been that India was in middle latitudes of the southern hemisphere during the late Cretaceous or early Eocene. This would also conform broadly to palaeogeographical reconstructions offered in the literature, according to which India once formed part of a southern super continent the constituents of which later dispersed.

Such an interpretation prompts the question to what extent the rest of what is now Asia participated in the hypothetical northward drift of India. It seemed that a promising source of evidence might reside in the palaeomagnetism of rock formations north of the Himalayas; in particular, the vast Siberian land mass offers manifold opportunities.

Consequently, in 1957, a request for some oriented samples from Siberia was made to Prof. V. V. Fedinsky of Moscow, then attending the eleventh Assembly of the International Union of Geodesy and Geophysics in Toronto. This was arranged without delay, and in 1958 the University of Alberta in Edmonton received a collection of trap rock from the northern part of the Enisei River system.

The samples are from five exposures in the valleys or basins of the Lower Tunguska, Severnaya and Dudinka Rivers, located as follows (Fig. 2): Site *A*, 66.0° N., 89.0° E.; Site *B*, 69.3° N., 88.0° E.; Site *C*, 66.5° N., 90.1° E.; Site *D*, 66.1° N., 89.0° E.; Site *E*, 66.5° N., 89.1° E. The formations are of Lower Triassic age, range in type from gabbro-diabase to diabase, and at all sites are steeply inclined to the horizontal. Gabbro and gabbro-diabase are elsewhere³ described as typical of the thick intrusive bodies which characterize the Siberian Traps in this region.

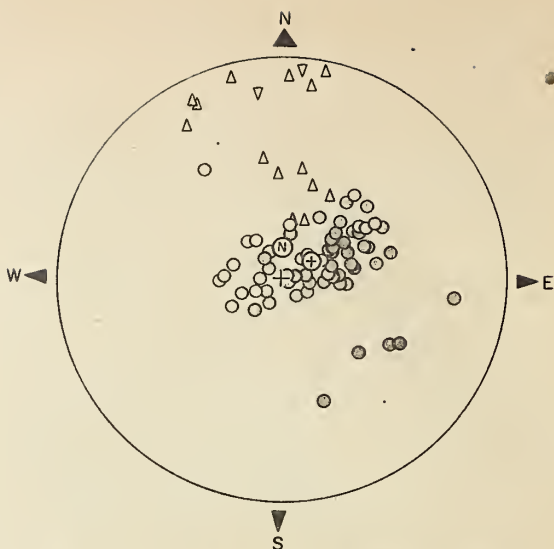


Fig. 1. Polar equal-area plot of the remanent magnetization. Δ , data for specimens from site *C*, N. pole pointing down; ∇ , site *C*, N. pole up; \circ all other sites, N. pole down; \oplus , mean direction for all samples, omitting site *C*; \odot in circle, theoretical dipole field at the sampling locality

Samples were cut into 1-3 cylindrical disks which will be referred to as 'specimens'. Direction and intensity of their magnetization were determined with a simple astatic magnetometer, mounted inside a hut belonging to the University of Alberta in Calgary, where we carried out the measurements during summer, 1960.

The stereogram (Fig. 1) shows results for all 83 specimens cut from 32 samples. With few exceptions, the vector extremities of the disks from sites *A*, *B*, *D* and *E* form part of a fairly dense central cluster. In contrast, the plot of points from Site *C* is anomalous and as their scatter exceeds that for any other site, the results were considered unreliable, and hence rejected. The resultant of 26 normalized vectors,

Table 1. MEAN REMANENT MAGNETIZATION OF SAMPLES FROM SITES *A*, *B*, *D* AND *E*

<i>S</i>	<i>N</i>	Declination	Dip	α_{50}	α_{95}	Intensity (c.g.s.)
67	26	N. 62° E.	+76° down	4.0°	8.5°	$(1.87 \pm 1.14) \times 10^{-3}$

S, number of specimens measured; *N*, number of samples; α_{50} , α_{95} , radii of 50 and 95 per cent circles of confidence, using Fisher's method. All averages are based on samples (*N*), not specimens.

all being specimen averages, then corresponds to a west-south-west—east-north-east axis dipping downward steeply towards the east (Fig. 1, Table 1).

In assessing whether this is a true record of the local field direction during Triassic times we make the usual assumption, which seems well supported by theory and some observation, that over periods of 500-1000 years the geomagnetic axis is that of a dipole coaxial with the spin axis. The magnetization of some specimens from each site had been provisionally determined in 1958, but was essentially the same after two years random storage. However, long-term stability may be inferred more compellingly from the data themselves, whenever the vectors form a compact group the mean direction of which is in misalignment with the present local, or dipole, field. The observed angle of deviation, though not large, was taken as significant, for it exceeds the semi-angle of the 95 per cent cone of confidence surrounding the mean vector. Because samples were used in the Fisher analysis, this cone is larger, but probably more indicative of the true scatter at the sampling locality than if all specimens had been weighted equally.

The direction of magnetization furnishes a Triassic north pole in eastern Siberia (Fig. 2, No. 1), as follows :

$$\begin{aligned}\text{Lat.} &= 65^{\circ} \text{ N. ; } \text{Long.} = 156^{\circ} \text{ E. ; } \delta m = 15\frac{1}{2}^{\circ} ; \\ &\delta p = 14\frac{1}{2}^{\circ},\end{aligned}$$

with δm , δp , semi-axes of the 95 per cent confidence ellipse. Since our investigation began, results of work in the same general area have been published³ (pole 2) ;

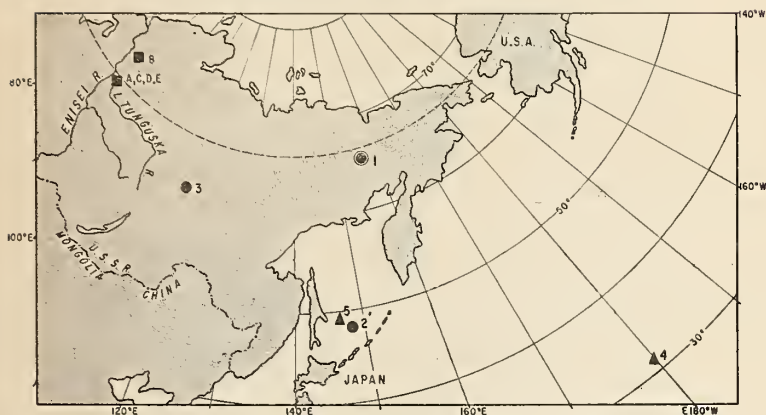


Fig. 2. Location of the north pole with respect to Siberia and Europe, from palaeomagnetic measurements on Triassic rocks. Numbers refer to results quoted in this article (1), and by Makarova (ref. 3) (2), Fineberg and Dashkevich (ref. 4) (3), Khramov (ref. 5) (4), and Nairn (ref. 6) (5). Sampling sites are represented by letters



Fig. 3. Location of the North Pole, estimated from palaeomagnetic measurements on Triassic rocks. Symbols represent polar plots with respect to: ●, Siberia; ▼, N. America; ■, Africa; ♦, Australia. Numbers indicate source material: 1, our results; 2, 3, other work on Siberian traps (refs. 3, 4); 6, Connecticut lavas (ref. 7); 7, Springdale Sandstone (ref. 8); 8, Brunswickian sediments (ref. 7); 9, New Oxford sediments (ref. 9); 10, Bechuanaland Cave sandstone (ref. 10); 11, Brisbane tuff (ref. 11). The solid line is a polar path relative to Europe, typical of versions published by various authors: *CM*, Cambrian; *D*, Devonian; *CB*, Carboniferous; *P*, Permian; *T*, Triassic; *E*, Eocene; *M*, Miocene

a report⁴ on the magnetization of trap rock from the Angara River basin is the source for pole 3.

Palaeomagnetic information unlocked from Triassic sedimentary exposures in Europe has yielded pole 4 relative to Russia⁵, and pole 5, which is an average quoted by Nairn⁶, of British, German and French data by different authors. Our pole, though located rather far north, conforms within limits of error to some point on the smoothed 'European' pole track (Fig. 3). This is not surprising, for it seems likely that in executing any movements inferred from this curve, Europe and northern Asia would have acted as one unit; hence, barring major changes in the Earth's radius, any two contemporary poles from Europe and Siberia should coincide.

Our result differs from three of four pole positions relating to North America⁷⁻⁹ and; more drastically, from the African¹⁰ and Australian¹¹ poles. Comparison of global non-Triassic data has revealed many similar discrepancies: the separation of the

European and Indian curves exceeds 90° in the Jurassic, the earliest period for which Indian data exist¹². One can interpret this by invoking large relative displacements between the two land masses, and probably by implication, between India and northern Asia. However, a direct comparison with the Siberian results must await examination of suitable Triassic exposures in India.

We are indebted to Prof. V. V. Fedinsky of the Physics of the Earth Institute, Moscow, and Dr. N. I. Marochkin, director of the Union Geological Research Institute, Leningrad, for making available the rock collection on which this work depended. At the University of Alberta, particular thanks are due to Dr. G. D. Garland, professor of geophysics, for providing workshop facilities and instrumentation, and for his continued interest.

¹ Clegg, J. A., Deutsch, E. R., and Griffiths, D. H., *Phil. Mag.*, Ser. 8, **1**, 419 (1956).

² Deutsch, E. R., Radakrishnamurty, C., and Sahasrabudhe, P. W., *Ann. de Geophys.*, **15**, 39 (1959).

³ Makarova, Z. V., *Bull. Acad. Sci. USSR.*, Geophys. Ser. 1959, 1520. Trans. Amer. Geophys. Un., 1081 (1960).

⁴ Fineberg, F. S., and Dashkevich, N. N., Report, Third Palaeomagnetic Conference, University of Leningrad (Oct. 1959).

⁵ Khramov, A. N., "The Palaeomagnetic Correlation of Sedimentary Strata" (Gostoptekhizdat, Moscow, 1958).

⁶ Nairn, A. E. M., *J. Geol.*, **68**, 285 (1960).

⁷ Du Bois, P. M., Irving, E., Opdyke, N. D., Runcorn, S. K., and Banks, M. R., *Nature*, **180**, 1186 (1957).

⁸ Runcorn, S. K., *Bull. Geol. Soc. Amer.*, **67**, 301 (1956).

⁹ Graham, J. W., *J. Geophys. Res.*, **60**, 329 (1955).

¹⁰ Nairn, A. E. M., *Phil. Mag. Supp.* **6**, 162 (1957).

¹¹ Irving, E., and Green, R., *Geophys. J. Roy. Astro. Soc.*, **1**, 64 (1958).

¹² Clegg, J. A., Radakrishnamurty, C., and Sahasrabudhe, P. W., *Nature*, **181**, 830 (1958).





Uncorrected
Proof.

("Geophysical Prospecting")

THE RELATIVE CONTRIBUTIONS OF REMANENT AND INDUCED MAGNETISM TO THE OBSERVED MAGNETIC FIELD IN NORTHEASTERN ALBERTA

BY

N. D. WATKINS *)

ABSTRACT

The ratios of induced to remanent magnetic intensities have been determined for samples of Precambrian Rock from part of the Canadian Shield in northeastern Alberta.

The relatively insignificant contribution of remanent magnetism to the observed field indicates that interpretation techniques based on the assumption of zero remanent intensity can be used.

Other implications of the magnetic measurements are briefly discussed.

Koenigsberger (1938), Hospers (1954) and many others have shown that igneous rocks frequently possess a remanent magnetization which is significantly different in direction from that of the earth's present magnetic field. Consequently, the use of interpretation methods which are based on the assumption that magnetic anomalies are caused solely by variations of induced magnetization has been questioned.

Methods of interpretation which involve the determination of the permanent magnetization vector have been suggested, but are often laborious. Green (1960) has shown that a modified induced magnetization interpretation method can be used when remanent magnetism data is available for the anomalous body. Some anomalies, of course, cannot be explained by induced magnetization alone, as has been shown by Gidler and Peter (1960).

A vast amount of aeromagnetic data has been obtained in Canada. Virtually all of this is concerned with the Precambrian Shield in either outcrop or subsurface. The commercial use of aeromagnetic surveys in western Canada is almost entirely restricted to use in oil exploration, where computed depths to the crystalline basement are used to estimate the thickness of the sedimentary cover. The broadscale nature of the work necessitates the use of rapid interpretation techniques such as that devised by Vacquier et alia (1951), which assumes the induced part to dominate in the observed field.

During a more intensive geological survey, J. D. Goffrey of the Research Council of Alberta collected twenty-three oriented samples from the Pre-

*) Present address: Dept. of Geology, University of Alberta, Edmonton, Alberta, Canada.

Sample No.	Sample Description	Vertical Induced Intensity (Oersted)	Vertical Induced Intensity (Gauss)	Vertical Induced Intensity (Oersted)	Vertical Induced Intensity (Gauss)
1	Granite Gneiss	10.4	10.4	10.4	10.4
2	Granite Gneiss	15.7	15.7	15.7	15.7
3	Granite Gneiss w/ quartz (pegmatite)	30.6	30.6	30.6	30.6
4	Granite Gneiss w/ quartz	30.6	13.8	44.4	0.450
5	Granite Gneiss (sheared)	531.0	25.3	556.3	0.047
6	Mylonitic porph.	16.6	1.9	18.5	0.114
7	Mylonitic porph.	9.22	1.25	10.47	0.135
8	Granite Gneiss (weathered)	21.8	1.0	22.8	0.046
9	Granite Gneiss (sheared)	127.0	-13.6	113.4	0.107
10	Banded Feldspathic Amphib.	166.0	18.6	184.6	0.112
11	Granite Gneiss (sheared)	43.8	0.5	44.3	0.011
12	Granite Gneiss	20.4	9.1	29.5	0.446
13	Granite Gneiss	21.8	1.4	23.2	0.064
14	Granite Gneiss	22.7	1.0	23.7	0.044
15	Granite Gneiss	34.4	6.28	40.68	0.182
16	Granite Gneiss (well banded)	47.0	3.66	50.66	0.078
17	Amphib. w/Quartz lenses and radioactive pegmatite	42.0	365.0	407.0	8.7
18	Granite Gneiss	2840.0	375.0	3215.0	0.132
19	Granite Gneiss (sheared)	1119.0	2110.0	3229.0	1.89
20	Amphibolite	45.6	10.3	56.1	0.230
21	Granite Gneiss	103.0	-34.2	69.8	0.332
22	Amphib. w/peg.	41.0	3.2	46.2	0.127
23	Mylon. Gran. Gneiss	12.1	1.0	13.1	0.083

Vertical field is approximated to the total field since the magnetic dip is about 80° at Bayonet Lake.

Vertical induced intensity calculated using H = 6 oersteds.

Q_v factor is here defined as $\frac{\text{Vertical Component of Remanent Intensity.}}{\text{Vertical Component of Induced Intensity}}$

Canadian Shield in northeastern Alberta, where aeromagnetic coverage is available. The location of the samples, together with the bedrock geology is given in Fig. 1(a). The aeromagnetic contours are shown in Fig. 1(b).

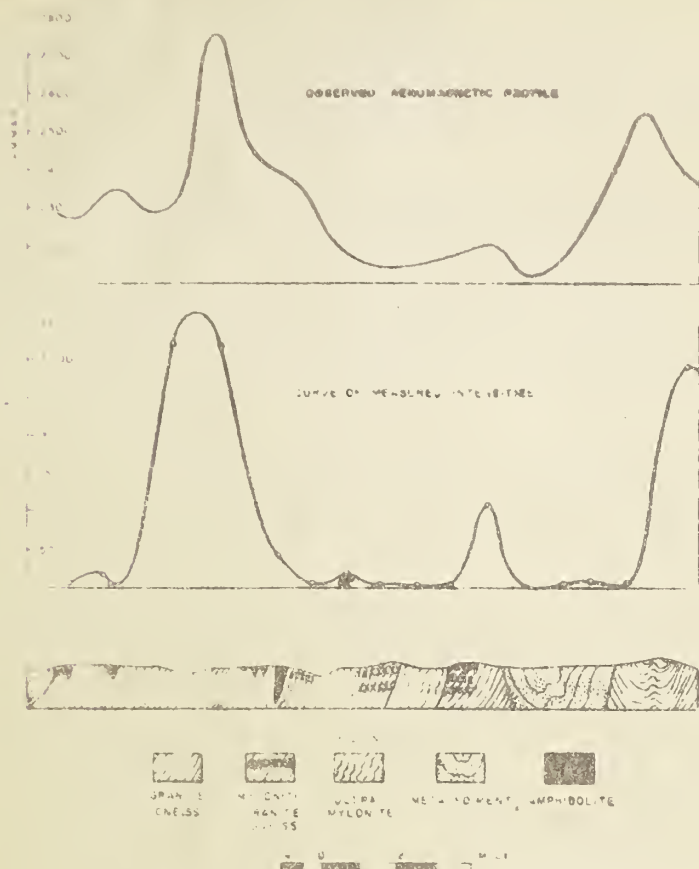


Fig. 2. Geological cross section, with observed aeromagnetic profile and curve of measured vertical magnetic intensity.

The magnetic properties of the samples were measured using an astatic magnetometer at the University of Alberta. The results are given in Table I. The Q_r factor is defined here as the ratio of the vertical components of induced to remanent intensities. In only two cases out of the twenty-three samples examined were the remanent intensities greater than the induced intensity, and one of these samples has anomalous petrological properties, while the other has anomalous magnetic intensity. The median Q_r factor is 0.1. Since it is seldom possible to obtain a basement depth to an accuracy of greater than 15%, it appears valid to use an assumption of dominant induced magnetic field in this

area, and hence utilize one of the many rapid interpretation techniques based on that assumption. Is the application of the Vacquier et alia (1951) interpretation method successful in western Canada because the buried PreCambrian Shield has negligible remanent magnetism?

It is of interest to note that two of the samples (Nos. 9 and 21) have reverse remanent vectors. Since the foliation planes throughout the area are very steep, the occurrence of reverse remanent magnetization could be indicative of overturned units.

Fig. 2 shows a profile of observed total magnetic intensity and a curve of the measured total intensity, with the near-surface geological cross-section. The correlation of observed and measured intensities indicates that the measurements are representative of the intensities existing in the metamorphic rocks. The flight level of the magnetometer (500 feet above ground level) agrees with the "depths" calculated using the Vacquier et alia (1951) system over this exposed magnetic surface. This gives some evidence of the vertical nature of the geological interfaces.

The measured low mean intensities agree with the statements by Hospers (1954) and others, that the mean intensity of remanent magnetization apparently decreases with age. The low Q_v values concur with Nagata's observations for older rocks.

It can be concluded that the geological age of the strata and the accuracy required should be equated when choosing the interpretation method to be used.

Other significant aspects of this study which are now under examination can be seen comparing the aeromagnetic contours and the geological map. The value of an aeromagnetic map as an aid to resolving some mapping problems in a highly diversified metamorphosed area is obvious. Determination of the magnetic properties serves to confirm the correlation between the aeromagnetic anomalies and distinct petrological units, and, as has been mentioned, the attitude of the geological interfaces can be suggested.

The measured intensities have shown that a gradation from granite gneiss to mylonitic granite gneiss to ultramylonite is synonymous with decrease in intensity of magnetization, which serves to emphasise the associated magnetic low, and the increase in quartz content to a maximum in the ultramylonite.

Attempts are presently being made to examine the relationship between the remanent magnetic vector and the foliation direction. Some anisotropy of susceptibility measurements are being carried out.

Acknowledgment is due to J. D. Godfrey for providing the samples and geological details, and to Dr. G. D. Garland for the instrumentation and interest shown.

REFERENCES

- DROLER, R. W. and PETER, G., 1960, An example of the Importance of Natural Remanent Magnetization in the Interpretation of Magnetic Anomalies, *Geoph. Prosp.* Vol. VIII, No. 3.
 EATON, R., 1960, Remanent Magnetization and the Interpretation of Magnetic Anomalies; *Geoph. Prosp.*, Vol. VIII, No. 1.
 JOSEPHS, J., 1954, Magnetic Correlation in Volcanic Districts; *Geol. Mag.*, Vol. 91, No. 5.
 KOENIGSBERGER, J. G., 1938, Natural Residual Magnetism of Eruptive Rocks, *Terr. Mag.*, Vol. 43.
 NAGATA, T., 1953, *Rock Magnetism*, (Tokyo, Maruzen & Co.).
 LACQUIER, V., STEENLAND, N. C., HENDERSON, R. G. and ZIETZ, I., 1951, Interpretation of Aeromagnetic Maps; *Mem. G.S.A.*, No. 47.

THE UNIVERSITY OF ALBERTA

STUDIES
IN
PALEOMAGNETISM

A THESIS
SUBMITTED TO THE FACULTY OF GRADUATE STUDIES
IN PARTIAL FULFILMENT OF
THE REQUIREMENTS FOR THE DEGREE
OF
MASTER OF SCIENCE

DEPARTMENT OF GEOLOGY

by

NORMAN DAVID WATKINS

B.Sc. (London) M.Sc. (Birmingham)

EDMONTON, ALBERTA

July 1961

ABSTRACT

The remanent magnetization of rocks from four different areas has been examined using an astatic magnetometer.

Samples of Siberian Lower Triassic dykes were obtained from Professor V. V. Fedinsky, of Moscow. From the five sampling sites near the Lower Tunguska River, twenty-three samples were obtained. Eighty-three specimens were made from the samples. Following the increasing of the sensitivity of the magnetometer, the magnetic vectors of the specimens were measured. A statistical analysis of the results gave a Triassic magnetic pole position at 65° North, 156° East. This pole position conforms, within the limits of error, to previously determined Triassic magnetic pole positions for European and western Asiatic rocks, suggesting that in executing any movements relative to North America, Northern Asia and Europe moved as a single unit.

Orientated samples were collected by J. D. Godfrey from the Precambrian Shield in the extreme northeastern corner of Alberta. The magnetic properties of the samples were determined using an astatic magnetometer, and a bridge-type susceptibility meter. The high ratio of induced to remanent magnetic intensities for the rocks indicates that the interpretation of local aeromagnetic anomalies can be made with theoretical methods which are based on the assumption that negligible remanent magnetic intensity exists in the anomalous bodies. The

measured combined vertical components of induced and remanent magnetic intensities correlate with the observed total magnetic intensity aeromagnetic profile, showing that the measured intensities are representative of the intensities existing in the rock units. The remanent magnetic vector does not appear to be in the foliation plane, as is indicated in other studies of metamorphic rocks.

Negative results were obtained from the two other studies.

Samples were collected from a lava near Cameron Lake and from a sill southwest of Cranbrook. The lava and sill are both situated in the Proterozoic Lewis thrust sheet. The relationship of the magnetic vectors in the respective igneous bodies of the west and east parts of the thrust sheet could aid in resolving the tectonic relationships within the thrust sheet, which may have suffered differential rotation along minor thrusts and faults. Measurement of the magnetic vectors in the lava has revealed a probable unstable component which has resulted in a wide scatter of the inclination of the magnetic vector, despite the existence of a fairly consistent azimuth of the magnetic vector. Removal of the unstable component of remanent magnetism was impossible because of lack of instrumentation. Even if satisfactory results could have been obtained from the Cameron Lake lava, however, the sill southwest of Cranbrook in the western part of the thrust sheet was so magnetically weak that no magnetic properties could be determined, and so a correlation of magnetic properties could not be made.

Proterozoic dykes in northeastern British Columbia were sampled, in order to integrate the results of the measurement of the magnetic vectors

with those from the Cameron Lake lava, into an attempt to determine a Proterozoic magnetic pole position. The magnetic intensity of the dykes proved to be so low that no measurements could be made with the available apparatus.

The studies have resulted in two publications:

- (1) A joint publication with Dr. E. R. Deutsch:

Direction of the Magnetic Field During the Triassic Period in Siberia; Nature; Volume 189, Number 4764, February 18th, 1961, pages 543 to 545;

- (2) A paper which has been accepted for publication by the editor of "Geophysical Prospecting" : The Relative Contributions of Remanent and Induced Magnetism to the Observed Magnetic Field in Northeastern Alberta.

ACKNOWLEDGEMENTS

I wish to thank the following people who have helped me with the preparation of this thesis:

Professor G. D. Garland who has provided instrumentation, frequent help and suggestions, constructive criticism of the results, publications, and thesis, and most particularly for his encouragement.

Dr. E. R. Deutsch, of Imperial Oil, who supervised the study of the Siberian rocks and conducted a major part of the analysis of the results. Dr. Deutsch also wrote the joint publication based on the Siberian results.

Professor V. V. Fedinsky of the Physics of the Earth Institute, Moscow; and Dr. N. I. Marochkin of the Union Geological Research Institute, Leningrad, who provided the Siberian samples.

Mr. J. D. Godfrey, of the Research Council of Alberta, who obtained the northeast Alberta samples, and provided the geological details for the study.

Professor R. E. Folinsbee, for guidance during the courses required to qualify to write this thesis, and for critical review of the results.

Mr. R. D. Miller, who prepared the Siberian samples for measurement.

Dr. G. Cummings, who supervised the preparation of the samples used in the attempted study of the Lewis Overthrust problem.

Mrs. Rhoda M. M. Warke, who typed the thesis.

Finally, I am indebted to the Department of Physics at the University of Alberta, for providing an assistantship during the period in which I qualified to write this thesis.

N.D.W.

TABLE OF CONTENTS

	Page
ABSTRACT-----	i
ACKNOWLEDGEMENTS-----	iv
TABLE OF CONTENTS-----	vi
LIST OF TABLES-----	xi
LIST OF ILLUSTRATIONS-----	xiii
LIST OF PLATES-----	xv
CHAPTER 1	
FUNDAMENTALS OF PALEOMAGNETISM-----	1
1. 1 Introduction-----	1
1. 2 Definitions-----	1
(i) Magnetic Field Intensity (H)-----	1
(ii) Intensity of Magnetization (I)-----	1
(iii) Susceptibility (k)-----	2
(iv) Curie Temperature-----	2
(v) Magnetic Domain-----	2
(vi) Coercivity-----	3
1. 3 Magnetic Minerals-----	3
1. 4 Thermo-Remanent Magnetization-----	5
1. 5 Isothermal Remanent Magnetization-----	7

1.6	Viscous Magnetization-----	8
1.7	Chemical Magnetization-----	8
1.8	Depositional Magnetization-----	9
1.9	Reverse Magnetization-----	9

CHAPTER 2

THE APPLICATION OF PALEOMAGNETIC STUDIES---		11
2.1	Basis of the Application of Paleomagnetic Studies	11
2.2	Continental Drift and Polar Wandering-----	12
2.3	The Expanding Earth-----	15
2.4	Local Correlation Problems-----	16
2.5	Local Tectonic Problems-----	16
2.6	Paleomagnetic Dating-----	17
2.7	Integration of Paleomagnetic Results into Other Geological Studies-----	17

CHAPTER 3

THE ASTATIC MAGNETOMETER-----		20
3.1	Description of the Blackett Magnetometer-----	20
3.2	Astatization of the Magnetometer-----	24
(i)	Selecting the Magnets-----	24
(ii)	Theoretical Moment of the Magnets-----	24
(iii)	Measuring and Equalizing the Magnetic Moments before Mounting-----	24
(iv)	Further Equalizing the Magnets After Mounting-----	26
(A)	Equalizing by free oscillation-----	26
(B)	Equalizing by forced oscillation-----	27

	Page
3.3 Sensitivity of the Magnetometer-----	27
(i) The Initial Measurement of the Sensitivity-----	27
(ii) Increasing the Sensitivity of the Magnetometer-----	28
(A) Measuring the thickness of the quartz fibre-----	29
(B) Making a quartz fibre-----	30
(iii) Final Calibration of the Apparatus-----	30
CHAPTER 4	
MEASUREMENT OF THE MAGNETIC VECTOR-----	32
4.1 Collecting and Preparing the Samples-----	32
4.2 Measurement of the Azimuth of the Magnetic Vector-----	34
4.3 Measurement of the Dip of the Magnetic Vector-----	38
4.4 Calculation of the Intensity of Magnetization of the Magnetic Vector-----	40
CHAPTER 5	
THE PROCESSING OF THE MEASUREMENTS OF THE MAGNETIC VECTOR-----	42
5.1 Correction for Geological Tilt-----	42
5.2 Computation of the Mean Azimuth and Dip----	46
5.3 Obtaining the Paleomagnetic Pole-----	47
5.4 Statistical Treatment of the Paleomagnetic Results-----	50
(i) The Circle of Confidence-----	50
(ii) The Oval of Confidence-----	52

CHAPTER 6

THE TRIASSIC MAGNETIC POLE IN SIBERIA-----	53
6.1 Motives of the Study-----	53
6.2 Location of the Samples-----	54
6.3 Geology of the Area-----	55
6.4 Field Orientation Technique-----	56
6.5 Measurement of the Magnetic Vector-----	56
6.6 Correction for Geological Dip-----	61
6.7 Representing the Results-----	67
6.8 Computing the Mean Azimuth and Dip for the Samples out of Specimens-----	67
6.9 Computing the Mean Azimuth and Dip for the Sites out of Samples-----	71
6.10 Computing the Mean Azimuth and Dip for the Area out of Sites-----	74
6.11 Obtaining the Paleomagnetic Pole-----	75
6.12 Determining the Circle of Confidence-----	78
6.13 Determining the Oval of Confidence-----	81
6.14 Plotting the Oval of Confidence-----	82
6.15 Significance of the Results-----	83
6.16 The Intensity of Magnetization-----	85
6.17 Stability Tests-----	92
6.18 Summary of the Results-----	93

CHAPTER 7

INVESTIGATION OF THE MAGNETIC PROPERTIES OF SOME ROCKS FROM NORTHEASTERN ALBERTA--	96
7.1 Geology of the Area-----	96

7.2	Determination of the Remanent Magnetic Vector-----	100
7.3	The Volume Susceptibility of the Rocks-----	102
	(i) Method of Measurement of the Susceptibility of the Specimens-----	103
	(A) Correction of the susceptibility result for specimen diameter-----	105
	(B) Correction of the susceptibility result for variation of length of the specimen-----	105
	(ii) The Results of the Measurement of the Susceptibility-----	107
7.4	The Relative Contributions of Induced and Remanent Magnetism to the Observed Field in the Bayonet Lake Area-----	110
7.5	Relationship of the Foliation Plane and the Remanent Magnetic Vector-----	117

CHAPTER 8

	UNSUCCESSFUL ATTEMPTS TO UTILISE THE PALEOMAGNETIC PROPERTIES OF ROCKS IN THE SOLUTION OF SOME GEOLOGICAL PROBLEMS-----	120
--	--	-----

8.1	The Lewis Overthrust-----	121
	(i) The Cameron Lake Lava-----	121
	(ii) The Irishman Creek Sill-----	126
	(iii) Other Work on Magnetism in the Lewis Overthrust-----	128
8.2	The Proterozoic Pole Position from Dykes in Northern British Columbia-----	129

	CONCLUSIONS-----	132
	BIBLIOGRAPHY-----	134
	APPENDIX-----	140

LIST OF TABLES

Table	Page
(i) The Azimuth and Dip of the Magnetic Vector in Each Specimen-----	58
(ii) Example of the Correction for Geological Tilt-----	62
(iii) In-Situ Azimuth and Dip of the Magnetic Vector-----	64
(iv) Example of the Determination of the Mean Azimuth and Dip for a Sample from Three Samples-----	69
(v) Mean Azimuth and Dip of Magnetic Vector in Samples-----	70
(vi) Example of the Determination of Mean Azimuth and Dip for a Site from Samples-----	72
(vii) Mean Azimuth and Dip of the Magnetic Vector for each Site-----	73
(viii) Determination of the Paleomagnetic Pole for the Four Sites A, B, D and E; and for Site A-----	77
(ix) Determination of the Circles of Confidence-----	80
(x) Example of the Determination of the Intensity of Magnetization-----	87
(xi) Intensity of Magnetization for all Specimens-----	89
(xii) Intensity of Magnetization for the Samples-----	91
(xiii) Summary of Results-----	94
(xiv) Petrological and Foliation Data for the Bayonet Lake Samples-----	99
(xv) The Results of the Measurement of the Remanent Magnetic Vector-----	100

Table	Page
(xvi) Calibration of the Susceptibility Bridge for Variation of Length of the Specimen-----	107
(xvii) Determination of the Volume Susceptibility of Rocks from the Bayonet Lake Area-----	108
(xviii) The Vertical Components of the Induced and Remanent Magnetic Intensities in the Bayonet Lake Area-----	113
(xix) The Magnetic Vectors of the Specimens from the Cameron Lake Area-----	123

LIST OF ILLUSTRATIONS

Figure		Page
1	Postulated Paleomagnetic Polar-Wandering Curves for Europe, North America, Australia, India and Japan-----	14
2	The Astatic Magnetometer-----	23
3	Measurement of Azimuth-----	36
4	Measurement of the Dip of the Magnetic Vector-----	39
5	Correction for Geological Dip of the Body-----	43
6	Relationships between Location of Sampling Site, Measured Remanent Magnetic Direction and Paleomagnetic Pole-----	49
7	Polar Equal-Area Plot of the Remanent Magnetization Vector-----	68
8	The Location of the North Pole with respect to Siberia and Europe from Paleomagnetic Measurements on Triassic Rocks-----	79
9	Location of the North Pole Estimated from Measurements on Triassic Rocks-----	84
10	The Geological and Total Magnetic Intensity Features of the Bayonet Lake Area, Northeastern Alberta-----	98
11	Simplified Circuit Diagram of the Susceptibility Bridge-----	104
12	Calibration of the Susceptibility Bridge for Variation of the Length of the Specimen-----	106

Figure		Page
13	Geological Cross-Section, with Observed Aero- magnetic Profile and Curve of Measured Vertical Magnetic Intensity in the Bayonet Lake Area-----	116
14	Stereographic Projections Showing Relationship of Foliation Plane and Remanent Vector Direction-----	119

LIST OF PLATES

Plate		Page
1	The Astatic Magnetometer-----	21
2	Operating the Astatic Magnetometer-----	35

CHAPTER I

FUNDAMENTALS OF PALEOMAGNETISM

1.1 Introduction

Paleomagnetic is a term describing the facility with which a rock retains magnetic characteristics which were acquired by the rock either contemporaneously or at a later date. This property is the remanent and not the induced magnetization. The vector representation of the induced magnetic field is entirely dependent on the ambient magnetic field at any given time.

1.2 Definitions

It is considered of value to define some of the terms used in this thesis.

(i) Magnetic Field Intensity (H):

This is numerically equal to the force in dynes exerted on unit pole in the field.

(ii) Intensity of Magnetization (I):

This is the magnetic moment per unit volume of the specimen concerned, i. e., $I = \frac{M}{V}$. This can be either the induced magnetization (I_i), or the remanent magnetization (I_r).

(iii) Susceptibility (k):

This is the intensity of magnetization per unit magnetic field intensity, i. e., $k = \frac{I}{H}$.

(iv) Curie Temperature (T_c):

At temperatures above the Curie point, a substance is paramagnetic (that is, the substance is feebly magnetized when situated in a magnetic field). At temperatures below the Curie point the substance becomes spontaneously magnetized.

(v) Magnetic Domain:

Weiss considered a ferromagnetic material (that is, a material which strongly magnetized in a magnetic field) to consist of a collection of regions or domains, in each of which a stable state of spontaneous magnetization exists. Modern research has shown that these domains form a closely-knit pattern with directions of magnetization so distributed among the domains that the resultant magnetic moment of an ordinary specimen is zero in the absence of an external field. When a field is applied, the domains which happen to be most favourably disposed with respect to the field grow at the expense of the neighbours, at first by a reversible extension of boundaries and then, in stronger fields, irreversibly. In a very strong field, there is a rotation of the direction of magnetization of the domains towards that of the field. Boundaries of domains may be revealed under the microscope by the clustering of colloidal magnetic particles along them when a suspension of such particles is applied to a polished face. The particles move into the strong local fields arising at the junction of domains. The resulting patterns

were first observed by Bitter (1931) and are termed 'Bitter Figures.'

(vi) Coercivity:

Remanent, or permanent magnetization results when the applied magnetic field is above a critical value termed the coercivity. This is the amount of energy needed to destroy magnetization. Above this value the direction of magnetization in a single domain will reorientate from its previous direction to that of the applied field, and will not return to the original direction.

1.3 Magnetic Minerals

Thellier (1959), Rimbart (1956), Haigh (1958), Nagata (1953), and Kobayashi (1959) have made important contributions to an understanding of magnetic minerals, and magnetizing processes.

An intensity of magnetization will result on the application of a magnetic field to a mineral which has a degree of susceptibility. These minerals will not necessarily be suitable for the creation of a permanent or remanent, magnetization.

The minerals which have been observed to be the agents of remanent magnetization in igneous rocks are composed of varying amounts of ferrous oxide (FeO), ferric oxide (Fe_2O_3) and titanium dioxide (TiO_2). The minerals are:

Ilmenite (FeTiO_3)

Ulvospinel (2FeOTiO_2)

Magnetite (Fe_3O_4)

Hematite (Rhombohedral Fe_2O_3)

Maghemite (Isometric Fe_2O_3)

The most strongly magnetic minerals of igneous rocks most frequently occur in the Ulvospinel to Magnetite series, and exist mainly as solid solutions.

The Ilmenite to Magnetite series features exsolution. That is, on cooling of a solid solution of the two minerals, some Ilmenite and Magnetite crystallizes, and also a mixture of the two minerals forms.

The Curie points of the minerals depend on their composition. The introduction of another ion (such the Al ion) into the solution will usually lower considerably the Curie point of the mineral.

The magnetic minerals of sedimentary rocks include a small percentage derived from igneous materials. Many sediments contain magnetic minerals which were formed after deposition. Siderite (FeCO_3) and Goethite $[\text{Fe}(\text{OH})]$ are such minerals, and could be formed from hematite grains, resulting in the loss of original magnetization. These unstable compounds might eventually form Hematite again.

Few studies have been made on the magnetic minerals of metamorphic rocks. These minerals are generally formed by reaction between the iron minerals of the material, resulting in a wide range of composition of magnetic minerals compared with those in igneous rocks.

A single rock will generally contain many magnetic minerals, which are different in physical dimensions and properties.

It has been shown by Graham (1953) that the observed permanent magnetization direction is caused by only a fraction of the parent rock's magnetic domains, since when very high external magnetic fields are applied to a rock specimen, a stronger magnetic intensity will be created.

There are six different types of remanent magnetization, which are classified according to the processes responsible for their origin. These types of magnetization are discussed in the following six sections.

1.4 Thermo-Remanent Magnetization

In passing through the Curie temperature (T_c) on cooling, an igneous rock develops a magnetization parallel to the earth's field. The resulting magnetization is termed thermo-remanent magnetization (T.R.M.). This property occurs in the most frequently used materials for the study of paleomagnetism. Partial thermoremanent magnetization (P.T.R.M.) is that magnetization which would result in a rock when cooling from below the Curie temperature to a given lower temperature. Thellier (1951) has demonstrated that P.T.R.M. is reversible since the destruction of such magnetization by heat features characteristic temperature limits for the initial and total loss of magnetic properties.

Neél (1955) has proposed a theory of T.R.M. for single domains. In Neél's theory the single grain possesses two mutually opposite directions in which the magnetic vector can occur at minimum energy. Separating these directions is an energy barrier given by:

$$E = \frac{v \cdot H_c \cdot I_s}{2} \quad \text{where } v = \text{the volume of the grain}$$

H_c = the coercive force

I_s = the spontaneous magnetization of the mineral

If E exceeds the thermal energy kT (k = Boltzmann's constant, T = Absolute Temperature), no movement of the magnetic direction across the barrier will result. With high temperatures, or small volumes, however, the

magnetic moment will cross the opposing barrier, to create a single orientation of the magnetic vector. With duplications in adjacent domains, an initial magnetization J_0 will result. After a given time, this value will decay to I_R where: $I_R = J_0 e^{-\frac{t}{\tau_0}}$ τ_0 is called the relaxation time

Néel defined τ_0 thus: $\frac{1}{\tau_0} = A \left(\frac{v}{T} \right)^{\frac{1}{2}} e^{-\frac{HcI_s}{2kT}} = A \left(\frac{v}{T} \right)^{\frac{1}{2}} e^{-\frac{\gamma v}{T}}$

The constants A and γ are dependent on the magnetic and elastic properties of the mineral. As A and γ are known for iron, Néel (1955) showed that τ_0 , $\frac{v}{T}$, and grain diameters at room temperature are related in the case of iron as follows:

$\frac{v}{T}$	τ_0	Grain Diameter
3.2×10^{-21}	0.1 secs.	120\AA
7.0×10^{-21}	340.0 years	160\AA
9.6×10^{-21}	3.4×10^9 years	180\AA

Thus the direction of magnetization in a grain with a diameter less than 120\AA is easily and quickly changed by the thermal fluctuations, and the application of a weak field to a number of such grains causes a net magnetization in the direction of the field.

The effect of grain size on coercivity was first observed by Koenigsberger (summarized 1947) and verified by Gottschalk (1935). An increase of coercivity with decreasing grain size was observed upon grinding magnetite powders.

The most successfully paleomagnetically examined igneous rocks

are basalts. From the above theory and observations, this is not surprising for basalts are characteristically fine-grained. The fine grain-size results in the direction of the ambient field at time of formation being easily assimilated by the basalt. The small grain size, on the other hand, results in high coercivity and thus the remanent magnetization is not easily destroyed. The suitability of basalts for paleomagnetic purposes was further emphasized by Deutsch (1956) who showed that the coercivity of basalts remains very high until very close to the Curie temperature, suggesting that reheating by later igneous activity need not necessarily modify greatly the originally created permanent magnetization. Furthermore, since basalts are usually associated with relatively passive volcanic events, the movement of material when below the Curie point is likely to be at a minimum.

Most magnetic materials in igneous rocks have Curie points between 550°C and 700°C , and the vast majority of igneous materials feature a T.R.M. type of natural remanent magnetism.

1.5 Isothermal Remanent Magnetization

If a rock is placed in a magnetic field which is larger than the smallest coercive force of the magnetic constituents of the rock, it will achieve isothermal remanent magnetization (I. R. M.).

Using Néel's terminology, domains with magnetic energy barriers with corresponding coercive forces less than the applied field orientate their magnetic moments with the field. The energy barrier prevents the return to the original direction upon removal of the ambient field.

As the earth's field is about 0.5 oersteds, and most rock forming minerals have coercivities of at least 100 oersteds, I. R. M. is rarely produced. An exception to this is the production of I. R. M. by lightning strikes.

1.6 Viscous Magnetization

Rimbert (1956) and Brynjólfsson (1957) have shown that a modification of the permanent magnetization may result if a rock is saturated in a magnetic field which is not sufficiently strong to cause I. R. M.

This viscous magnetization is a long process, and is due to the Boltzmann distribution of thermal energy, which upon conversion into magnetic energy aids the crossing of energy barriers by magnetic domains which would not normally do so, when in the earth's field. Thus a preferential realignment towards the direction of the applied magnetic field results.

1.7 Chemical Magnetization

Doell (1956), and Martinez and Howell (1956), have shown that magnetization of sediments may be due to chemical changes occurring after consolidation. A remanent magnetization can be acquired during chemical change, such as the reduction of hematite to magnetite.

This type of magnetization has enabled paleomagnetic investigations of sediments to be made, such as that carried out on the Triassic Red Sandstones of Britain by Clegg, Almond and Stubbs (1954).

The process of acquiring Chemical Magnetization is somewhat

similar to the I. R. M. process, for Haigh (1958) has demonstrated that as the magnetic grains grow chemically, the critical diameter is passed, and great magnetic stability results.

1.8 Depositional Magnetization

King (1955) has shown that magnetic particles are deposited with preferential alignment parallel to the external field. The magnetic stability of such deposits is only slight, but the resulting magnetic vectors have been utilized for paleomagnetic studies, such as the work by Griffiths (1955) on Quarternary varved clays.

1.9 Reverse Magnetization

In addition to the five types of remanent magnetism discussed above, frequent observation has been made of reversed magnetization, which could be described as a subdivision of T. R. M. or P. T. R. M. This phenomenon indicates either reversal of the earth's magnetic field or self-reversed magnetization, where a rock may become magnetized in the opposite direction to the applied field.

One explanation of self-reversed magnetization is by Néel (1951); a rock has two magnetic constituents A and B. Constituent A has a higher Curie point than B and acquires a T. R. M. During cooling, the Curie point of B is reached. The T. R. M. of A induces a magnetization in B opposite to that of A, and thus reversed relative to the original applied field. If, after cooling, the magnetic intensity of B is greater than that of A, self-reversed magnetization will be observable.

The above six different types of paleomagnetism certainly include almost all types of remanent magnetism so far observed in nature, but it is impossible to state whether or not the classification may be widened as the study of the subject continues.

CHAPTER 2

THE APPLICATION OF PALEOMAGNETIC STUDIES

In the previous chapter it was shown that measurement of the magnetic vector in a rock can provide evidence of the direction of the earth's magnetic field at the time of formation of the rock. As with present day magnetic measurements of magnetic dip and declination, a geographical location relative to the magnetic pole can be determined from the magnetic data obtainable from suitable rocks. Thus these determinable relative paleolocations can be used to aid in the resolution of geological problems involving relative positions of parts of the earth's surface. Such problems are continental drift, the expanding earth, and local correlation problems in tectonically disturbed areas. The method can also be used to study the more directly applicable problem of wandering of the magnetic pole, and with an established curve of the wandering of the magnetic pole, magnetic dating of strata is possible.

2.1 Basis of the Application of Paleomagnetic Studies

There exist several assumptions in paleomagnetic studies. In the case of applying the method to polar wandering and continental drift problems, the crucial assumption is that the earth's field is, and always has been, dipolar, and coaxial with the axis of rotation of the earth.

Spherical Harmonic Analysis of the earth's magnetic field by Chapman and Bartels (1940), has indicated that the field has three components: a magnetic dipole inclined at $11\text{-}1/2^{\circ}$ to the spin axis and located at the centre of the earth; a non-dipole component; and a very small contribution from above the earth's surface. The $11\text{-}1/2^{\circ}$ inclination to the axis of rotation of the dipole results in the expression of this dipole on the earth's surface (as the magnetic pole) being close to, but not coincident with the geographic pole. The non-dipole component has been observed to be a relatively rapidly changing small component, and it is assumed that the effect of this component is averaged out in the number and varying age of the samples collected.

Although Cox (1957) has shown that for certain observation points, the angular departure of the earth's present field from the axial dipole field ranges up to 17.3° , both theoretical and observational evidence (Hospers 1955) tend to confirm the necessary assumption that when averaged for periods of several thousands of years, the earth's rotational or geographical axis and magnetic axis have generally been coincident. This substantiates the dynamo theories of geomagnetism by Elsasser (1946 and 1947) and Bullard (1949).

2.2 Continental Drift and Polar Wandering

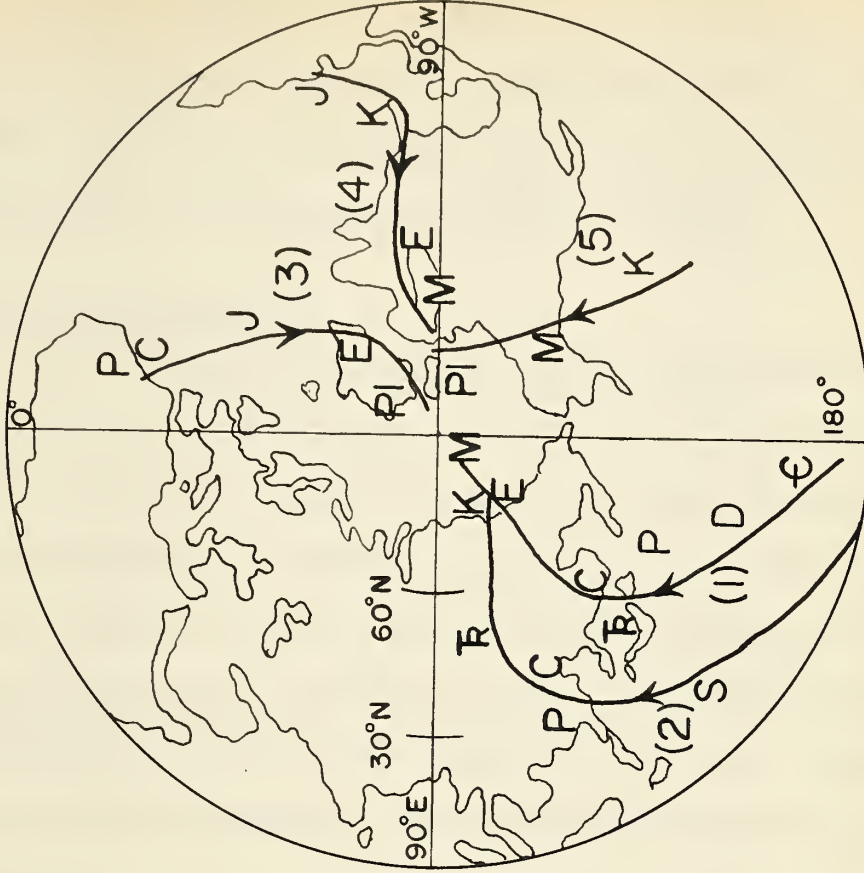
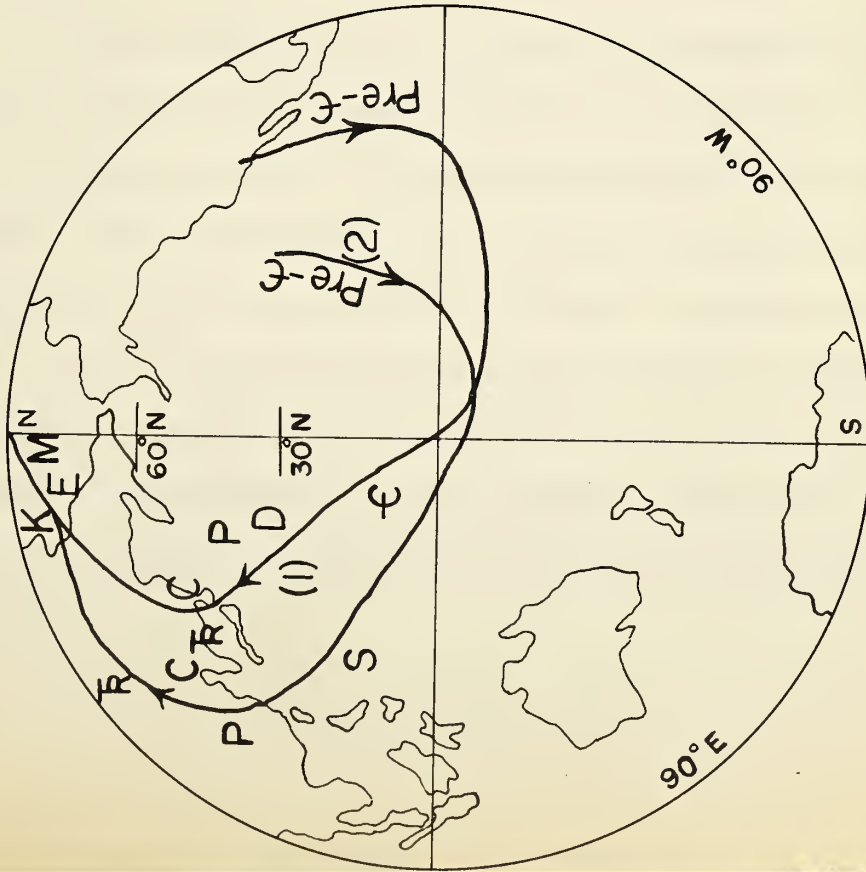
It is generally believed that Continental drift was first suggested by Taylor (1908) and Wegener (1910) on the basis of various geological, paleobotanical, and other data. The idea was, however, first published by Snider (1858) on the basis of the similarity of North American and

European Carboniferous fauna, in addition of course, to the complementary nature of the respective coastlines.

The fact that the mean geomagnetic pole and the rotational axis have been parallel in late Pleistocene and Recent times at least suggests that, in applying the principle of uniformitarianism to paleomagnetic data which differs from the present magnetic field, either continental drift or polar wandering may have occurred in geologic history.

Runcorn (1956 b), Irving (1956) and others have suggested that the separation of curves of paleomagnetic poles observed for North America and Europe (Figure 1) is due to a rotational drifting apart of the continents of 24° of longitude since Triassic times. This has been confirmed compellingly by more recent work (Collinson and Runcorn 1960) where the curves again suggest a drifting apart, although in the case with up to 30° of longitude drift since Triassic times. This recent data features pole curves which are marked by a kink at the Permian-Carboniferous stages in both the European and North American curves. Similar to data from India, Japan and Australia (Figure 1) demand much larger movements of the continents to create a unique polar wandering path.

Other land movements have been postulated by Nairn (1956), whose investigation of Carboniferous and Precambrian strata indicated a 20° counterclockwise rotation of Newfoundland with respect to the rest of North America. Clegg et al. (1957), using Triassic magnetic poles from Spain, suggests a rotation of Spain relative to France and England. Similar rotations have been proposed for Japan relative to continental Asia, by Irving (1959), for Oregon with respect to the rest of North



Pl - Pliocene
 M - Miocene
 E - Eocene
 K - Cretaceous
 J - Jurassic
 R - Triassic
 P - Permian
 C - Carboniferous
 D - Devonian
 S - Silurian
 E - Cambrian
 Pre-E - Precambrian

- (1) Europe (After Creer, Irving and Runcorn, 1957)
 (2) North America (After Clegg, et al., 1958)
 (3) Australia (After Irving and Green, 1958)
 (4) India (After Clegg, et al., 1958)
 (5) Japan (After Nagata, et al., 1959)

Fig. 1.

POSTULATED PALEOMAGNETIC POLAR-WANDERING CURVES FOR EUROPE, NORTH AMERICA, AUSTRALIA, INDIA, AND JAPAN

America (Irving 1959), and Creer (1958) suggests a drift of South America with respect to Africa, based on Jurassic paleomagnetic data. Irving and Tarling's (1961) investigation of the Aden Volcanics suggests that the Red Sea was at one time non-existent, and its present configuration is due to a drifting apart of the present east and west shores.

2.3 The Expanding Earth

Carey (1958), on the basis of a study of deformation of mountain ranges and the distribution of faults and oceans, proposed that since the Paleozoic the earth's area has increased by 45%. The physiography of mid-ocean ridges gave Heezen (1959) the impression that the earth is actively expanding. Egyed (1956 and 1960) calculated on the basis of the paleogeographical decrease in ocean area a rate of the increase of the earth's radius of 0.4 to 0.8 millimetres per year, and Egyed (1960) has expressed the suitability of paleomagnetism as a tool for testing these ideas.

Cox and Doell (1961) have applied the available data from the Permian of Western Europe and Siberia to a simple test, which is, if the earth's radius increases, the geocentric angle between two points increases. The ancient angle is observable paleomagnetically. Although the magnetic studies of the Permian indicate a relatively steady magnetic field at that time, the accuracy of the data available together with correlation dependability, is not sufficient to confirm or deny Egyed's calculation. Carey's hypothesis does seem to be rejected. Beck (1961) comes to a similar conclusion, on the basis of energy considerations.

2.4 Local Correlation Problems

The direction of the magnetic vector in a sample is determined by the local magnetic field at the time of formation. Thus rocks with similar stable remanent moments are very likely the same age; and conversely, rocks which have different remanent directions are unlikely to have been formed at the same time.

Using this principle, DuBois (1959) has shown the contemporaneity or noncontemporaneity of some Keweenawan rocks from the Lake Superior district. The results agree with the older geological results.

A similar study has been carried out by Belshé (1957) on the Carboniferous of England.

2.5 Local Tectonic Problems

Hood (1961) has made an investigation of the paleomagnetic properties of the Precambrian nickel eruptive of the Sudbury basin. The difference of forty degrees in the vertical angle of the remanent vectors between the south and north ranges are symmetrically distributed about the vertical and the east-west axis. This difference is explained by assuming that there has been relative tilting about the east-west axis through the middle of the basin.

Norris (1959 and 1960) has used the similarity of the horizontal component of the magnetic vector within the same formations of the Flathead and Clarke ranges to suggest that little if any differential rotation in a horizontal plane has taken place during thrust faulting of the parent Lewis Overthrust.

The use of only one component is a dubious practice, unless the horizontal component in use is very different from the earth's present field; and Norris has not yet published details of the direction of the horizontal component which he used.

2.6 Paleomagnetic Dating

Gusev (1959) has used sixteen hundred orientated rock samples from the Maymechu-Kotuy region of Russia to obtain a paleomagnetic pole position for the rocks, which he has compared with the paleomagnetic results already published, to suggest a Permian to early Triassic age for the samples.

This result disagrees with the previously proposed age based on paleontological methods, but agrees with a recent isotope age determination using the potassium-argon method.

This method is obviously only applicable where reliable pole positions have been previously determined. In rocks older than the Tertiary, with the exception of Permian and Triassic, the present data is not well-enough defined to enable anything more than a first approximation of the age to be obtained from magnetically stable rocks.

2.7 Integration of Paleomagnetic Results into other Geological Studies

It has already been shown above how the magnetic pole positions determined from the measurement of the magnetic properties of rocks can aid in geological problems where some degree of movement has taken place either locally or on a global scale.

Obviously, any phenomenon which is dependent on its location relative to a well-defined geographical zone in past ages can be studied using suitable methods, together with the paleomagnetic method for the relative location aspect of the particular study.

Opdyke and Runcorn (1960) have used the method first proposed by Shotton (1937) for determining ancient wind directions in aeolian sandstones, in their study of the Tensleep, Caspar, and Weber formations of the Permo-Pennsylvanian in the Western United States. The method is simply to determine the direction of the slip face of ancient sand dunes, and thus map the direction of ancient winds. Assuming that a trade wind belt has been a feature of the general circulation of the atmosphere in ancient times, as it is at present, the relative position of the ancient trade wind belts and the paleomagnetically determined equator can be mutually affirmative or contradictory.

Opdyke and Runcorn (1960) have shown that the inferred wind directions and the paleomagnetic equator in their study agree with each other.

Eaton (1960) has suggested that the distribution of volcanic ash interstratified with sediments is a far more reliable function of ancient contemporaneous wind directions, since, as volcanic ash is frequently carried at high altitudes, local land surface irregularities will not affect the high altitude wind direction, as might be the case in ancient ground level winds which determine the direction of the slip faces of ancient sand dunes.

The use of paleomagnetism as a geological tool is undeniable, but the precision of this tool must always be weighed against the precision of the geological investigation which it is related to, prior to drawing confirmatory or contradictory conclusions.

CHAPTER 3

THE ASTATIC MAGNETOMETER

There are two main types of magnetometer used for determining the magnetic vector in rock samples. They are the spinner type magnetometer, which operates by the inducing of an electro-motive force into a coil by the rapid spinning of the magnetic sample in the coil; and the simple astatic magnetometer.

All the measurements of permanent magnetization carried out for the purpose of this thesis were made using an astatic magnetometer. (See plate 1).

3.1 Description of the Blakett Magnetometer

The principle of the operation of an astatic magnetometer is: a regularly shaped specimen is placed centrally beneath an astatic pair of magnets; the deflection observed is due to the horizontal moment of the specimen perpendicular to the plane of the magnets, and is proportional to the difference in the horizontal fields acting on the two different magnets.

To construct the instrument, an astatic pair of magnets four millimetres long, with four square millimetres cross-sectional area



Plate 1

THE ASTATIC MAGNETOMETER

are mounted one above the other in opposition on an aluminium housing. A plane mirror is mounted on the housing beam, for optical measuring purposes. (See Figure 2). The housing is suspended on a very fine quartz fibre. In the original magnetometer designed by Blackett (1952) the magnets were suspended in a magnetic field free space which was produced by three pairs of mutually perpendicular Helmholtz coils. The magnetometer used by the author, however, does not feature the Helmholtz coils, and is operated at a high astatization which is obtained by use of the trimmer magnets mounted on the aluminium housing. The quartz fibre is suspended from a torsion head. This enables the system to be raised and lowered, or rotated by applying a twist to the fibre.

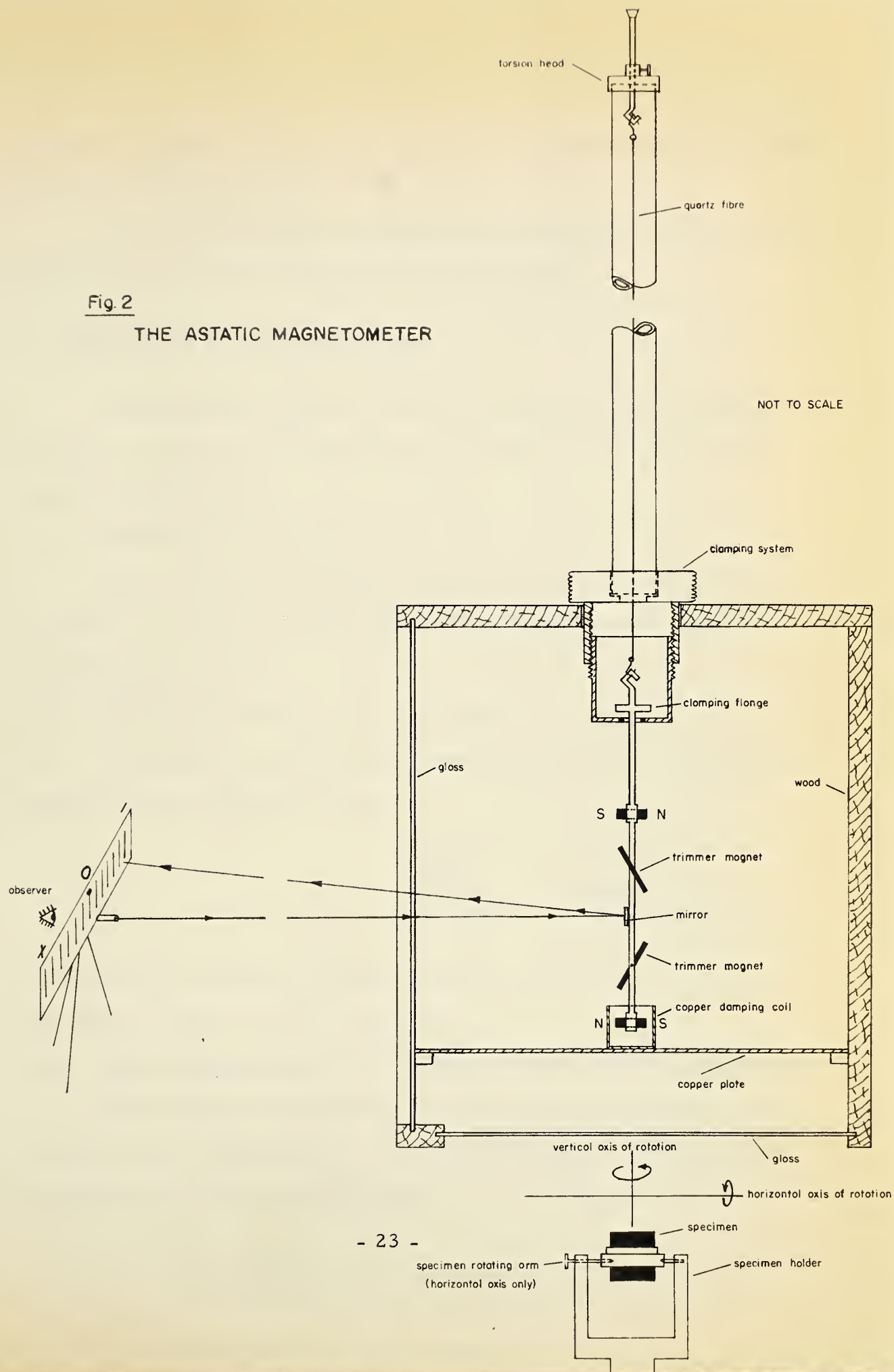
Damping of the system is accomplished by placing a copper plate under the lower magnet. The eddy currents set up by the magnet provide a brake for the oscillation of the system. The damping was increased in the apparatus used, by allowing the lower magnet to rotate inside a ring of copper raised above the damping plate.

The plastic specimen holder is capable of being raised or lowered directly underneath the suspended magnets, according to the magnetic intensity of the specimen. The holder is also capable of rotation through any vertical or horizontal plane, in order to measure the chosen components.

The whole aluminium housing can be clamped by the raising of a flange so that the corresponding rim on the housing is raised, thus preventing tension on the fibre. (See Figure 2). The magnetic housing is enclosed in a draught free box, with glass on one side for the optical

Fig. 2

THE ASTATIC MAGNETOMETER



measuring process. Other minor features of the apparatus are levelling screws, and a bubble level.

The whole apparatus is mounted on a concrete block on a concrete floor to minimize the transmission of any vibration.

3.2 Astatization of the Magnetometer

This operation consists of making the moments of the magnets as equal as possible and antiparallel in direction. There are several stages in this operation:

(i) Selecting the Magnets:

Select two small cylindrical magnets which have been cut from the same bar of Alnico. At this stage, they should be of precisely the same length and weight.

(ii) Theoretical Moment of the Magnets:

The magnets used in the apparatus were Alnico II. The residual of Alnico II is 7,200 gauss. Given

Diameter	= 0.106"
Length	= 0.180"
Volume	= 0.026 cm.
I Residual	= $\frac{7200}{4\pi} = 570$ c. g. s.

The theoretical maximum magnetic moment of the magnets are therefore equal to $0.026 \times 570 = 14.8$ c. g. s.

(iii) Measuring and Equalizing the Magnetic Moment before Mounting:

The moments were measured using a vertical variometer. The variometer was calibrated at 20 γ per scale division. The moment of the magnets was measured as follows:

$$H = \frac{2M}{d^3}$$

d = distance of centre of magnet from vario-
meter magnetic blades mount

M = magnetic moment of magnet

H = observed magnetic field

For the first magnet, at a distance of 29.0 cm.; the deflection was 2.1 s.d.

$$H = 42 \times 10^{-5} = \frac{2M}{29^3}$$

$$\underline{M = 5.3 \text{ c. g. s.}}$$

For the second magnet, at a distance of 29.0 cm., the deflection was 1.7 s.d.

$$H = 34 \times 10^{-5} = \frac{2M}{29^3}$$

$$\underline{M = 4.3 \text{ c. g. s.}}$$

Since neither magnet had approached its theoretical maximum magnetic moment, nor were they equal, an attempt was made to saturate both magnets simultaneously in a strong magnetic field provided by a strong electric magnet.

Result of this operation was:

For both magnets, at a distance of 28.4 cm., the deflection was 2.6 s.d.

$$H = 52 \times 10^{-5} = \frac{2M}{28.9^3}$$

$$\underline{M = 11.9 \text{ c. g. s.}}$$

Thus the magnets were equalized and their magnetic moments were increased to almost saturation, to facilitate a maximum deflection with a given fibre.

(iv) Further Equalizing of the Magnets after Mounting:

Although the magnets were equalized as far as possible prior to mounting, the accuracy of the measurements was limited by the sensitivity of the vertical variometer. Furthermore the possibility of magnetic field gradients occurring around the magnets when suspended necessitates further equalization of the suspended magnets. Therefore two further operations were carried out with the magnets in their suspended position:

(A) Equalizing by free oscillation

The magnets were mounted in the aluminum housing, without being cemented. The north pole of each magnet was marked. The system was suspended from the torsion head by a torsionless fibre such as silk at the permanent operating location. From the position of the system after it had come to rest, it could be seen which of the two magnets was the stronger. From the equation:

$$T = 2\pi \sqrt{\frac{I}{c + \Delta MH}}$$

T = periodic time
I = moment of inertia of the system
c = torsion constant of the fibre
 ΔM = difference in magnetic moments
of the two magnets
H = ambient field

it can be seen that the magnetic moments will approximate the same magnitude when the period of oscillation is at a maximum. Periods of oscillation were observed with the upper magnet in four different positions, each at 90° to each other along the long axis. The position of the magnet corresponding to the largest periodic time was noted, and the magnet was cemented permanently into that position.

The operation was repeated for the lower magnet.

(B) Equalizing the Magnets by use of the Trimmer Magnets and
Helmholtz Coil (Forced Oscillation)

Final astatization of the system was accomplished using a Helmholtz coil and the trimmer magnets. The coil was mounted so that the uniform field produced was vertical and along the axis of the housing, that is, perpendicular to the horizontal planes through the long axis of each magnet. Now from the above equation in (A), it can be seen that with no difference in the magnetic moment of the magnets, variation of the ambient field will produce no change in the oscillation rate. The upper trimmer magnet was rotated about its horizontal axis until a position was found where variation of the current in the Helmholtz coils (that is, variation of the uniform ambient field) had a minimum effect on the period of oscillation of the magnetic system. The upper trimmer magnet was then cemented into a permanent position. The operation was repeated for the lower trimmer magnet.

The apparatus was then considered to be as astatized as was possible with the equipment available.

3.3 Sensitivity of the Magnetometer

(i) The Initial Measurement of the Sensitivity:

The astatized magnetic system was mounted on a quartz fibre which was obtained from Mr. S. Worden. The first calibration of the apparatus was then made by use of a magnet of known moment. Since the net deflecting field is, neglecting the magnetic length of the magnet:

$$H = M \left\{ \frac{1}{Z_u^3} - \frac{1}{Z_l^3} \right\} \text{ where } Z_u = \text{distance of upper magnet to centre of calibrating magnet}$$

Z_l = corresponding distance for lower magnet

M = magnetic moment of calibrating magnet

The sensitivity was determined by:

$$\begin{aligned} \text{Moment of calibrating magnet} &= 100 \text{ c. g. s. units} \\ Z_u &= 46.2 \text{ cms.} \\ Z_l &= 51.3 \text{ cms.} \end{aligned}$$

$$\begin{aligned} \text{Net deflecting field is } H &= M \left\{ \frac{1}{Z_u^3} - \frac{1}{Z_l^3} \right\} \\ &= 100 (27.5 \times 10^{-6}) \\ &= 2.75 \times 10^{-4} \text{ oersteds} \end{aligned}$$

Deflection produced by this field is 28 scale divisions. Thus reciprocal sensitivity is 1×10^{-5} oersteds per scale division. This sensitivity was found adequate for most samples of the major study of this thesis (Chapter 6) where the average 2.5×10^{-3} c. g. s. intensity would produce a maximum of forty scale divisions deflection, if orientated so that the total component of the magnetic vector creates the deflection. Other components will produce a smaller deflection, of course, depending on the orientations with respect to the total vector. The other studies undertaken for this thesis were with much older and magnetically weaker rocks. Thus it was decided to try to increase the sensitivity in order to make more accurate measurements of the younger rocks, and to make some measurements at least of the older materials.

(ii) Increasing the Sensitivity of the Magnetometer

It has already been described how the astatization of the magnetometer was carried out.

A source of insufficient sensitivity could be the thickness of the quartz fibre. It can be shown that a thickness of 10 microns is needed for a sensitivity of about 10^{-6} c.g.s. per scale division under normal conditions.

(A) Measuring the thickness of the quartz fibres.

In order to determine whether or not the quartz fibre was responsible for the low sensitivity of the instrument, the thickness of the fibre was measured using the equations:

$$c = \frac{n \pi r^4}{2l} \quad \text{where } c = \text{torsion constant for the quartz fibre}$$

$n = 3.0 \times 10^{11}$ dynes/cm² for quartz
 r = radius of quartz fibre
 l = length of quartz fibre

c is obtained from:

$$T = 2\pi \sqrt{\frac{I}{c}} \quad \text{where } T = \text{period of oscillation}$$

I = moment of inertia of the body suspended
by the fibre and

I was obtained from:

$$I = \frac{mL^2}{12} \quad \text{where } m = \text{mass of a long thin bar}$$

L = length of the bar. (The bar was suspended
at its middle point)

The results were:

$$T = 15.21 \text{ seconds}$$

$$I = 0.513 \text{ gm. cm.}^2$$

$$c = \frac{4\pi^2 0.513}{15.21^2} = 0.0875 \text{ dynes cms.}$$

Substituting this in $c = \frac{n \pi r^4}{2l}$ with $l = 18.6$ cm., we obtain

$$3.0 \times 10^{11} \times \pi \times r^4 = 0.0875 \text{ giving } r^4 = 3.46 \times 10^{-12}$$

$$r = 1.364 \times 10^{-3} \text{ cm.} = 13.64 \text{ microns}$$

$$\text{thickness} = 27.28 \text{ microns}$$

Thus the fibre is almost three times the thickness usually required for a sensitivity of about 10^{-6} c.g.s. per scale division. It was therefore decided to manufacture a thinner quartz fibre.

(B) Making a quartz fibre

The jet of an oxyacetylene apparatus was adjusted so that the flame was vertical and about six inches long, with the inner cone about half an inch long. A black velvet cloth about three feet square was pinned to a board about two feet above the oxyacetylene jet. A one-eighth of an inch diameter quartz rod was held horizontally at the top of the inner cone of the jet, and when a molten state was reached, the two halves of the rod were drawn apart by raising one half upwards. A filament of quartz was carried up in the flame as the two halves parted. The molten ends of the rod were joined, and the process repeated many times. A 'cobweb' of fibres eventually formed on the velvet cloth. After selection and cutting, small brass hooks were attached to both ends of each fibre with wax.

(iii) Final Calibration of the Apparatus

Several extremely thin fibres were not able to bear the weight of the aluminum housing. The apparatus was eventually successfully operated using a fibre which led to the following calibration, based on two experiments with a magnet of intensity 276 c.g.s. units:

$$\begin{array}{ll} (1) \text{ } Z_u = 67.7 \text{ cm.} & (2) \text{ } Z_u = 92.0 \text{ cm.} \\ \text{ } Z_L = 72.8 \text{ cm.} & \text{ } Z_L = 97.1 \text{ cm.} \end{array}$$

$$\text{Total Deflection } 2D_1 = 302 \text{ s.d.} \qquad 2D_2 = 83 \text{ s.d.}$$

$$\text{Now } H = \frac{M}{Z^3} \qquad \text{where } H = \text{the horizontal field at the astatic magnets}$$
$$\qquad \qquad M = \text{the magnetic moment of the calibration magnets}$$
$$\qquad \qquad Z = \text{the distance between the astatic magnets}$$

Therefore the field gradient is $\frac{dH}{dZ} = -3MZ^{-4}$

$H = + \frac{3ML}{Z^4}$ oersteds/cm. where Z = the distance from the calibrating magnet to the centre of the astatic pair

L = the separation of the astatic magnets

For the two experiments $Z_1 = 70.2$ cm., $Z_2 = 94.5$ cm.,
 $M = 276$ c.g.s., and $L = 5.1$ cm.

$$\text{Then } H_1 = \frac{15.3 \times 276}{2.43 \times 10^7} = 1.74 \times 10^{-4} \text{ oersteds}$$

$$H_2 = \frac{15.3 \times 276}{7.98 \times 10^{-7}} = 0.53 \times 10^{-4} \text{ oersteds}$$

Now the deflection produced was: $2D_1 = 302$ s.d.
 $2D_2 = 83$ s.d.

Thus the sensitivity of the apparatus was:

$$S_1 = \frac{D_1}{H_1} = \frac{151}{1.24 \times 10^{-4}} = 0.866 \times 10^6 \text{ s.d. /oersted}$$

$$S_2 = \frac{D_2}{H_2} = \frac{41.5}{0.53 \times 10^{-4}} = 0.783 \times 10^6 \text{ s.d. /oersted}$$

$$\text{Average sensitivity } S_{av} = 0.825 \times 10^6 \text{ s.d. /oersted}$$

or reciprocal sensitivity is $\frac{1}{S_{av}} = 1.214 \times 10^{-6} \text{ oersteds/s.d.}$

Thus it seems that the manufacture of a thinner quartz fibre improved the sensitivity of the instrument by a factor of eight.

Immediately following calibration, the intensity of a standard specimen was measured, for daily use during operation of the instrument. Details of the calculations of the intensities of the calibration specimen will be given in Chapter 6, together with the details of the intensities for the other specimens in the collection.

CHAPTER 4

MEASUREMENT OF THE MAGNETIC VECTOR

The astatic magnetometer is basically a very simple instrument. In order to compute the magnetic vector it is only necessary to measure the various components of the vector. Measurement of the remanent magnetism, however, will only have significance if it is relatable to the ancient magnetic field, and therefore suitable collection, orientation, and preparation methods must be observed.

4.1 Collecting and Preparing the Samples

Whatever orientating method is used in sampling, two conventions should be adhered to. Samples should be collected from as fresh exposures as possible, since the weathering processes can result in the decay of magnetic properties. When a sample has suffered weathering, an effort should be made to disregard the outer weathered parts of the sample. Over-localized information can be dangerous, particularly if the paleomagnetic pole is being investigated for a particular formation. In sampling an outcrop, collection from as widely scattered an area as is possible and from a large vertical extent should be attempted, to give the collection a random nature.

The samples are collected from the field using a suitable

orientation convention. Any method whereby the sample can be uniquely orientated into a position so that the in-situ magnetic vector can be measured and then related to the original formational position is suitable. For example, magnetic north or any other bearing on the upper surface, and horizontal lines on at least two different faces will be sufficient to enable the unique position to be recreated for later coring.

It is frequently convenient to orientate samples from an undisturbed intrusive, for example, with reference to the dipping face of the body. It would be necessary, therefore, after computing the vector relative to the dyke face, to rotate the vector until it is relative to the horizontal, or whatever plane is thought to be the old reference datum, in order to duplicate the old magnetic field. Sampling using this method would need data concerning the dip and strike of the body to apply the necessary rotation.

A similar correction would be necessary, depending on the sampling technique, for bodies which have undergone movement since formation, always assuming that the amount of movement since formation can be determined. For this purpose, sedimentary bedding planes, which frequently can be found near dykes, are assumed to have been formed horizontally.

By use of the orientation markings made in the field, the samples have their field orientation reproduced in the workshop, usually with the aid of plaster of paris. This orientation may be with reference to the horizontal, or the face of the particular body. The samples are then cored using a high-speed drill featuring a hollow diamond impregnated bit. These cores are then cut into what will be referred to as specimens. Care is taken to transfer accurately the magnetic north or bearing line

to the specimen, on to the upper surface or "top" indicator of the specimen. The other orientations are known since the core orientation is known. The length of the cylindrical specimens should be a maximum of one inch, which is also the diameter size. Wilson (1959) has stated that a uniformly magnetized cube has a magnetic field which is the same as that of a dipole to within 1% at distances from the centre of the cube greater than the length of its sides. A cylinder of height equal to its diameter also features the same approximation.

4.2 Measurement of the Azimuth (Declination) of the Magnetic Vector

The first operation on the prepared cylindrical specimen is the measurement of the horizontal component or azimuth of the magnetic vector in the specimen. This measurement is made with respect to a fixed horizontal (on the specimen) line, designated by "B" in Figure 3. This is the bearing line, and can be either the magnetic north or a bearing, the angle of which, with reference to magnetic north, is known.

Suppose the magnetometer has been set up so that the north seeking end of the lower magnet faces west (left in Figures 2 and 3). Then, the diagrams in Figure 3 show the specimen and lower magnet above it, in plan view. "B" represents the bearing arrow, and the other arrow is the azimuth of the vector which is to be determined. The observer is situated on the left hand side, as shown in Figure 2. The operations are as follows:

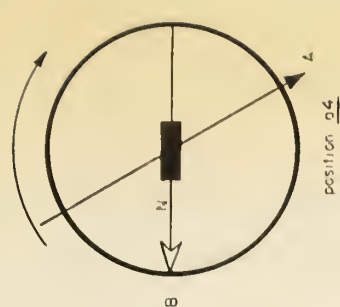
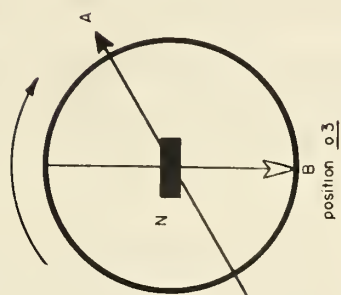
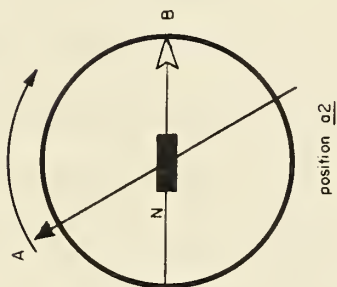
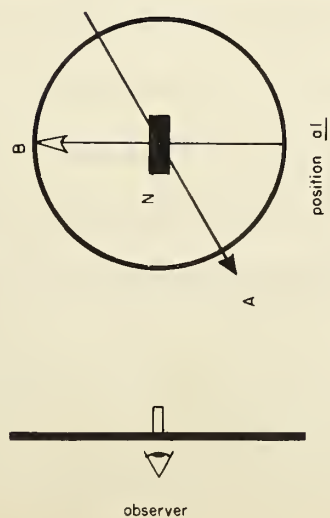
(a) Insert the cylinder in the holder, with the top face perpendicular to the vertical axis, and the bearing arrow pointing north as in Figure 3a1.



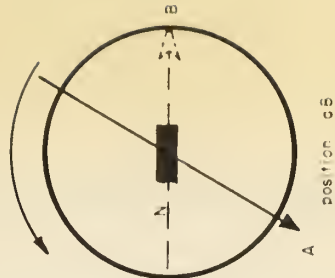
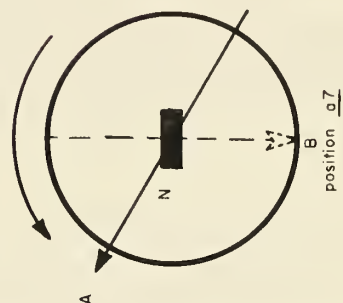
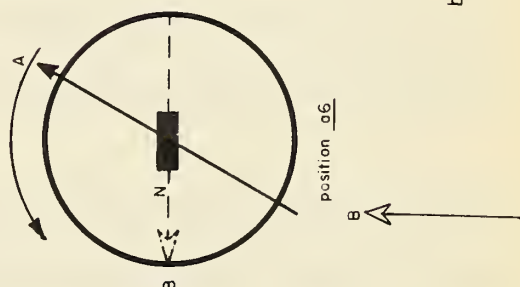
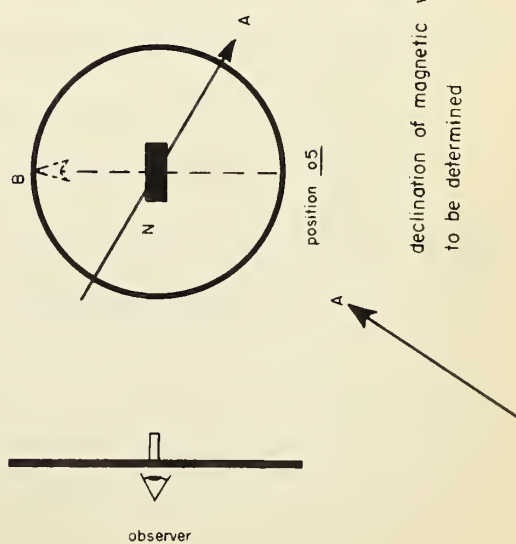
Plate 2

OPERATING THE ASTATIC MAGNETOMETER

(i) TOP OF SAMPLE UPWARDS



(ii) TOP OF SAMPLE DOWNWARDS



declination of magnetic vector
to be determined

bearing line

direction of rotation of specimen
about a vertical axis

Fig.: 3 MEASUREMENT OF AZIMUTH
(Plan View)

With the azimuth as shown, a deflection to the left of the observer, which is negative by convention, will result.

(b) Rotate the cylinder clockwise through 90° about a vertical axis to the position shown in Figure 3a2. The deflection will be to the right of the observer (positive) and larger in magnitude than the first reading.

(c) Observe the deflections after rotation clockwise to positions 3a3 and 3a4, which will give small positive and large negative readings respectively.

(d) From 3a4 position the specimen is rotated once again through 90° to repeat the 3a1 position. If drift has occurred in the fibre, a different observation will be made, and this difference is then distributed with time over the four readings.

(e) Remove the specimen and reinsert with bottom face on top with the bearing arrow still pointing northwards as in Figure 3a5. A small and negative reading will result.

(f) Rotate the specimen anticlockwise about a vertical axis, making readings every 90° . With homogenous magnetizations, a similar sequence of readings will be observed, as in the case of the five readings for the upright specimen. The drift of the fibre is similarly distributed.

(g) If the readings after drift correction are a_1 , a_2 , a_3 , and a_4 , corresponding to the bearing arrow being north, east, south, and west, respectively, in the upright specimen case; and a_5 , a_6 , a_7 , and a_8 , corresponding to the bearing arrow being north, west, south, and east, respectively, for the inverted specimen; then after adding

$$a_1 + a_5 = b_1 \quad a_2 + a_6 = b_2$$

$$a_3 + a_7 = b_3 \quad a_4 + a_8 = b_4$$

it can be shown that the angle between the bearing direction and the magnetic azimuth is

$$\Theta = \tan^{-1} \frac{b_4 - b_2}{b_1 - b_3}$$

Care must be taken with the signs of the numerator and denominator, in order to arrive at the correct tangent quadrant.

(h) Finally it is obvious that

$$A = B + \Theta \quad \text{where } A = \text{final azimuth}$$

B = angle between bearing and magnetic north

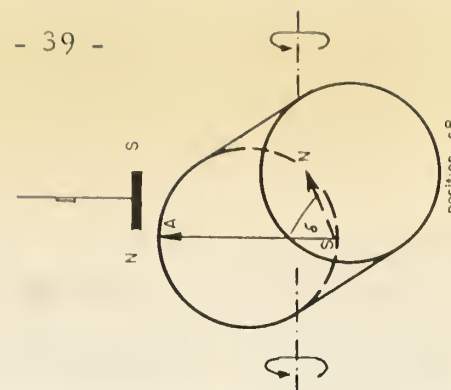
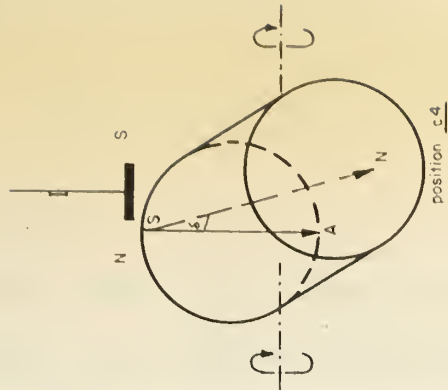
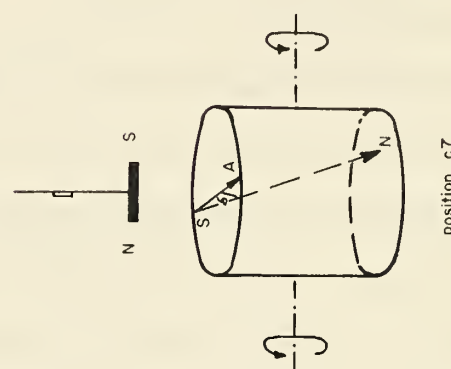
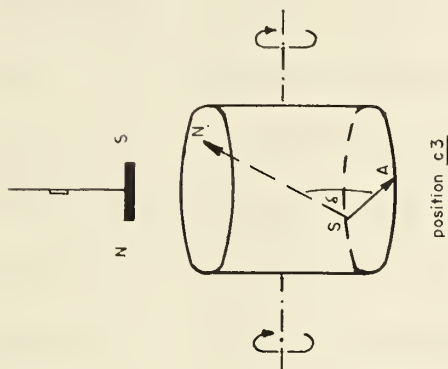
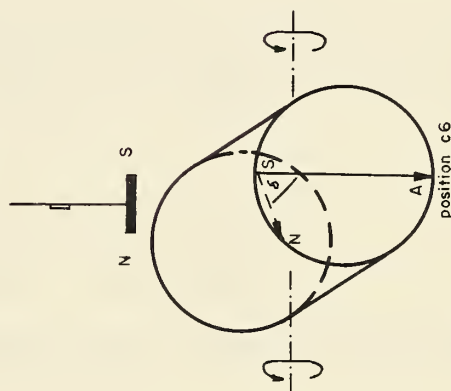
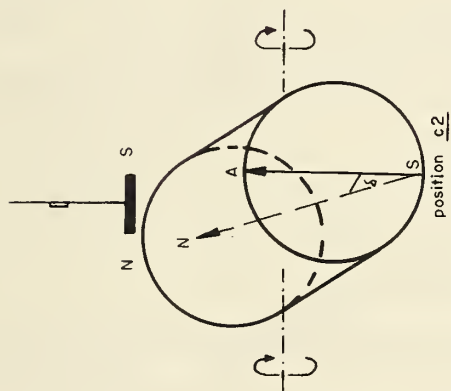
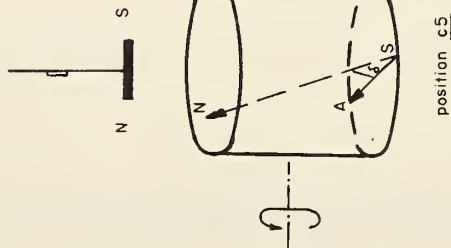
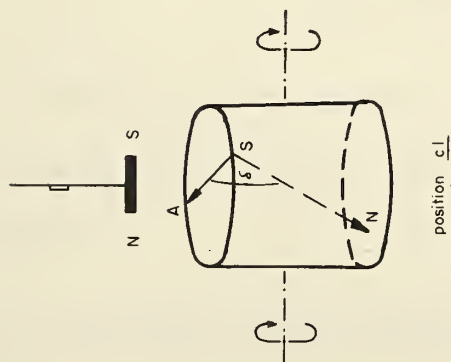
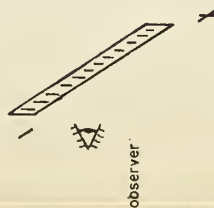
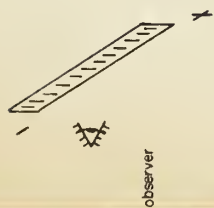
Thus the azimuth or declination with respect to magnetic north can be obtained for a cylindrical specimen.

4.3 Measurement of the Dip or Inclination of the Magnetic Vector

After having determined, as described above, the declination of the magnetic vector in the specimen, the declination direction is marked on the top of the specimen. The measurement of the declination is made by rotating the specimen about a horizontal axis, in the plane of the previously determined declination; for obviously, the magnetic vector lies in this plane. The procedure is as follows:

(a) The specimen is mounted with the top face perpendicular to the vertical axis (that is, with the top face horizontal) and the previously determined declination pointing north as in Figure 4c1. A positive reading will result in the case shown.

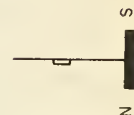
(b) The specimen is then rotated clockwise to the observer through 90° about a horizontal axis to the 4c2 position. A large negative reading



dip of the magnetic vector which is in the
plane of declination, and is to be determined.

declination, as determined previously (see fig.:3)

diagrammatic representation of the lower
ostatic magnet and mirror



MEASUREMENT OF THE DIP OF THE MAGNETIC VECTOR

Fig.: 4

results.

(c) Similarly, rotations through 90° to 4c3 and 4c4 positions will give negative and positive readings respectively. A fifth reading, duplicating the 4c1 position, is made to determine the drift, if any, which is then distributed with time, as in the case of the declination measurements.

(d) The specimen is then placed with the top face downwards, and horizontal, with the declination arrow again pointing north, as in Figure 4c5. The specimen is rotated anticlockwise to the observer, about the horizontal axis, and five more readings are taken, to get four readings corrected for drift, corresponding to positions 4c5, 4c6, 4c7 and 4c8, in Figure 5.

(e) If the first four corrected readings are called c_1, c_2, c_3 and c_4 ; and if the second set of four readings are called c_5, c_6, c_7 and c_8 , addition will give

$$d_1 = c_1 + c_5 \quad d_2 = c_2 + c_6$$

$$d_3 = c_3 + c_7 \quad d_4 = c_4 + c_8$$

It can then be shown that the angle of dip, which the vector makes with the horizontal is

$$\delta = \tan^{-1} \frac{d_4 - d_2}{d_1 - d_3}$$

The denominator will be observed to be always positive. Thus the sign of the dip is always that of the numerator. Downdip is positive; updip is negative.

4.4 Calculation of the Intensity of Magnetization of the Magnetic Vector

The two above operations will yield the declination and dip of the

magnetic vector in a given sample. To complete the data concerning the magnetic vector, it remains to calculate the intensity of magnetization of the sample. This is done using the following equation:

The intensity of magnetization

$$J = \frac{1}{S.A.} \left[\frac{D}{t \cos \delta \left\{ \frac{ZL}{(ZL^2 - t^2)^2} - \frac{Zu}{(Zu^2 - t^2)^2} \right\}} \right] \quad \text{e.m.u. / c.c}$$

where S = sensitivity of the instrument in millimetres per oersted

t = thickness of specimen in cms.

A = cross sectional area of specimen in cm.²

δ = dip of the magnetic vector from the horizontal

ZL = distance from the centre of the specimen to the centre of the lower astatic magnet

Zu = the corresponding distance to the upper astatic magnet

D = deflection produced on a scale at a certain distance from the mirror

D is the deflection caused by the horizontal component of the magnetic vector when it is at right angles to the astatic magnets. This occurs when the specimen is in the first and third position during dip determination.

The average deflection D is thus taken as

$$D = 1/4(d_1 - d_3)$$

The intensity is then found using the above equation.

The measuring of the declination, inclination and intensity of magnetization of the magnetic vector can thus be carried out for each specimen. There are other methods for measuring the vector using the astatic magnetometer, but the method given in this chapter enables more cancellation of random errors than any other method.

Examples of the calculations of the magnetic vector from first observations will be given in later chapters.

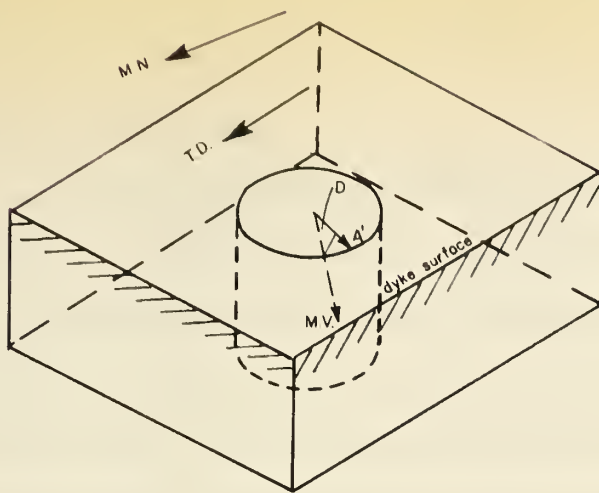
CHAPTER 5

THE PROCESSING OF THE MEASUREMENTS OF THE MAGNETIC VECTOR

Obtaining the direction of a stable magnetic vector, as shown in the previous chapter, merely furnishes information about the direction of the magnetic field at the sample site at the time of formation of the rock. Several operations on the results are necessary before a position of the paleomagnetic pole can be obtained.

5.1 Correction for Geological Tilt

If, subsequent to the acquisition of remanent magnetism, the geological body involved is structurally deformed, in order to obtain accurate information, the vectors must be transformed back into a position which, by some indication, such as bedding planes, is that in which they were originally deposited. Alternatively, if steep bodies, such as dykes, are sampled, and measurements of the magnetic vector are made with respect to the dip and strike of the body, the measured vectors must be rotated to give a result relative to the original horizontal at the time of deposition, which can be obtained from adjacent sedimentary bedding planes, or from the dip and strike of the dyke itself, if it has remained undisturbed since formation. The operation is



T.D. = tilt (geological dip) direction

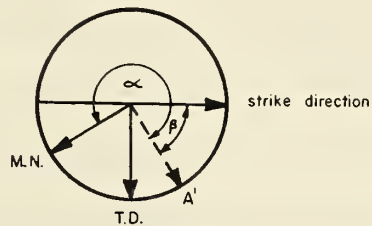
A' = azimuth of measured magnetic vector

D = dip of magnetic vector

M.V. = magnetic vector

M.N. = magnetic north

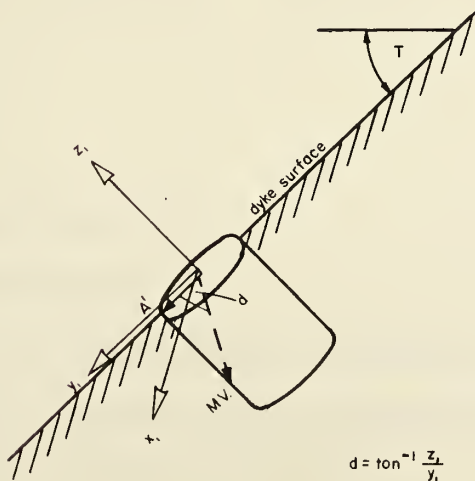
b) cross-section of the core :



α = azimuth wrt magnetic north

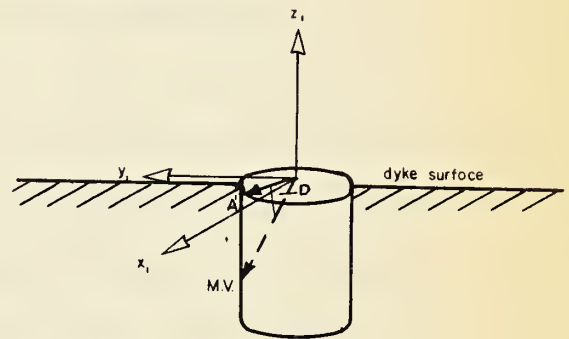
β = azimuth wrt strike direction

d) after projection of the magnetic vector on to the vertical plane through the tilt direction, rotation through the geological tilt about the x_1 axis :



T = geological dip (tilt) of the dyke

c) first set of axes :

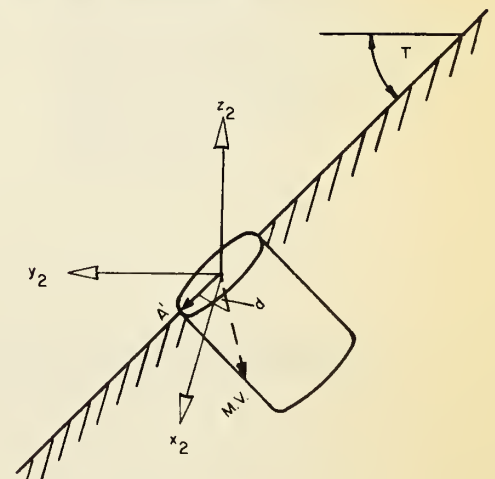


x_1 = strike direction

y_1 = tilt (geological dip) direction

z_1 = perpendicular to dyke surface

e) the axes for the in-situ magnetic vector



x_2 = strike direction

y_2 = tilt direction

z_2 = vertical

Fig.: 5

CORRECTION FOR GEOLOGICAL DIP OF THE BODY

similar in both cases.

The details of the operation given below are those which have been applied to the specimens used for the study in Chapter 6.

The samples were collected using an orientation system where the dip direction and/or strike direction of the parent dyke was marked on the top of the sample. The cores were obtained so that the top of each specimen was parallel to the dipping surface of the dyke, so that the bearing line on the top of the specimen is in fact the dip or strike line. Before correction for tilt, the results were given in terms of magnetic north for the azimuth, and the dip was relative to the top of the specimen (Figure 5a). The first part of the operation is to substitute a new coordinate system, with strike (X_1), geological tilt or dip direction (Y_1), and the normal to the top of the cylinder (Z_1) for the original magnetic north, east-west, and normal to the top of the specimen coordinate system; (Figures 5b and 5c). This is done using the equations:

$$X_1 = \cos \phi \cos D \text{ where } D = \text{uncorrected dip of the magnetic vector}$$

$$Y_1 = \sin \phi \cos D \quad \text{and } \phi = A^1 - S^1 \text{ where } A^1 = \text{uncorrected azimuth of the magnetic vector}$$

$$\text{and } S^1 = \text{strike direction of the body (} S^1 \text{ is always } 90^\circ \text{ less than the dip direction)}$$

$$Z_1 = Z = \sin D$$

By convention:

X_1 is positive if this component is in the same direction as bearing

Y_1 is positive in the downtilt direction

Z_1 is positive downwards

The uncorrected magnetization vector is then projected upon the vertical plane in which the tilt direction lies, and the dip of the projected vector relative to the top of the sample is then:

$$d = \tan^{-1} \frac{Z_1}{Y_1}$$

d is positive downwards in the +Y₁ direction, and upwards

in the -Y₁ direction.

This projection is tilted through the angle of dip of the geological body, which was measured in the field (Figure 5d). In this way, the original in situ of the magnetic vector is then duplicated.

The coordinates are then projected back to a new set of axes X₂, Y₂, Z₂, which occupy the same position of the old X₁, Y₁, Z₁ axes before tilting (Figure 5e).

X₂ = X₁ (since the rotation back to the position of the old axes takes place on the horizontal axis through X₁, there is no change in X₂)

$$Y_2 = Y_1 \frac{\cos (d + T)}{\cos d} \quad \text{where } T = \text{angle of dip of the body}$$

$$Z_2 = Z_1 \frac{\sin (d + T)}{\sin d} \quad d = \tan^{-1} \frac{Z_1}{Y_1}$$

Then the in-situ azimuth of the magnetic vector, relative to the dip direction is:

$$A_1 = \tan^{-1} \frac{Y_2}{X_2} = \tan^{-1} \frac{Y_2}{X_1}$$

given the bearing B, relative to magnetic north, the in-situ azimuth of the vector relative to magnetic north is simply: A₁' = A₁ + B

In the particular area studies no correction for geomagnetic declination was needed since magnetic north coincided with geographic north.

The in-situ dip of the magnetic vector is:

$$D_1 = \tan^{-1} \frac{Z_2}{(X_2^2 + Y_2^2)^{\frac{1}{2}}} = \tan^{-1} \frac{Z_2}{(X_1^2 + Y_2^2)^{\frac{1}{2}}}$$

Throughout all the calculations in the operation, great care must be taken in order to obtain the correct quadrants for the particular trigonometrical functions. Examples of the application of this "tilt correction" technique will be given in the next chapter.

5.2 Computation of the Mean Azimuth and Dip

When several specimens from a single sample have had their in-situ remanent magnetic vectors measured and calculated, it is usually necessary to determine a mean azimuth and dip for the sample. Similarly, when several samples from a collecting site have had their mean vectors determined, the mean azimuth for the site can be obtained.

This is carried out using the components of the measured vector along north-south, east-west, and vertical directions, which have been designated X_2 , Y_2 , and Z_2 in the previous section of this chapter. X_2 , Y_2 , and Z_2 are positive if they are North, East, and downwards, respectively. Now for each specimen

$$X_2 = P \cos A \cos D \quad \text{where } A = \text{in-situ azimuth of the magnetic vector}$$

$$Y_2 = P \sin A \cos D \quad D = \text{in-situ dip of the magnetic vector}$$

$$Z_2 = P \sin D \quad \text{and } P \text{ is a constant vector}$$

By letting P be the unit vector, and averaging out all the values of X_2 , Y_2 , and Z_2 , for the specimens of a particular sample, the resultant average values can be used to determine the mean vector in the sample.

$$\text{mean azimuth } \bar{A} = \tan^{-1} \frac{Y_{2av}}{X_{2av}}$$

$$\text{mean Dip } \bar{D} = \tan^{-1} \frac{Z_{2av}}{(X_{2av}^2 + Y_{2av}^2)^{\frac{1}{2}}}$$

Similarly the components from the samples

$$X_3 = P \cos \bar{A} \cos \bar{D}$$

$$Y_3 = P \sin \bar{A} \cos \bar{D}$$

$$Z_3 = P \sin \bar{D}$$

can be added and averaged, and then used to determine a mean azimuth for the collecting site:

$$\text{mean azimuth for the site } \bar{\bar{A}} = \tan^{-1} \frac{Y_{3av}}{X_{3av}} \quad \text{and}$$

$$\text{the mean dip for the site } \bar{\bar{D}} = \tan^{-1} \frac{Z_{3av}}{(X_{3av}^2 + Y_{3av}^2)^{\frac{1}{2}}}$$

The mean azimuth and declination for a series of sites can be similarly determined.

No such refined operations are necessary to determine the mean intensity of magnetization of the samples. These are merely averaged.

Examples of the use of these averaging methods are given in the next chapter.

5.3 Obtaining the Paleomagnetic Pole

In many paleomagnetic studies, it is desirable to present the vector measurements in terms of the geocentric dipole that would produce the

measured field direction. This is usually done by specifying the geographic coordinates of the geomagnetic pole that corresponds to the orientation of this inferred dipole. Once the mean azimuth and dip have been established for a site, the paleomagnetic pole which produced that permanent magnetic direction can be obtained using the following equations, based on Figure 6:

$$\sin \Theta^1 = \sin \Theta \cos P = \cos \Theta \sin P \cos D$$

$$\sin (\phi^1 - \phi) = \frac{\sin P \sin D}{\cos \Theta^1}$$

$$\cot P = \frac{1}{2} \tan I$$

where I = inclination of the vector

D = declinate of the vector

Θ = latitude of sampling site

ϕ = longitude of sampling site

Θ^1 = latitude of paleopole

ϕ^1 = longitude of paleopole

P = angular distance from sampling site to paleopole

This group of equations can be expressed alternatively as

$$\cos a = \cos C \cos p + \sin c \sin p \cos A$$

$$\sin (b - d) = \frac{\sin p \sin A}{\sin a}$$

$$\cot p = \frac{1}{2} \tan I$$

where I = inclination of vector

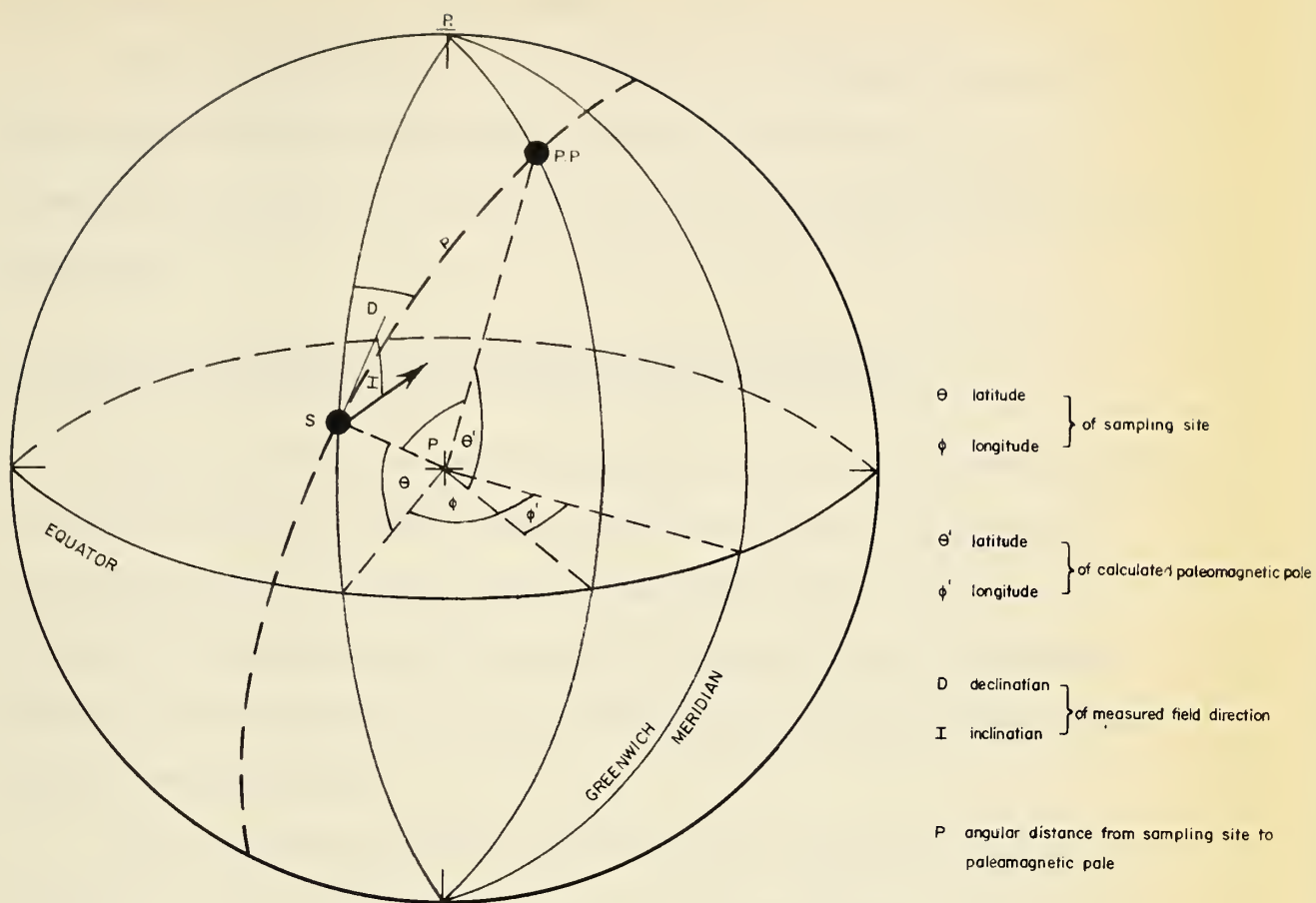
A = declination of azimuth of vector

a = colatitude of ancient pole

b = longitude of ancient pole (East is +, West is -)

c = colatitude of sampling site

d = longitude of sampling site



P - GEOGRAPHIC POLE
 S - OBSERVATORY LOCATION
 $P.P.$ - PALEOMAGNETIC POLE

Fig.: 6

RELATIONSHIPS BETWEEN LOCATION OF SAMPLING SITE, MEASURED
 REMANENT MAGNETIC DIRECTION, & PALEOMAGNETIC POLE

The above relationships will uniquely determine a paleomagnetic pole position for a given in-situ magnetic vector.

Lack of coincidence of pole positions for various sites may be due to a lack of exact stratigraphic correlations; or the scatter in a formation may be due to a departure of the observed field from the ideal dipole field.

5.4 Statistical Treatment of the Paleomagnetic Results

Errors in the study of paleomagnetism can occur during sampling, coring and measuring, apart from during the necessary calculations. Very minor movements of the studied formations after deposition are usually unrecognizable, and thus another source of error is available. Thus it is very desirable to treat statistically the results of any paleomagnetic investigation.

Fisher (1953) developed a method for the statistical analysis of paleomagnetic data. The method is generally applicable to the analysis of any data consisting of a set of vectors or lines in space.

(i) The circle of confidence

The applicability of Fisher's method is based on two conditions; the vectors in the analysis must have an axial symmetrical distribution about their mean direction; and the density of the vectors must decrease with increasing angular displacement ψ from the mean direction according to the probability density function:

$$P = \left(\frac{k}{(4 \pi \sinh k)} \right) e^{k \cos \psi}$$

The constant k is called the precision parameter and describes the tightness of a group of vectors about their mean direction. High k values indicate tight groups, while a zero value would indicate vectors uniformly distributed over a unit sphere. The meaning of P is that when an area of dA on a unit sphere at an angular distance ψ from the mean of a series of points, the proportion of points in the area dA is $Pd\psi$.

Fisher shows that the best estimate of the true mean direction of a number of results is the vector sum N of the unit vectors. The sums of the component values of the in-situ vectors are used:

$$X = \sum_{i=1}^n \cos I_i \cos A_i \quad (\text{north component})$$

$$Y = \sum_{i=1}^n \cos I_i \sin A_i \quad (\text{east component})$$

$$Z = \sum_{i=1}^n \sin I_i \quad (\text{downward component})$$

where I = inclination or dip of magnetic vector

A = azimuth of the magnetic vector

$$\text{Length of resultant vector } R = \sqrt{X^2 + Y^2 + Z^2}$$

$$\text{Inclination of resultant vector } I_R = \sin^{-1} \frac{Z}{R}$$

$$\text{Azimuth of resultant vector } A_R = \tan^{-1} \frac{Y}{X}$$

At a probability level of $1 - P$ the true mean direction of the given group of vectors lies within a circular cone about the resultant vector R with a semi-vertical angle $\alpha(1 - p)$ given by Fisher to be

$$\cos \alpha(1 - p) = 1 - \frac{N - R}{R} \left[\frac{(1)}{(P)} \frac{1}{N - 1} - 1 \right]$$

In paleomagnetic analysis the values α_{95} and α_{50} are usually determined. These correspond to a 1 in 20 chance and a 1 in 2 chance that the true mean direction of the vectors lies outside the cone of confidence.

(ii) The oval of confidence

The circle of confidence just discussed occurs is a closed curve around the mean paleomagnetic pole. Because of its occurrence within the geoid, the closed curve is more an oval than a circle.

Given α , the semivertical angle of the circle of confidence, the semi axes δ_p and δ_m of the oval of confidence about the mean geomagnetic pole can be obtained from:

$$\delta_p = \frac{1}{2} (1 + 3 \cos^2 P) \cdot \alpha \qquad \delta_m = \frac{\sin P}{\cos I} \cdot \alpha$$

where P = ancient colatitude of the site

I = mean remanent vector inclination

δ_p = semi axis along the great circle from collecting site
to the paleomagnetic pole

δ_m = at right angles to δ_p

If α is calculated to a probability of 95%, there is a 95% chance that the paleomagnetic pole lies in the oval given by δ_p and δ_m .

Examples of the use of Fisher's statistical methods will be given in the next chapter.

CHAPTER 6

THE POSITION OF THE TRIASSIC MAGNETIC POLE IN SIBERIA

6.1 Motives for the Study

The determination of the magnetic pole for any given period is of value in the assessment of the significance of paleomagnetism with respect to the geological problems discussed in Chapter 2.

The Triassic period has become particularly significant as the initial paleomagnetic studies have become published, for the data have indicated that a separation of 30° has occurred between North America and Europe since the Triassic period. (See Figure 1, Chapter 2).

Paleomagnetic investigations in India by Clegg et al. (1956), and Deutsch et al. (1959), have suggested that India was in southern middle latitudes during the late Cretaceous or early Eocene, and has drifted to its present position since that time. This suggested paleoposition agrees with the Gondwanaland concept of Wegener (1910), which was based on paleogeographic reconstructions.

Thus there exist two motives for determining the Triassic magnetic pole in Siberia. Such a study can aid in answering the question concerning the extent that Asia participated in the northward drift of India; and also the Triassic Pole position in Siberia will be valuable in confirming the available European data, or suggesting whether or not

Asia has moved as a unit with Europe. It would also be possible to suggest an expansion of the earth if the paleomagnetic data between Western Europe and Asia so indicated.

In the summer of 1957, a request for a collection of orientated Triassic basaltic rocks from Siberia was made to Professor V. V. Fedinsky of Moscow, who was then attending the eleventh Assembly of the International Union of Geodesy and Geophysics, in Toronto. The collection was received at the University of Alberta in 1958.

6.2 Location of Samples

The samples were taken from five exposures in the valleys of the Lower Tunguska, Severnaga, and Dudinka Rivers (Figure 8). The locations of the five sites with the number of samples, and the number of specimens are:

<u>Site</u>	<u>Latitude</u>	<u>Longitude</u>	<u>No. of Samples</u>	<u>No. of Specimens</u>
A	60.0° N	89.0° E	8	23
B	69.35° N	88.0° E	7	20
C	66.5° N	90.1° E	6	17
D	66.1° N	89.0° E	6	17
E	66.5° N	89.1° E	5	10

The specimens were numbered as follows:

First letter	(A)	is the sample
Second letter	(A)	is the core from the sample
The figure	(1)	is the specimen from the core

6.3 Geology of the Area

The sampling sites are all situated on the western flank of the Tunguska syncline, which is in the northern part of the Siberian platform.

The samples have been given field identification of gabbro-diabase to diabase, and are from the "trap rock" of the Induan stage, which is the lower part of the Lower Triassic.

The sediments of the Induan stage are zoned on species of the following ammonites: Otoceras, Pachyprotychites, and Paranorites. According to Sachs and Strelkov (1960), on the northern side of the Siberian platform a thick volcanic series is related to the trap series of the western flank of the Tunguska syncline. This volcanic series is dated on phyllopods (Estheria gutta and Estheria aequale) and leaf impressions (Podozamites lanceolatus, Cladophlebia andata, and Retinosporites siberica) in the interbedded sediments.

At the time of writing, efforts to obtain further geological details have been unsuccessful. Additional geological data will be included in the Appendix when such data are available.

6.4 Field Orientation Technique

The field orientation was made with respect to the dipping face of the dykes. Consequently, the samples featured on their surfaces a bearing arrow which represents the dip direction (or strike direction in the case of vertical dykes). The dip and azimuth of this dip or strike arrow with respect to magnetic north, which is also geographic north in the area, were tabulated for each sample.

The samples were cored, and sliced into discs which are the specimens, in Edmonton, during the summer of 1958. They were orientated so that the surface of the specimen is the same as the dipping surface of the intrusive, as in figure 5.

6.5 Measurement of the Magnetic Vector

From the 32 samples, 87 specimens were obtained. The magnetic vector was measured using an astatic magnetometer set up at the University of Alberta Physics Department in Calgary, during the summer of 1960. The method for measuring has been described in Chapter 4. Examples of the determination of the azimuth and dip of the magnetic vector are, using the nomenclature given in Chapter 4.2:

Site, Sample and Specimen	Scale Divisions				$\theta^{\circ} = \tan^{-1} \frac{b_4 - b_2}{b_1 - b_3}$
	b_1	b_2	b_3	b_4	
AA1	-275	-214	-242	-306	250
AA2	-291	-239	-266	-328	254
AA3	-171	- 56	-127	-245	257

A correction was then applied to the azimuth, since the measurement was made with respect to a line diametrically across the specimen and not relative to a chord across the specimen, which marked the bearing direction. (The chord and diametrical line had a common point on the edge of the specimen.) The final azimuths with respect to the bearing line were:

AA1: 280°

AA2: 284°

AA3: 292°

It was then necessary to obtain the azimuth with respect to magnetic north. This was obtained using the original field strike or dip direction data for the sample:

Site, Sample and Specimen	Measured Azimuth°	Bearing Used	Azimuth° of Bearing°	Vector Azimuth° Relative to Magnetic North
AA1	280	Strike	35	315
AA2	284	"	"	324
AA3	292	"	"	327

The dip of the magnetic vector was then measured, using the method given in Chapter 4.3.

Site, Sample and Specimen	Scale Divisions				$D^\circ = \tan^{-1} \frac{d_4 - d_2}{d_1 - d_3}$
	d ₁	d ₂	d ₃	d ₄	
AA1	+136	+101	+ 71	+103	+ 2°
AA2	+139	+108	+ 92	+124	+19°
AA3	+ 85	- 35	-104	+ 11	+14°

The results for all samples giving the azimuth relative to magnetic north, and the dip of the magnetic vector, are shown in Table (i).

TABLE (i)

AZIMUTH AND DIP OF THE MAGNETIC VECTOR
IN EACH SPECIMEN

Site, Sample and Specimen	Measured Azimuth ^o	Bearing Used	Azimuth ^o of Bearing	Vector Azimuth ^o w. r. t. Mag. North	Dip ^o of Measured Vector
AA1	280	S	35	315	+ 2
AA1	284	S	35	324	+19
AA3	292	S	35	327	+14
AB1	334	D	205	179	+45
AB2	352	D	205	197	+50
AB3	336	D	205	181	+44
Ar1	22	D	300	322	+28
Ar2	32	D	300	332	+25
A ^A 1	3	D	265	268	0
A ^A 2	6	D	265	271	+ 3
A ^A 3	9	D	265	274	+15
AX1	9	D	255	264	+69
AX2	356	D	255	251	+53
A ^A 1	260	D	280	180	+77
A ^A 2	indeterminate				
A ^A 3	359	omit because of complete incompatibility			
A ^A 4	16	D	280	296	+89
AH1	220	D	60	80	+73
AH2	13	D	60	73	+54
AH3	354	D	60	54	+40
AO1	37	D	58	95	-23
AO2	10	D	58	68	+25
AO3	6	D	58	64	+14

TABLE (i) -- Continued

Site, Sample and Specimen	Measured Azimuth ^o	Bearing Used	Azimuth ^o of Bearing	Vector Azimuth ^o w. r. t. Mag. North	Dip ^o of Measured Vector
B _U 1	355	D	0	355	+15
B _U 2	32	D	0	32	+ 3
B _U 3	356	D	0	356	0
B _A 1	11	D	130	141	+29
B _A 2	351	D	130	121	-25
B _A 3	340	D	130	110	+16
B _Z 1	29	D	124	153	-16
B _Z 2	6	D	124	130	-15
B _Z 3	17	D	124	141	+25
B _M 1) B _M 2)	omit because of complete incompatibility (possibly unstable)				
BK1	354	D	43	37	+15
BK2	12	D	43	55	0
BK3	353	D	43	36	- 1
BH1	352	D	38	30	+11
BH2	1	D	38	29	-11
BH3	14	D	38	52	-13
BO1	322	D	17	339	-14
BO2	336	D	17	353	+14
B _W 1	332	D	95	67	- 8
B _W 2	345	D	95	80	0
B _W 3	346	D	95	81	-19
C _U 1	217	S	85	302	-79
C _U 2	32	S	85	117	-79
C _U 3	102	S	85	187	-74
Cr1	291	S	75	6	-37
Cr2	291	S	75	6	-29
Cr3	284	S	75	359	-20
Cz1	57	S	35	92	+22
Cz2	57	S	35	92	+ 3
Cz3	298	omit because of marking ambiguity			

TABLE (i) -- Continued

Site, Sample and Specimen	Measured Azimuth ^o	Bearing Used	Azimuth ^o of Bearing	Vector Azimuth ^o w. r. t. Mag. North	Dip ^o of Measured Vector
C^1	4	D	0	4	-22
C^2	351	D	0	351	-46
CO1	355	S	345	340	+26
CO2	351	S	345	336	+16
CO3	347	S	345	332	+22
Cn1	238	S	70	308	-77
Cn2	247	S	70	317	-75
Cn3	241	S	70	311	-66
DA1	20	D	248	268	+72
DA2	20	D	248	268	+77
DA3	14	D	248	262	+68
DB1	354	D	42	36	-10
DX1	343	D	88	71	-14
DX2	341	D	88	69	-17
DX3	329	D	88	57	-16
Dn1	321	D	185	146	+39
Dn2	specimen lost				
Dn3	328	D	185	153	+33
D^1	70	S	60	130	-13
D^2	72	S	60	132	-12
D^3	72	S	60	132	-7
DM1	350	D	75	65	-22
DM2	omit because of complete incompatibility				
DM3	340	D	75	55	-9
DM4	38	D	75	113	-31
E^1	282	S	15	297	-13
E^2	274	S	15	289	+9
Er1	16	D	157	173	+1
E^1	19	D	227	246	0
Ez1	262	S	308	210	+21
Ez2	266	S	308	214	+4
Ez3	268	S	308	216	+2

TABLE (i) -- Continued

Site, Sample and Specimen	Measured Azimuth ^o	Bearing Used	Azimuth ^o of Bearing	Vector Azimuth ^o w. r. t. Mag. North	Dip ^o of Measured Vector
EO1	262	S	342	244	+ 8
EO2	262	S	342	244	+ 3
EO3	273	S	342	255	+ 9

Measured Azimuth: refers to the azimuth of the magnetic vector
in the specimen

Bearing Used: S^o = Strike, D^o = Dip Direction.

Strike is used only when the geological dip of
the sample is 90^o

Azimuth Bearing: This is measured clockwise from magnetic
north.

6.6 Correction for Geological Dip

It has been shown in Chapter 5.1 how the correction for geological tilt of the sample is applied to convert the measured dip and azimuth, with respect to magnetic north, into the in-situ magnetic vector. Examples of this correction are given below in Table (ii).

TABLE (ii)

EXAMPLE OF THE CORRECTION FOR GEOLOGICAL DIP

	Sample Numbers		
	AA1	AA2	AA3
T. D. ° = Tilt (Dip) Direction	305	305	305
S° = Strike Direction	215	215	215
A ¹ = Uncorrected Azimuth of Magnetic Vector	315	324	327
ϕ = Azimuth in New Coords. ($\phi = A^1 - S^\circ$)	100	109	112
cos ϕ	-0.1736	-0.3256	-0.3746
sin ϕ	+0.9848	+0.9455	+0.9272
D° = Uncorrected dip of Magnetic Vector	+ 2	+19	+14
cos D°	+0.9994	+0.9455	+0.9703
X ₁ = cos ϕ cos D	-0.1735	-0.308	-0.364
Y ₁ = sin ϕ cos D	+0.9842	+0.8950	+0.9000
Z ₁ = sin D	+0.0349	+0.3256	+0.2419
Z ₁ /Y ₁	+0.0355	+0.3620	+0.2690
d° = tan ⁻¹ Z ₁ /Y ₁	+ 2	+20	+15
cos d	+0.9994	+0.9400	+0.9660
sin d	+0.0349	+0.3420	+0.2590
T° = tilt (dip) of body = tilt of bearing line	+90	+90	+90
(d + T)°	+92	+110	+105
cos (d + T)	-0.0349	-0.342	-0.259
sin (d + T)	+0.9994	+0.940	+0.966

TABLE (ii)--Continued

		Sample Numbers		
		AA1	AA2	AA3
m	$= \frac{\cos (d + T)}{\cos d}$	-0.0349	-0.364	-0.277
n	$= \frac{\sin (d + T)}{\cos d}$	+28.64	+2.75	+3.73
X ₂	= X ₁	-0.1735	-0.308	-0.364
Y ₂	= mY ₁	-0.0343	-0.336	-0.249
Z ₂	= nZ ₁	+0.995	+0.895	+0.905
Y ₂ /X ₂		+0.1977	+1.09	+0.685
A ₁ ⁰	= tan ⁻¹ Y ₂ /X ₂	191	227	214
X ₂ ²		+0.0301	+0.0950	+0.1330
Y ₂ ²		+0.0012	+0.1130	+0.0620
(X ₂ ² + Y ₂ ²)		+0.0313	+0.2080	+0.1950
(X ₂ ² + Y ₂ ²) ^{$\frac{1}{2}$}		+0.1769	+0.4501	+0.4416
P	$= \frac{Z_2}{(X_2^2 + Y_2^2)^{\frac{1}{2}}}$	+5.6506	+1.962	+2.049

Finally:

tan ⁻¹ P = D ₁ ⁰ = In-situ Dip of Magnetic Vector	+80	+63	+64
A ₁ ¹ ⁰ = In-situ Azimuth of Magnetic Vector = A ₁ +S	+46	+82	+69

Thus the in-situ dip and azimuth, with respect to magnetic and geographic north, of the magnetic vector are obtained for three specimens from one sample. This was carried out for all the specimens; the results are given below in Table (iii).

TABLE (iii)

IN-SITU AZIMUTH AND DIP OF THE MAGNETIC VECTOR

(Corrected for Geological Dip)

Site, Sample and Specimen	Azimuth A°	Dip D°
AA1	46	+80
AA2	82	+63
AA3	69	+64
AB1	87	+69
AB2	48	+77
AB3	88	+71
Ar1	60	+70
Ar2	46	+60
AA1	273	+69
AA2	284	+71
AA3	321	+80
AX1	69	+56
AX2	83	+72
A\1	238	+70
A\2	100	+87
A\3	omit; measurements incompatible	
A\4	99	+79
AH1	204	+80
AH2	95	+74
AH3	50	+64
AO1	96	+24
AO2	109	+78
AO3	76	+71

TABLE (iii) -- Continued

Site, Sample and Specimen	Azimuth A°	Dip D°
B \bar{C} 1	225	+83
B \bar{C} 2	80	+54
B \bar{C} 3	338	+79
B \bar{A} 1	242	+80
B \bar{A} 2	119	+40
B \bar{A} 3	62	+69
Bz1	162	+41
Bz2	133	+50
Bz3	218	+75
BK1	313	+84
BK2	82	+71
BK3	67	+73
BH1	10	+73
BH2	40	+53
BH3	59	+50
BO1	325	+40
BO2	268	+67
B \bar{n} 1	49	+48
B \bar{n} 2	59	+64
B \bar{n} 3	76	+48
C \bar{A} 1	10	+68
C \bar{A} 2	351	+44
CO1	11	+ 4
CO2	1	+ 9
CO3	8	+12
C \bar{n} 1	333	+11
C \bar{n} 2	334	+14
C \bar{n} 3	328	+20
C \bar{C} 1	346	+ 7
C \bar{C} 2	5	- 6
C \bar{C} 3	352	-16
Cr1	10	+48
Cr2	18	+54
Cr3	19	+67

TABLE (iii) -- Continued

Site, Sample and Specimen	Azimuth A ^o	Dip D ^o
Cz 1	358	+51
Cz 2	29	+54
Cz 3	omit; measurements incompatible	
DA 1	58	+53
DA 2	62	+48
DA 3	58	+56
DB 1	29	+63
DX 1	55	+58
DX 2	55	+55
DX 3	39	+49
DM 1	68	+67
DM 2	Specimen lost	
DM 3	79	+63
DA 1	94	+66
DA 2	45	+68
DA 3	80	+72
DM 1	51	+66
DM 2	omit; measurements incompatible	
DM 3	8	+70
DM 4	121	+43
EU 1	328	+73
EU 2	81	+80
Er 1	250	+75
EA 1	317	+71
Ez 1	58	+68
Ez 2	83	+84
Ez 3	83	+87
EO 1	117	+79
EO 2	142	+82
EO 3	270	+81

6.7 Representing the Results

All the above in-situ magnetic vectors have been plotted on a polar equal-area stereographic projection (Figure 7). This represents the results for all 83 specimens cut from 32 samples.

The mean direction for all samples is derived in part 10 of this chapter.

6.8 Computing the Mean Azimuth and Dip for Samples out of Specimens

It has been shown in Chapter 5.2 how the mean azimuth and dip of the in-situ magnetic vector can be calculated for the samples, from the data for specimens.

An example of the computation of the mean azimuth and dip for one sample, involving three specimens, is given in Table (iv).

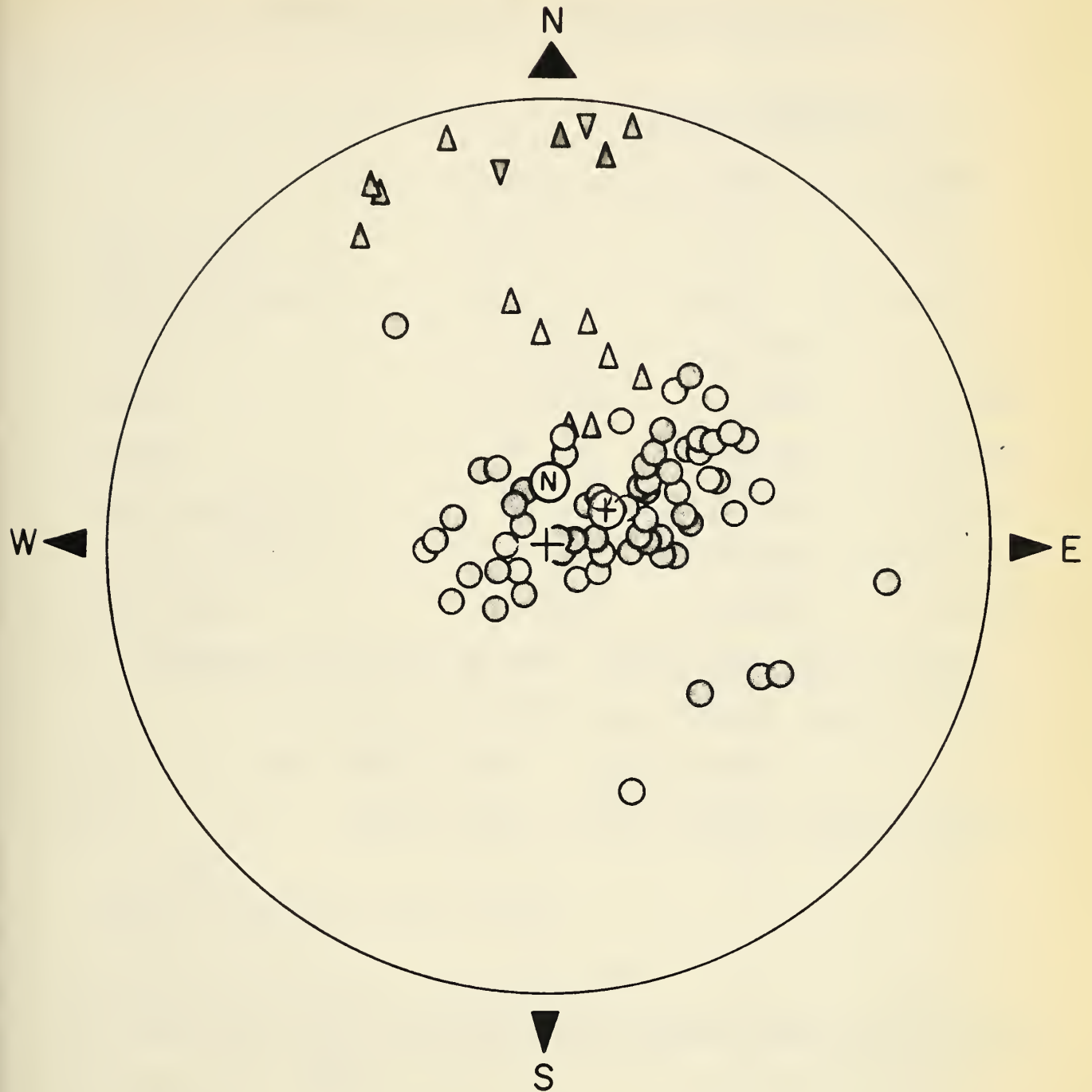


Fig. 7

POLAR EQUAL-AREA PLOT OF THE REMANENT MAGNETIZATION VECTOR

- ▲ Results for site C. North pole down
- ▼ Results for site C. North pole up
- All other sites North pole down
- ⊕ Mean direction for all samples, omitting site C.
- ⊙ Theoretical dipole field at mean sampling site

TABLE (iv)

EXAMPLE OF THE DETERMINATION OF THE MEAN AZIMUTH
AND DIP FOR A SAMPLE FROM THREE SPECIMENS

	SAMPLE NUMBERS		
	AA1	AA2	AA3
$A^\circ = \text{In-situ}$	46	82	69
$D^\circ = \text{In-situ Dip}$	+80	+63	+64
$\cos A^\circ$	+0.6947	+0.1392	+0.3584
$\sin A^\circ$	+0.7193	+0.9903	+0.9336
$\cos D^\circ$	+0.1736	+0.4540	+0.4384
$X_2 = \cos A \cos D$	+0.1206	+0.0632	+0.1571
$Y_2 = \sin A \cos D$	+0.1249	+0.4496	+0.4093
$Z_2 = \sin D$	+0.9848	+0.8910	+0.8988

$$\text{For Sample AA: } \sum X_2 = +0.3409 \quad \sum Y_2 = +0.9838 \quad \sum Z_2 = +2.7746$$

$$\text{and } X_{2av} = +0.1136 \quad Y_{2av} = +0.3279 \quad Z_{2av} = 0.9249$$

$$\text{Now } X_2^2_{av} = 0.129 \quad Y_2^2_{av} = 0.1075$$

$$X_2^2_{av} + Y_2^2_{av} = 0.1204. \quad (X_2^2_{av} + Y_2^2_{av})^{\frac{1}{2}} = 0.3470$$

$$\frac{Z_{2av}}{(X_2^2_{av} + Y_2^2_{av})^{\frac{1}{2}}} = 2.6654 = \tan \bar{D}$$

$$\text{Mean Dip of Magnetic Vector} = \bar{D} = +69^\circ$$

$$\text{and } \bar{A} = \tan^{-1} \frac{Y_{2av}}{X_{2av}} = \text{mean azimuth of magnetic vector} = \tan^{-1} 2.8864$$

$$\bar{A} = 71^\circ$$

Thus the mean azimuth and dip for each of 32 samples was calculated. The complete results are given below in Table (v).

TABLE (v)

MEAN AZIMUTH AND DIP OF MAGNETIC VECTOR IN SAMPLES

Site	Sample	No. of Specimens	A° = Mean Azimuth	D° = Mean Dip
A	A	3	71	+69
A	B	3	78	+73
A	r	2	49	+66
A	A	3	287	+74
A	X	2	74	+64
A	λ	3	193	+86
A	H	3	80	+79
A	O	3	39	+59
B	B	3	65	+81°
B	A	3	109	+71°
B	λ	3	158	+58°
B	K	3	66	+79°
B	H	3	42	+60°
B	O	2	306	+57°
B	π	3	62	+54°
C	B	3	354	- 5
C	r	3	15	+56
C	λ	2	13	+54
C	λ	2	354	+56
C	O	3	7	+ 8
C	π	3	332	+15
D	A	3	59	+52
D	B	1	29	+63
D	X	3	49	+54
D	λ	2	73	+60
D	λ	3	90	+69
D	M	3	78	+68
E	B	2	3	+82
E	r	1	250	+75
E	A	1	317	+71
E	z	3	65	+80
E	O	3	153	+86

6.9 Computing the Mean Azimuth and Dip for Sites out of Samples

It was shown in Chapter 5.2 how the mean azimuth and dip of the magnetic vector of a site could be computed, using the average of the added components of the samples.

An example, (for the A site) is given in Table (vi).

TABLE (vi)

EXAMPLE OF THE DETERMINATION OF MEAN AZIMUTH AND
DIP FOR A SITE FROM SAMPLES

Sample No.	Mean Coordinates		
	X_{3av}	Y_{3av}	Z_{3av}
AA	+0.1136	+0.3279	+0.9249
AB	+0.0602	+0.2835	+0.9512
Ar	+0.2592	+0.3030	+0.9027
AA	+0.0775	-0.2610	+0.9546
AX	+0.1191	+0.4144	+0.8901
Aλ	+0.0734	-0.0167	+0.9733
AH	-0.0331	-0.1799	-0.9483
AO	-0.0281	+0.4737	+0.7768

Therefore for site A: $\sum X_3 = +0.5612$ $\sum Y_3 = +1.7047$ $\sum Z_3 = +7.3221$

$$X_{3av} = +0.0702 \quad Y_{3av} = +0.2131 \quad Z_{3av} = +0.9153$$

$$X_{3av}^2 = +0.0049 \quad Y_{3av}^2 = +0.0454$$

$$X_{3av}^2 + Y_{3av}^2 = +0.503 \quad (X_{3av}^2 + Y_{3av}^2)^{\frac{1}{2}} = +0.2243$$

$$\text{Mean Dip} = \overline{D} = \tan^{-1} \frac{Z_{3av}}{(X_{3av}^2 + Y_{3av}^2)^{\frac{1}{2}}} = \tan^{-1} 4.0807$$

Mean Dip of the Magnetic Vector for a site, out of samples: $\overline{D} = 76.2^\circ$

$$\text{Mean Azimuth} = \overline{A} = \tan^{-1} \frac{Y_{3av}}{X_{3av}} = \tan^{-1} 3.0356$$

Mean Azimuth of the Magnetic Vector for a site, out of samples: $\overline{A} = 71.8^\circ$

The mean azimuth and dips of the magnetic vectors for the other sites are similarly determined. The results are given below in Table (vii).

TABLE (vii)

MEAN AZIMUTH AND DIP OF THE MAGNETIC VECTOR
FOR EACH SITE

Site	No. of Samples	Mean Coordinates		
		X_{3av}	Y_{3av}	Z_{3av}
A	8	+0.0702	+0.2131	+0.9153
B	7	+0.0765	+0.1708	+0.9153
C	6	+0.7397	-0.0362	+0.8514
D	6	+0.2172	+0.3918	+0.8549
E	5	+0.0589	-0.0532	+0.9684

Site	Mean in-situ Azimuth of Magnetic Vector	Mean in-situ Dip of Magnetic Vector
A	71.8°	+76.2°
B	65.9°	+77.6°
C	357.2°	+31.7°
D	61.0°	+62.3°
E	317.9°	+85.3°

6.10 Computing the Mean Azimuth and Dip for the Area out of Sites

It can be seen from Figure 7 that selectivity must be applied to get the best mean azimuth and dip of the magnetic vector for the entire study, based on the mean azimuth and dip for the sites.

With few exceptions, the vector extremities of the specimens from sites A, B, D and E form part of a dense central cluster in Figure 7. In contrast, the points representing the results from site C seem anomalous. The scatter in site C exceeds that for any other site. Thus the results were considered unreliable, and rejected.

The mean declination and azimuth for the area was determined as follows:

Sites	No. of Specimens	$\sum \sum X_4 =$	$\sum \sum Y_4 =$	$\sum \sum Z_4 =$
A, B, D & E	26	+2.6943	+4.9850	+23.2529

Sites	X_{4av}	Y_{4av}	Z_{4av}
A, B, D & E	+0.10362	+0.19173	+0.89434

$$X_{4av}^2 = +0.01074 \quad Y_{4av}^2 = +0.03676$$

$$X_{4av}^2 + Y_{4av}^2 = +0.04750 \quad (X_{4av}^2 + Y_{4av}^2)^{\frac{1}{2}} = +0.21795$$

$$\frac{Z_{4av}}{(X_{4av}^2 + Y_{4av}^2)^{\frac{1}{2}}} = + 4.1034 = \tan \text{ dip}$$

$$\underline{\underline{\text{Mean Dip} = + 76.30^{\circ}}} \quad \text{and}$$

$$\frac{Y_{4av}}{X_{4av}} = 1.8503 = \tan \text{ Azimuth}$$

$$\underline{\underline{\text{Mean Azimuth} = 61.61^{\circ}}}$$

Thus the mean azimuth and dip of the in-situ magnetic vector for the area can be determined from the sites.

6.11 Obtaining the Paleomagnetic Pole

It has been shown in chapter 5.3 how the paleomagnetic pole is obtained from the magnetic vector measurements. The ancient pole was obtained for all sites, and for the area as a whole using the following equation:

$$\cos a = \cos C \cos p + \sin C \sin p \cos A$$

$$\sin (b - d) = \frac{\sin p \sin A}{\sin a}$$

$$\cot p = 1/2 \tan D \text{ where}$$

D = dip of vector

A = azimuth of vector

a = colatitude of ancient pole

b = longitude of ancient pole (East is +; West is -)

c = colatitude of site

d = longitude of site

p = angular distance from site to ancient pole

The following information was used:

Site	A° = Mean Azimuth of Vector	D° = Mean Dip of Vector	C° = Colatitude of Site	d° Longitude of Site
A	71.8	+76.2	24.42	89.02
B	65.9	+77.6	20.83	88.00
C	357.2	+31.7	23.71	90.07
D	61.0	+62.3	23.94	88.59
E	317.9	+85.3	23.72	89.05
A, B, D&E	61.6	+76.3	23.21	88.65

Determination of p:

Site	$\tan D$	$p^0 = \cot^{-1} \frac{1}{2} \tan D$
A	+2.0404	+26.1
B	+2.2728	+23.7
C	+0.3090	+72.8
D	+0.9542	+46.3
E	+6.0980	+ 9.3
A, B, D&E	+2.0517	+25.98

The paleomagnetic pole can then be determined. The details of the determination of the pole position for the group of sites A, B, D & E, and for site A separately, are given in Table (viii).

TABLE (viii)

DETERMINATION OF THE PALEOMAGNETIC POLE
FOR THE FOUR SITES A, B, D AND E; AND FOR SITE A

	A, B, D & E	A
p°	+25.98	+26.1
C°	+23.21	+24.4
$\cos p^{\circ}$	+ 0.8990	+ 0.8980
$\cos C^{\circ}$	+ 0.9190	+ 0.9170
$\cos C \cos p = m$	+ 0.8262	+ 0.8178
$\sin p^{\circ}$	+ 0.4381	+ 0.4399
$\sin C^{\circ}$	+ 0.3942	+ 0.4131
A°	61.6	71.8
$\cos A$	+ 0.4754	+ 0.3123
$\sin p \sin C = n$	+ 0.1727	+ 0.1817
$n \cos A = Q$	+ 0.0567	+ 0.0821
$m + Q = \cos a$	+ 0.9083	+ 0.8745
a° (colatitude of ancient pole)	+24.73	+29.0
$\sin a$	+ 0.4184	+ 0.4848
$\sin (b - d) = \frac{\sin p \sin A}{\sin a}$	+ 0.9210	+ 0.8620
$b - d$	+67.07	+59.5
d°	+88.65	+89.0
b° (<u>Longitude of ancient pole</u>)	<u>155.72°E</u>	<u>148.5°E</u>
$90^{\circ} - a^{\circ}$ (<u>Latitude of ancient pole</u>)	<u>65.27°N</u>	<u>61.0°N</u>

The results for all the collecting sites and for the group of sites are:

Site	Longitude	Latitude
A	148.5°E	61.0°N
B	152.9°E	66.1°N
C	86.6°E	40.9°N
D	175.7°E	50.7°N
E	68.4°E	72.2°N
A, B, D & E	155.7°E	65.3°N

The result of the study is represented by the pole position for the group of sites at 155.7° East and 65.3° North in Figure 8 and 9 (pole 1). The result is also given in Figure 7 as the \oplus symbol.

6.12 Determining the Circle of Confidence

In Chapter 5.4, the significance of the circle of confidence was explained. The semi-vertical angle of a circular cone about the resultant vector R is given by:

$$\cos \alpha_{(1-p)} = 1 - \frac{(N - R)}{N} \left[\left(\frac{1}{p} \right) \frac{1}{N - 1} - 1 \right] \quad \text{See Chapter 5.4 for the explanation of this equation.}$$

The details of the determination of the circle of confidence for site A, and the group of sites A, B, D and E at a probability level of 95% are given in Table (ix). The details of the determination of the circle of confidence for the group of sites is also given for a probability level of 50%.

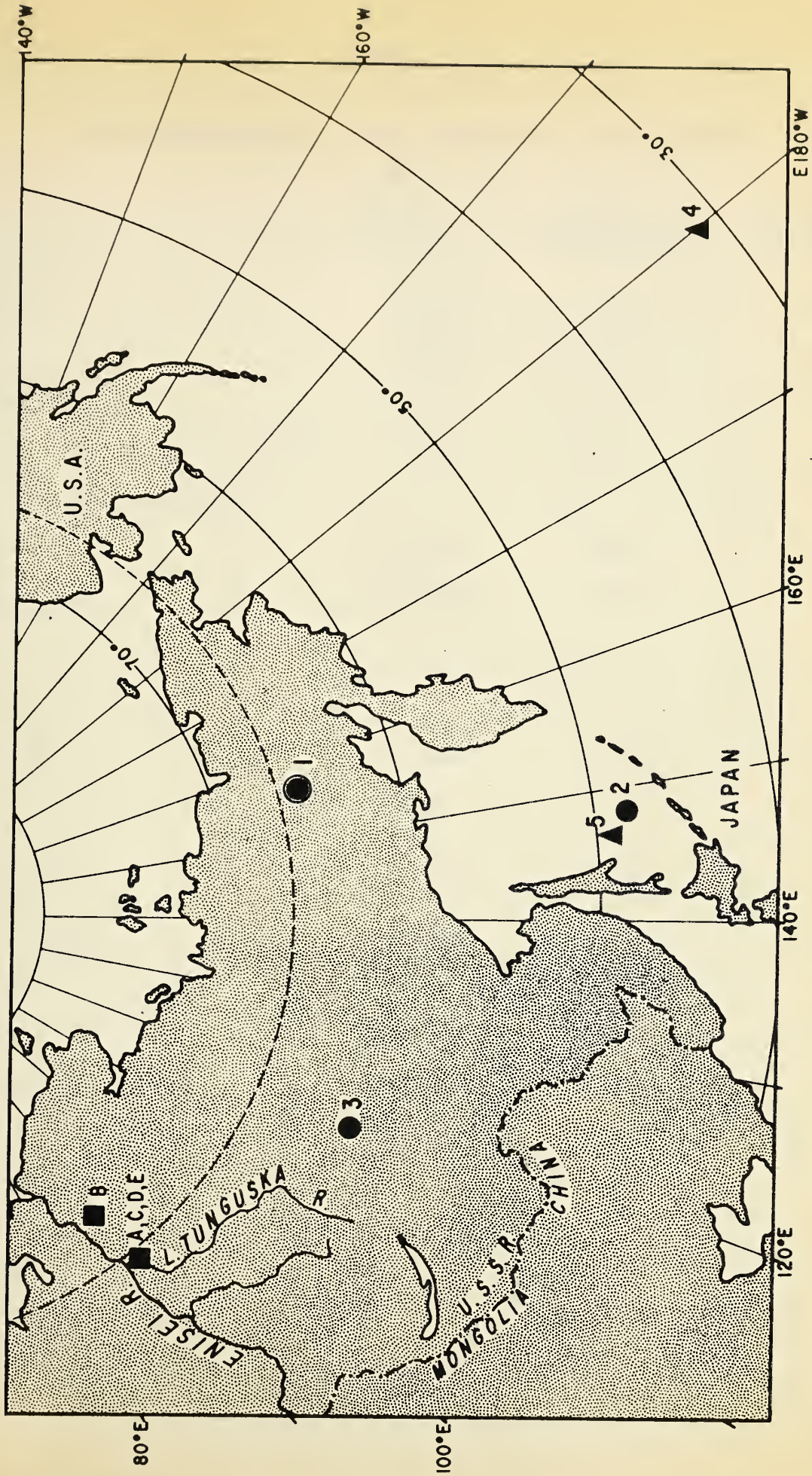


Fig. 8 LOCATION OF THE NORTH POLE WITH RESPECT TO SIBERIA AND EUROPE FROM PALEOMAGNETIC MEASUREMENTS ON TRIASSIC ROCKS

- 1 : pole determined in this thesis
- 2 : Motarova (1960)
- 3 : Fineberg and Dashkevitch (1959)
- 4 : Khromov (1959)
- 5 : Nalrn (1960)

A, B, C, D, E are the sampling sites for this study

TABLE (ix)

DETERMINATION OF THE CIRCLES OF CONFIDENCE

	α_{45} for A	α_{45} for A, B, D & E	α_{50} for A, B, D & E
$\sum X_3^2$	0.315	7.259	7.259
$\sum Y_3^2$	2.906	24.850	24.850
$\sum Z_3^2$	53.613	540.806	540.806
$R = (X_3^2 + Y_3^2 + Z_3^2)^{\frac{1}{2}}$	7.539	23.934	23.934
N (No. of Specimens)	8	26	26
N - R	0.461	2.066	2.066
$\frac{N - R}{R} = F$	0.0612	0.0863	0.0863
N - 1	7	25	25
$\frac{1}{N - 1}$	0.1429	0.0400	0.0400
p	0.05	0.05	0.50
$\left(\frac{1}{p}\right)^{\frac{1}{N - 1}}$	1.5343	1.1273	1.0281
$\left(\frac{1}{p}\right)^{\frac{1}{N - 1}} - 1 = G$	0.5343	0.1273	0.0281
F. G.	0.03270	0.01099	0.00243
$1 - F. G. = \cos \alpha$	0.96730	0.98901	0.99757
α°	14.7°	8.50°	4.00°

The complete results for the oval of confidence are:

	<u>α_{95}</u>	<u>α_{50}</u>
A	14.7°	--
B	25.22°	--
C	28.62°	--
D	13.96°	--
E	14.65°	--
A, B, C & E	8.50°	4.00°

From these values, the oval of confidence is determined.

6.13 Determining the Oval of Confidence

The significance of the oval of confidence and the details of the equation which is used to determine the oval of confidence are given in Chapter 5.4.

Determining δ_p from $\delta_p = \frac{1}{2}\alpha(1 - 3 \cos^2 p)$

	<u>$\alpha_{50} \quad N = 26$</u>	<u>$\alpha_{95} \quad N = 26$</u>
p°	25.98	25.98
$3 \cos^2 p$	2.4237	2.4237
$1 + 3 \cos^2 p$	3.4237	3.4237
α°	4.00	8.50
$\alpha(1 + 3 \cos^2 p)$	13.695	29.10
$\frac{1}{2}\alpha(1 + 3 \cos^2 p) = \delta_p$	6.85°	14.55°

Determining δ_m from $\delta_m = \frac{\sin p \cdot \alpha}{\cos D}$

	<u>$\alpha_{50, N} = 26$</u>	<u>$\alpha_{95N} = 26$</u>
p	25.98	25.98
log sin p	1.6416	1.6416
D	+76.30	+76.30
log cos D	1.3745	1.3745
α	4.00	8.00
log α	0.6021	0.9294
$\delta_m = \frac{\sin p \cdot \alpha}{\cos D}$	7.40°	15.72°

Thus the final values for the oval of confidence were:

- (i) for α_{50} , $\delta_p = 6.85^\circ$ (ii) for α_{95} , $\delta_p = 14.55^\circ$
 $\delta_m = 7.40^\circ$ $\delta_m = 15.72^\circ$

6.14 Plotting the Oval of Confidence

It has been determined that:

- (i) δ_p , the semi axis of the oval of confidence along the great circle from the collecting site to the paleomagnetic pole is 6.85° for a circle of confidence of 50%, and 14.55° for a circle of confidence of 95%.
- (ii) δ_m , the semi axis of the oval of confidence at right angles of δ_p is 7.40° for a circle of confidence of 50%, and 15.72° for a circle of confidence of 95%.

By using a stereogram, the latitude and longitude of the end points of these axes can be determined. They are:

$$\begin{aligned}\delta_m: \quad m_1 &= 75.7^\circ \text{ N}; \quad 168.5^\circ \text{ W} \\ m_2 &= 51.0^\circ \text{ N}; \quad 142.0^\circ \text{ E} \\ \delta_p: \quad p_1 &= 69.7^\circ \text{ N}; \quad 118.9^\circ \text{ W} \\ p_2 &= 55.1^\circ \text{ N}; \quad 176.3^\circ \text{ E}\end{aligned}$$

The oval of confidence was then plotted on Figure 9.

6.15 Significance of the Result

The paleomagnetic pole position for the Triassic in Siberia has been plotted in Figures 8 (pole I), and 9. The oval of confidence is plotted in Figure 9.

In Figure 8, results of other Triassic studies are plotted. A study in the same area by Makerova (1960) is the source of pole number 2. Triassic intrusives were also studied by Fineberg and Dashkevitch (1959) to determine pole number 3. Paleomagnetic information unlocked from Triassic sedimentary exposures in Europe has yielded pole number 4 (Khramov (1958) relative to Russia, and pole number 5 is an average quoted by Nairn (1960) from British, German and French data by different authors.

In Figure 9, the smoothed polar path from Cambrian to recent times relative to Europe is indicated. The result of the study by the author is indicated. The oval of confidence is given for the result, together with the oval of confidence for the work by Makerova.

North American Triassic pole positions are given as pole numbers 6, 7, 8 and 9 in Figure 9. The first three pole positions differ markedly from the result of the study described in this thesis. These pole positions, of course, conform to the North American polar wandering



Fig. 9

LOCATION OF THE NORTH POLE ESTIMATED FROM MEASUREMENTS ON TRIASSIC ROCKS

Symbols indicate polar plates with respect to :

- Siberia
- ▼ North America
- Africa
- ★ Australia

Numbers indicate source material:

1. Pale measured for this thesis
2. Siberian Triassic by Mokerova (1960)
3. Siberian Triassic, Fineberg & Dashkevitch (1959)
4. Connecticut Lavas, Dubois et al (1957)
5. Springdale Sandstone, Runcorn (1956)
6. Brunswickian Sediments, Dubois et al (1957)
7. New Oxford Sediments, Graham (1955)
8. Bechuanaland Cove Sandstone, Nairn (1957)
9. Brisbane Tuff, Irving & Green (1958)
10. Bechuanaland Cove Sandstone, Nairn (1957)
11. Brisbane Tuff, Irving & Green (1958)

The solid line is a polar path relative to Europe, typical of versions published by authors.

curve of Figure 1.

The resulting pole position conforms within the limits of the oval to the smoothed polar curve for Europe. This is not surprising, for it seems likely that in executing any movements inferred from this curve and the North American curve (Figure 1), Europe and Northern Asia would have acted as one unit; and so barring major change in the earth's radius, any two contemporary poles from Europe and Siberia should coincide.

The Triassic pole positions numbers 10 and 11 are for Africa and Australia respectively. It has already been discussed in Chapter 2 how very great relative displacements of these southern continents are needed to conform to a unique pole position.

The Indian data for the late Mesozoic suggests a large displacement for India relative to Siberia and Europe. It is not possible to suggest the Triassic position of India relative to Asia until Indian Triassic results are obtained. If India did in fact drift to its present position from southern latitudes, it appears from the Siberian Triassic pole position that Northern Asia did not participate in the drift northwards. The great Himalayan area might be the demarcation between the relatively stable Eurasian mass and the mobile Indian peninsula. As has been stated, lower Mesozoic Indian pole studies might aid in the resolving of this anomalous paleomagnetic situation.

6.16 The Intensity of Magnetization

It is usual in paleomagnetic studies to give the intensity of magnetization of the rocks used. This parameter is of no significance

in the determination of the paleomagnetic pole position, but is useful should the induced intensity be compared to the remanent intensity (Chapter 7), which would give an index of stability of the remanent magnetism. In analysis of local magnetic anomalies, the intensity of remanent magnetization is of paramount importance.

In Chapter 4.4 the equation for the determination of the intensity of magnetization was given:

$$J = \frac{1}{S.A.} \left[\frac{D}{t \cos \delta \left\{ \frac{Z_L^2 - t^2}{4} \right\}^2 + \frac{Z_u^2 - t^2}{4} \right]} \right] \text{ e.m.u/cc.}$$

where

- S = sensitivity of the instrument in millimetres per oersted
- t = thickness of the specimen in cms.
- A = cross sectional area of the specimen in cm^2
- Z_L = distance from the centre of the specimen to the centre of the lower astatic magnet
- Z_u = the corresponding distance to the upper astatic magnet
- D = deflection produced on a scale at a certain distance from the mirror

It was shown in Chapter 3.3 (iii) how the apparatus was calibrated at a reciprocal sensitivity of 1.214×10^{-6} oersted/s.d. The scale used in the optical part of the apparatus featured scale divisions at a spacing so that 1 millimetre = 1.61 s.d. Thus the reciprocal sensitivity is

1.956×10^{-6} oersted/mm; or the sensitivity is 5.11×10^5 mm/oersted.

As was stated in Chapter 3.3, a standard specimen was used, and the apparatus was calibrated frequently during use. It was found that the sensitivity varied from day to day. This was probably due to variation of the ambient field.

An example to the calculation of the intensity of magnetization is given below, for the AA specimens, in Table (x).

TABLE (x)
EXAMPLE OF THE DETERMINATION
OF THE INTENSITY OF MAGNETIZATION

	AA1	AA2	AA3
Z_{Lcms}	5.8	5.8	5.8
Z_L^2	33.64	33.64	33.64
$t cms$	0.543	0.558	0.648
$\frac{t^2}{4}$	0.07	0.08	0.68
$Z_L^2 - \frac{t^2}{4}$	33.57	33.56	32.96
$(Z_L^2 - \frac{t^2}{4})^2$	1127	1126	1086
$\frac{Z_L}{(Z_L^2 - \frac{t^2}{4})^2} = F$	0.00515	0.00515	0.00534
$Z cms$	10.9	10.9	10.9
Z^2	118.81	118.81	118.81
$Z^2 - \frac{t^2}{4}$	118.74	118.73	118.13
$(Z^2 - \frac{t^2}{4})^2$	14100	14100	13600
$\frac{Z}{(Z^2 - \frac{t^2}{4})^2} = G$	0.00077	0.00077	0.00080
$(F - G) cms.$	0.00438	0.00438	0.00454

TABLE (x)--Continued

	AA1	AA2	AA3
cos D	-1.000	-0.946	-0.970
t cos D	0.543	0.528	1.599
(F - G), t cos D, cms. ⁻² = K	0.002378	0.002313	0.007259
4 D units	64.5	47	189.5
$\frac{4 D \text{ units cms.}^2}{K}$	27, 120	20, 320	26, 110
$\frac{1}{4} \frac{(1)}{S.A.} \text{ oersted/units.cm}^2$	5.782×10^{-8}	5.782×10^{-8}	4.482×10^{-8}
$\frac{D}{(S.A.) K} = I (\times 10^{-3} \text{ c. g. s.})$	<u>1.57</u>	<u>1.17</u>	<u>1.17</u>

Thus the intensity of magnetization can be determined. The results for all specimens are given below in Table (xi).

TABLE (xi)

INTENSITY OF MAGNETIZATION FOR ALL SPECIMENS

Area, Sample and Specimen	Intensity of Magnetization $I \times 10^{-3}$ c. g. s.	Area, Sample and Specimen	Intensity of Magnetization $I \times 10^{-3}$ c. g. s.
AA1	1.57	BA1	-
AA2	1.17	BA2	-
AA3	1.17	BA3	0.65
AB1	2.19	BZ1	0.66
AB2	2.48	BZ2	0.58
AB3	2.34	BZ3	1.35
Ar1	0.99	BK1	2.47
Ar2	1.25	BK2	2.82
		BK3	2.70
AM1	1.58	BH1	1.77
AM2	3.97	BH2	2.40
AM3	0.80	BH3	3.65
AX1	0.80	BO1	1.20
AX2	0.95	BO2	-
AX1	0.71	B71	1.07
AX2	0.74	B72	1.71
AX3	-	B73	1.45
AX4	0.93		
AH1	0.74	CA1	2.10
AH2	1.28	CA2	0.60
AH3	1.10		
AO1	1.12	CO1	8.70
AO2	0.77	CO2	9.01
AO3	0.46	CO3	15.36
BE1	1.79	C71	2.47
BE2	2.08	C72	0.90
BE3	2.06	C73	-
DA1	3.59	DM1	2.11
DA2	3.01	DM2	-
DA3	-	DM3	8.77
		DM4	3.97

TABLE (xi) -- Continued

Area, Sample and Specimen	Intensity of Magnetization $I \times 10^{-3}$ c. g. s.	Area, Sample and Specimen	Intensity of Magnetization $I \times 10^{-3}$ c. g. s.
DB1	2.26	E Γ 1	0.14
		E Γ 2	0.82
DX1	3.67		
DX2	3.90	Er1	0.83
DX3	2.70		
		E Δ 1	0.99
D ∇ 1	2.79		
D ∇ 2	-	Ez1	1.91
D ∇ 3	3.06	Ez2	0.35
		Ez3	1.65
D Δ 1	4.04		
D Δ 2	4.05	EO1	2.41
D Δ 3	4.18	EO2	2.11
		EO3	2.18

From five sites and thirty-two samples, eighty-three specimens were used. Values for the intensity of Magnetization were obtained for 77 specimens.

The intensities of magnetization of the specimens were then averaged for each sample. The results are given in Table (xii).

TABLE (xii)

INTENSITY OF MAGNETIZATION FOR THE SAMPLES

Area	Sample	No. of Specimen Averaged	Intensity of Magnetization $I \times 10^{-3}$ c. g. s.
A	A	3	1.30
A	B	3	2.34
A	r	2	1.12
A	A	3	2.12
A	X	2	0.88
A	λ	3	0.76
A	H	3	1.04
A	O	3	0.78
B	G	3	1.98
B	A	3	0.65
B	z	3	0.86
B	K	3	2.66
B	H	3	2.61
B	O	2	1.20
B	π	3	1.41
C	G	3	2.47
C	r	3	3.43
C	z	2	2.54
C	π	2	1.35
C	O	3	11.02
C	π	3	1.68
D	a	3	3.30
D	B	1	2.26
D	X	3	3.42
D	N	2	2.93
D	λ	3	4.09
D	M	3	4.95
E	G	2	0.48
E	r	1	0.83
E	A	1	0.99
E	z	3	1.30
E	O	3	2.23

The mean intensity of magnetization for each site was then determined, from the values for the samples.

Site	Intensity of Magnetization $I \times 10^{-3}$ c. g. s.	Standard Deviation from Mean Intensity in c. g. s. units $\times 10^{-3}$
A	1.29	± 0.57
B	1.62	± 0.75
C	3.75	± 3.32
D	3.49	± 0.85
E	1.17	± 0.59

Finally, from the above figures, the mean intensity of magnetization was obtained from the sites A, B, D, E as

$$\underline{I = 1.87 \pm 1.14 \times 10^{-3} \text{ c. g. s.}}$$

6.17 The Stability of the Remanent Magnetization

If the remanent magnetism contained in any rock is unstable (that is, if the remanent vector has undergone change in direction since formation) then paleomagnetic measurements are useless if the attitude of the in-situ vector is sought. Obviously tests must be made to determine the stability of the vector if meaning is to be attached to the results.

Consistency among the directions of magnetization is often used as a criterion for stability. This assumption is only likely to be valid if the direction is significantly different from the earth's present field. A much stronger indication of stability would be if the tightly grouped directions of magnetizations featured some anti-parallel vectors; that is, if some of the rocks were reversely magnetized.

Graham (1949) has postulated the folding test for magnetic stability. In this very simple test, an indication of stability is strongly evident if

directions of magnetization from either side of a synclinal or anticlinal feature coincide after 'unfolding' of the structure. Somewhat similar to this is the result of the Siberian study, for here intrusives with different attitudes have combined to give similar in-situ magnetic vectors.

Thellier (1954) has proposed a simple test for magnetic stability. A re-measurement of the magnetic vector in the specimen after storage with the magnetic vector at 90° to the earth's present field should indicate a degree of instability if the vector has rotated towards the present field direction; or a degree of stability if no change of the vector in the Siberian specimens was observed.

It is assumed here that in the case of sites A, B, D and E, a strong stability is evident, for three reasons. They are: the grouping of the results about a mean direction significantly different from the earth's present field; the similarity of the in-situ magnetic vector direction from intensives with different attitudes; and the lack of change of the direction of the magnetic vector after two years' storage with the vector in random directions.

Several different laboratory experiments can be made on rock specimens, in order to separate the unstable from the stable components in the magnetic vector. Instrumentation was not available for such studies, but in any case, such experiments do not seem necessary in the case of the Siberian samples, although site C certainly could have been investigated for the existence of an unstable component.

6.18 Summary of the Results

It is considered of value to summarise the results which have been given in this chapter, in Table (xii).

TABLE (xiii)

SUMMARY OF RESULTS

	Site A	Site B	Site C	Site D	Site E
Longitude of site	89.02°E	88.00°E	90.07°E	88.59°E	89.05°E
Latitude of site	65.58°N	69.17°N	66.29°N	66.06°N	66.28°N
No. of samples averaged	8	7	6	6	5
Mean coords. of vector:					
X	+0.0702	+0.0765	+0.7397	+0.2172	+0.0589
Y	+0.2131	+0.1708	-0.0362	+0.3918	-0.0532
Z	+0.9153	+0.8514	+0.4577	+0.8549	+0.9684
Azimuth of Mag. Vector	71.8°	65.9°	357.2°	61.0°	317.9°
Dip of Mag. Vector	+76.2°	+77.6°	+31.7°	+62.3°	+85.3°
Intensity of Magnetization (1×10^{-3} c. g. s. units)	1.27	1.62	3.75	3.49	1.17
Standard Deviation from mean intensity in 10^{-3} c. g. s. units	± 0.57	± 0.75	± 3.32	± 0.85	± 0.59
Radius of oval of confidence (95%)	14.7°	25.2°	28.6°	14.0°	14.7°
Ancient pole longitude	148.5°E	152.9°E	86.4°W	177.7°W	68.4°E
Ancient pole latitude	61.0°N	66.1°N	40.9°N	50.7°N	72.2°N

	Site A, B, D and E
Mean Latitude	67.0°N
Mean Longitude	88.8°E
Present Dipole Direction	Azimuth 0° Dip +77.9°
Total No. of Samples averaged	26
Total No. of Specimens averaged	67
Mean Azimuth of Magnetic Vector	61.6°
Mean Dip of Magnetic Vector	+76.3°
Coordinates of magnetic Vector	X = +0.1036 (+X is north) Y = +0.1917 (+Y is east) Z = +0.8943 (+Z is down)
Mean Intensity of Magnetization	$1.87 \pm 1.14 \times 10^{-3}$ c. g. s.
Ancient pole longitude	155.7°E
Ancient pole latitude	65.3°N
Radius of Circle of Confidence	95% (α 95) = 8.50° 50% (α 50) = 4.00°
Semi-axes of the Oval of Confidence in the computed pole position (for α 95)	$\delta_p = 14.55^\circ$ $\delta_m = 15.72^\circ$
Semi-axes of the Oval of Confidence in the computed pole position (for α 50)	$\delta_p = 6.85^\circ$ $\delta_m = 7.40^\circ$

CHAPTER 7

INVESTIGATION OF THE MAGNETIC PROPERTIES OF SOME ROCKS FROM NORTHEASTERN ALBERTA

During the summer of 1959, J. Godfrey of the Research Council of Alberta was conducting a detailed geological survey of part of the Canadian Shield which outcrops in northeastern Alberta. A collection of orientated samples was made where aeromagnetic coverage is available. These samples have had their magnetic properties examined.

The survey is centred on Bayonet Lake at $110^{\circ} 19'W$; $59^{\circ} 54'N$. This is some five miles west of the much larger Andrew Lake which gives its name to the government local aeromagnetic map, and to the published geological work carried out in the vicinity, by J. Godfrey (1961).

7.1 Geology of the Area

The surface geology of the area in the vicinity of the samples is given in figure 10 (a). The inferred surface geological cross-section is included in figure 13. Details of the geology immediately east of the Bayonet Lake Area are given in "Geology of the Andrew Lake, North District" by J. D. Godfrey (1961).

Metamorphism has played the major role in the geological history of the Bayonet Lake area. The geology is complex in both the lithologic

and structural sense. The main feature is the alternation of northerly trending major bands of granite gneiss, porphyroblastic biotite granite, and metasedimentary rocks, with some mylonization and ultramylonization associated with the granite gneiss. This ultramylonization is the extreme manifestation of crushing, shearing and plastic flowage which has occurred commonly throughout the area.

The distinction between lithologic units is not always clear, and some difficulty was experienced in the definition of rock types and the establishment of some lithologic boundaries. The high degree of deformation, with metamorphism, and the obliteration of most original structures, has produced a complex of mixed rock types over much of the area. Sometimes three or four different rock types may be present in a single outcrop, and so the map representation of lithologic units shows the predominant lithology only. J. D. Godfrey has not attempted to interpret the geological history of the area because of the apparent complexities and the limited area so far studied.

The glacial lakes, sand plains, drumlins and eskers, highly polished striated rock surfaces, glacial erratics and glacially smoothed outcrops characterize the appearance of the area as a typical example of recently glaciated terrain.

The sample numbers and locations are given in Figure 10 (a). The field petrological descriptions are included in the following Table:

FIGURE 10(a)

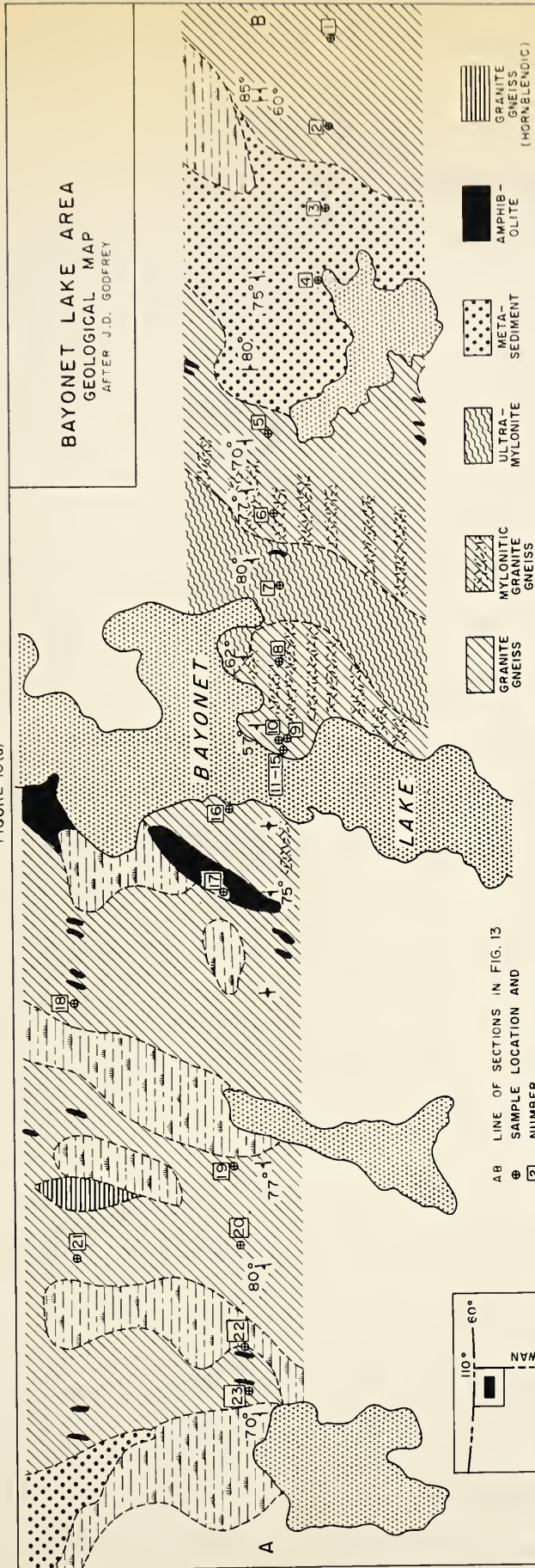
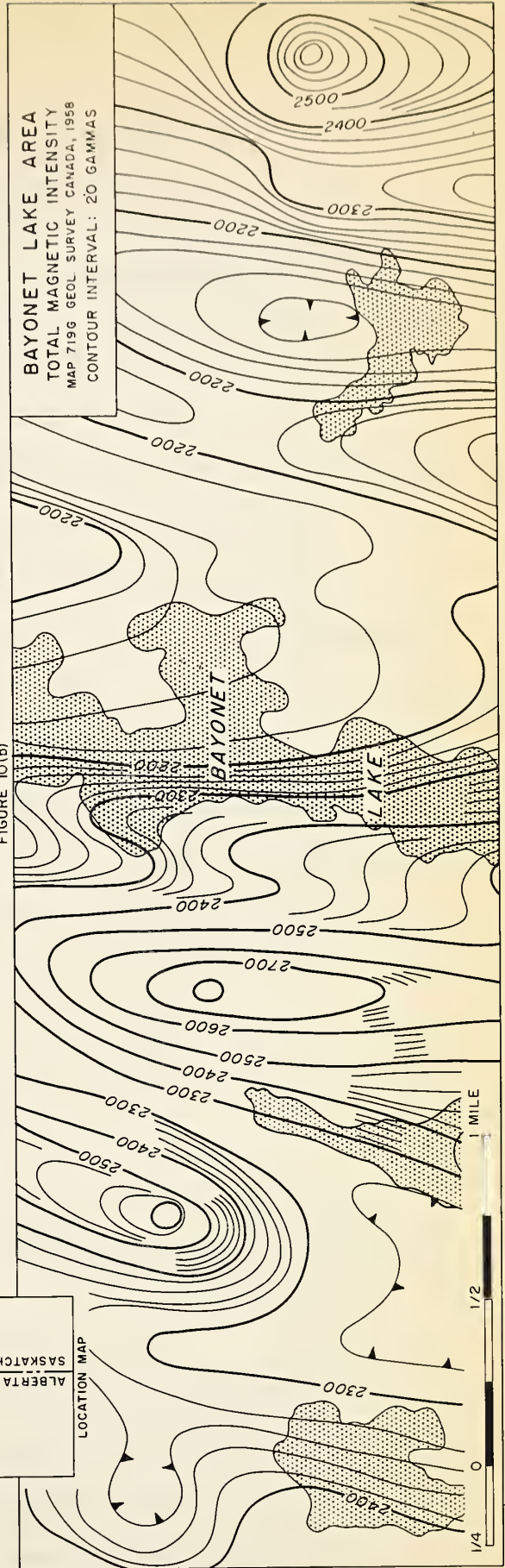


FIGURE 10(b)



THE GEOLOGICAL AND TOTAL MAGNETIC INTENSITY FEATURES OF THE BAYONET LAKE AREA, NORTHEASTERN ALBERTA

FIGURE 10

PETROLOGICAL AND FOLIATION DATA
FOR THE BAYONET LAKE SAMPLES

Sample No.	Foliation Direction	Dip	Petrological Description
1	N 0°E	88°E	Granite Gneiss
2	N 46°E	-	Granite Gneiss
3	N 12°E	-	Metasediment w/ granite pegmatite
4	N 2° to 15°W	75°W	Metasediment w/garnet
5	N 5°W	70°W	Granite Gneiss (sheared)
6	N 15°E	77° - 82°W	Mylonitic Porphyritic Amphibolite
7	N 18°E	59°W	Mylonitic Porphyritic Granite Gneiss
8	N 10°E	83°W	Granite Gneiss (weathered)
9	N 30°E	65° - 85°W	Granite Gneiss (sheared)
10	N 45°E	65° - 85°W	Banded Feldspathic Amphibolite
11	-	-	Granite Gneiss (sheared)
12	-	-	Granite Gneiss
13	-	-	Granite Gneiss
14	-	-	Granite Gneiss
15	-	-	Granite Gneiss
16	N 26°E	90°	Granite Gneiss (well banded)
17	N 32°E	75°W	Amphibolite w/ Quartz lenses and radio-active pegmatite
18	N 0°E	65° - 80°W	Granite Gneiss
19	N 2°E	70° - 80°W	Granite Gneiss (sheared)
20	N 26°E	70° - 80°W	Amphibolitic Granite Gneiss
21	N 10°E	68°W	Granite Gneiss
22	N 2°E	65° - 75°W	Amphibolite w/ pegmatite
23	N 30°E	65° - 80°W	Mylonitic Granite Gneiss

7.2 Determination of the Remanent Magnetic Vector

The measurements were carried out in exactly the same way as the measurements on the Siberian samples. In the case of the Alberta samples, however, all the cores were obtained after the sample had been orientated into a position which enabled in-situ vertical cores to be obtained.

It was found very difficult to obtain cores from the metamorphic samples since the high quartz content made drilling very slow. Not all samples, therefore, have more than one specimen from which the magnetic constants were determined.

The following Table gives results of the measurement of the magnetic vector. Details of these measurements are not given in the Table, but are available from a folder on file in the Geophysics Department at the University of Alberta.

TABLE (xv)

THE RESULTS OF THE MEASUREMENT OF THE REMANENT MAGNETIC VECTOR

Specimen Number	Azimuth ^o of Magnetic Vector	Dip ^o of Magnetic Vector	Intensity Magnetiza- tion $\times 10^{-6}$ c. g. s.
1	340	+67	1190
2	38	+56	2.84
3A	211	+ 4	29.8
3B	160	+10	609.0
3C	174	+47	152.0

TABLE (xv)--Continued

Specimen Number	Azimuth ^o of Magnetic Vector	Dip ^o of Magnetic Vector	Intensity Magnetiza- tion x 10 ⁻⁶ c. g. s.
4	100	+22	36.6
5A	256	+75	26.7
5B	338	+71	1143
6	321	+64	2.09
7	127	+22	3.37
8	T O O W E A K		
9	247	-15	52.60
10	281	+58	21.90
11	344	+76	0.52
12A	211	+24	32.10
12B	200	+14	21.66
13	207	+27	3.04
14A	T O O W E A K		
14B	T O O W E A K		
15	210	+25	114.8
16A	185	+ 3	53.8
16B	183	+ 7	33.8
16C	190	+ 7	33.9
17	302	+85	366.0
18A	353	+85	116.2
18B	52	+26	1009.0
18C	123	+47	718.0

TABLE (xv) -- Continued

Specimen Number	Azimuth ^o of Magnetic Vector	Dip ^o of Magnetic Vector	Intensity Magnetiza- tion x 10 ⁻⁶ c. g. s.
19	156	+75	2190
20	285	+51	13.43
21	36	-65	37.8
22	40	+45	7.33
23	T O O W E A K		

Azimuths are taken clockwise from magnetic north.

Dips are positive in the downwards direction.

The letters A, B and C refer to the first, second or third cores taken from an individual sample.

7.3 The Volume Susceptibility of the Rocks

Volume susceptibility data is a standard requirement in all magnetic surveys, and is defined as the susceptibility of unit volume of the material.

Susceptibility is defined as:

$$k = \frac{I}{H} \quad \text{where} \quad k = \text{susceptibility in c. g. s.}$$

I = Intensity of Magnetization

H = Magnetic Field Strength

7.3(i) Method of Measurement of the Susceptibility of the Specimens

The susceptibility of a material can be determined in several different ways. Basically, susceptibility is determined by observing the intensity of magnetization produced by a given magnetic field.

The susceptibility of the samples from northeastern Alberta was determined using a bridge-type alternating current circuit, manufactured by the Geophysical Specialties Company, of Hopkins, Minnesota. The susceptibility is measured by inserting the specimen into an air-core coil which forms part of one arm of the bridge. The inductance of the coil changes if the material is paramagnetic, and decreases if it is diamagnetic. The change of inductance causes the bridge to be thrown out of balance, and restoration of the balance provides a measure of the susceptibility.

A simplified circuit diagram of the bridge is given in Figure 11. The air-core coil is shown as L in the circuit. It can be shown that in the condition of balance (that is, when there is no potential difference between A and B), then

$$\frac{R_1}{R_3} = \frac{R_2}{R_4} \text{ and } L = C.R_2.$$

The bridge is balanced prior to inserting the cylindrical specimen into the coil, by adjusting C and R_2 until no sound is heard in the headphones, indicating that no potential difference exists between A and B, and that the bridge is balanced. The specimen is then inserted, and C and R_2 are readjusted until balance is reestablished. The difference in the C and R_2 readings between the air-filled coil and the coil with the

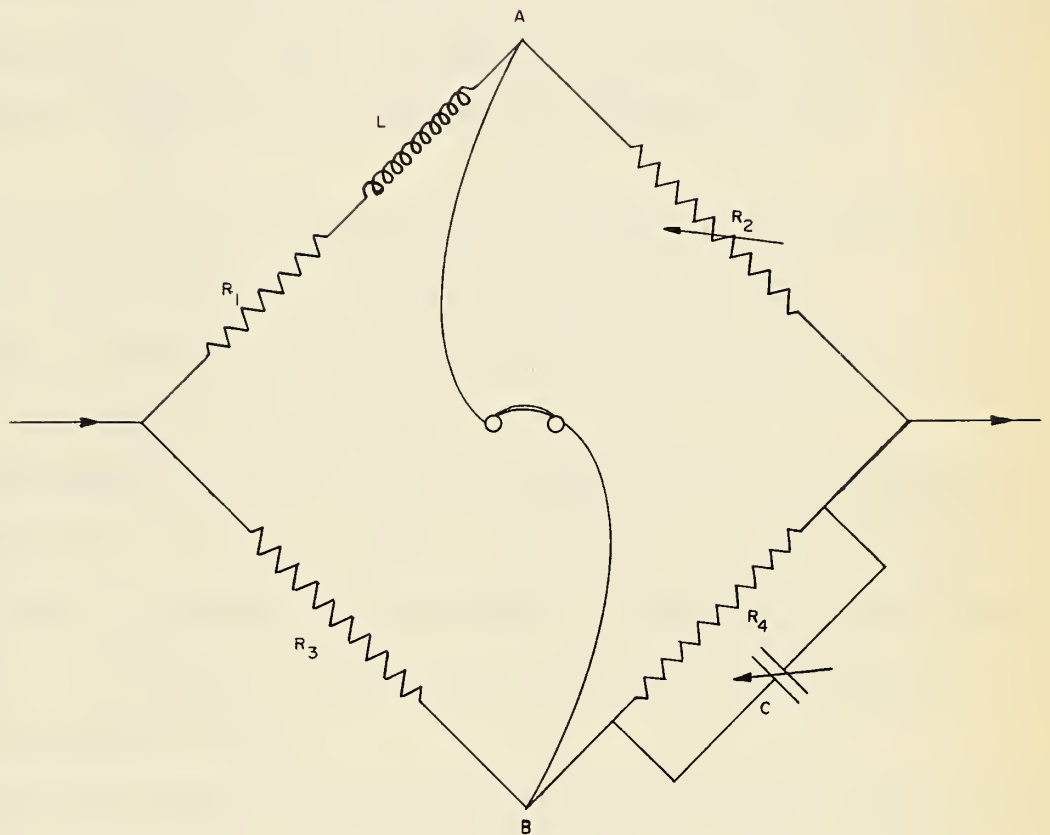


Fig.: II

SIMPLIFIED CIRCUIT DIAGRAM OF THE MS-3 SUSCEPTIBILITY BRIDGE

specimen inserted is noted, and the calibration curve provided by the manufacturers is then used to determine the susceptibility. The result obtained must then be corrected for variation of two parameters:

- (A) Correction of the susceptibility result for specimen diameter difference relative to the coil diameter:

According to the manufacturers, the factor for correction of the result, if the specimen is smaller in diameter than the hole in the coil is:

$$\text{Result} \times \frac{1.413}{d^2} \text{ where } d = \text{diameter of specimen in inches}$$

Since all cores are one inch in diameter, the factor for correction due to specimen diameter difference relative to the coil is $\times 1.413$.

- (B) Correction of the susceptibility result for variation of length of the specimen:

The manufacturers state that their calibration curve is intended for specimens of 2.5 inches in length, and no factor for the variation in specimen length is included. It was quickly determined that this variation is not linear. The apparatus was therefore calibrated empirically for variation of specimen length.

Two long specimens were sliced into various lengths. The susceptibility was assumed to be homogeneous throughout each sample. The standard length of 2.5 inches was assigned the unity factor, and smaller lengths were given lesser factors based on their measured susceptibilities. Table (xvi) is a list of the figures used for the calibration curve given in Figure 12.

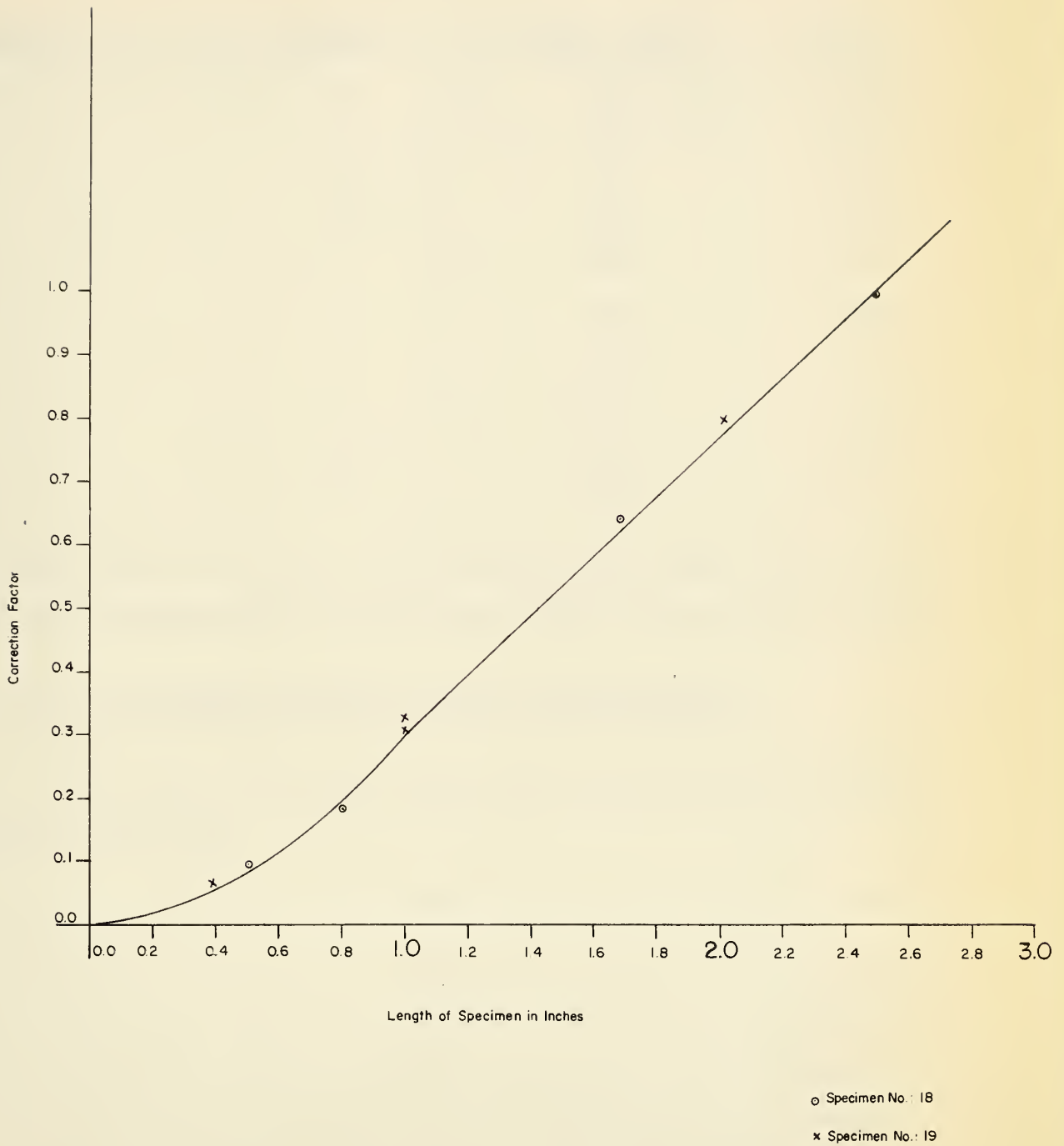


Fig.:12

CALIBRATION OF SUSCEPTIBILITY BRIDGE FOR VARYING LENGTHS OF SPECIMENS

TABLE (xvi)

CALIBRATION OF THE SUSCEPTIBILITY BRIDGE
FOR VARIATION OF LENGTH OF THE SPECIMEN

Sample	Length	$\Delta(R_2 \text{ and } C)$	Factor
18	0.5	86	0.095
18	0.8	163	0.188
18	1.675	560	0.646
18	2.5	869	1.0
19	0.4	25	0.061
19	1.0	128	0.31
19	1.0	135	0.33
19	2.0	330	0.8

In Figure 12, it can be seen that the length of the sample varies linearly with the correction factor for specimens greater than one inch in length.

7.3 (ii) The Results of the Measurement of Susceptibility

The measurements and results of the susceptibilities are given below in Table (xvii).

TABLE (xvii)

DETERMINATION OF THE VOLUME SUSCEPTIBILITY OF ROCKS
FROM THE BAYONET LAKE AREA

Sample Number	ΔR	Uncorrected $K \times 10^{-6}$ c. g. s.	Length corr. Factor	Combined Length & Diameter Corr. Fact.	Final corrected $K \times 10^{-6}$ c. g. s.
1	175.5	585	0.30	4.70	2850.0
2A	8	26.0	0.27	5.21	136.0
2B	6	19.5	0.30	4.70	91.8
3A	14	45.0	0.98	1.44	65.0
3B	21	68.0	0.94	1.50	102.0
4	10	32.5	0.91	1.55	51.0
5	176	590	0.94	1.5	885.0
6	2	6.50	0.33	4.25	27.6
7	3	9.75	0.91	1.55	15.2
8	2	6.50	0.25	5.6	36.4
9	14	45.0	0.30	4.7	212.0
10	15	49.0	0.27	5.21	266.0
11	4	13.0	0.25	5.6	73.0
12	6.5	21.0	0.87	1.62	34.0
13	2	6.5	0.25	5.6	36.5
14A	3	9.75	0.3	4.7	46.0
14B	2	6.50	0.3	4.7	29.5
15	6	19.5	0.48	2.94	57.3

TABLE (xvii)--Continued

Sample Number	ΔR	Uncorrected $K \times 10^{-6}$ c. g. s.	Length corr. Factor	Combined Length & Diameter Corr. Fact.	Final corrected $K \times 10^{-6}$ c. g. s.
16A	14	45.0	1.00	1.413	63.2
16B	8	26.0	0.35	4.04	105.0
17	4	13.0	0.27	5.4	70.0
18	882	3200	0.96	1.47	4710.0
19	121	394	0.30	4.7	1860.0
20	15	49.0	0.91	1.55	76.0
21	7	22.75	0.19	7.4	168.0
22	1.5	4.85	0.10	14.1	68.5
23	1	3.25	0.23	6.2	20.2

ΔR : indicates the difference in the reading on the susceptibility bridge between the air-filled coil and the coil with the specimen inserted.

Length Correction Factor:

the length of the specimen, if required, can be read from Figure 13 using these figures. N.B. The uncorrected reading must be divided by the length correction factor.

Combined Length and Diameter Correction Factor:

This is simply the diameter correction factor ($\times 1.413$), which is the same for all specimens, divided by the length correction factor.

7.4 The Relative Contributions of Induced and Remanent Magnetization to the Observed Field in the Bayonet Lake Area

The interpretation of aeromagnetic or ground magnetic anomalies is usually based on the theoretical anomaly, which would be created by a given regular anomalous body with a given constant susceptibility contrast with the surrounding media. This theoretical anomaly can be compared directly with the observed magnetic anomaly to give an estimate of the unknown parameters, or, as is more often attempted, certain indices of the observed anomalies can be used in theoretical equations to arrive at a solution. The unknown parameters associated with magnetic anomalies are usually numerous, and consequently there can exist many possible ambiguities in the resulting interpretations, particularly when the latter are made without the aid of geological control of the unknown parameters.

Almost all the available theoretical interpretation methods use the earth's present magnetic field as the predominant source of the magnetic intensity of the unknown anomalous body, in magnetic survey problems. This conveniently eliminates an important parameter, which is the direction of the magnetic intensity vector in the anomalous body whose theoretical magnetic effect is to be calculated. The direction of the magnetic intensity vector is taken to be that of the earth's present magnetic field wherever the anomalous body exists. That is, the induced magnetic intensity of the body is assumed to create the magnetic anomaly, and the effects of remanent or permanent magnetization are ignored.

Koenigsberger (1938), Hospers (1954) and many others have shown that igneous rocks frequently possess a remanent magnetization which is

significantly different in direction from that of the earth's present magnetic field. Consequently, the use of the many interpretation methods which are based on the assumption that magnetic anomalies are caused solely by variations of induced magnetization has been questioned.

Methods of interpretation which involve the determination of the permanent magnetization vector have been suggested, but are often laborious. Green (1960) has shown that a modified induced magnetization interpretation can be used when remanent magnetism data are available for the anomalous body. Some anomalies, of course, cannot be explained by magnetization alone, as has been shown by Girdler and Peter (1960).

A vast amount of aeromagnetic data has been obtained in Canada. Virtually all of this is concerned with the Precambrian Shield in either outcrop or subsurface. The commercial use of aeromagnetic surveys in western Canada is almost entirely restricted to use in oil exploration, where computed depths to the crystalline basement are used to estimate the thickness of the sedimentary cover. The broadscale nature of the work necessitates the use of rapid interpretation techniques such as that devised by Vacquier et al. (1951), which assumes the induced part to dominate in the observed field. Zietz (1960) has stated that the success of the method when applied to magnetic anomalies over sedimentary basins can be explained by some recently developed empirical relationships which consider inclinations of magnetization different from the earth's present field.

Thus the ratio of the induced to the remanent magnetic intensity for rocks in any area can aid in the selection of an interpretation method,

should magnetic anomalies require investigation.

The susceptibility and remanent magnetic properties of the orientated samples collected by J. D. Godfrey near Bayonet Lake have already been given in this chapter in Tables (xv) and (xvii). In order to determine the induced intensity of magnetization it is necessary to apply the following equation to the susceptibility results:

$I = kH$ where I = Intensity of magnetization in c. g. s. units

k = Susceptibility in c. g. s. units

H = Earth's magnetic field strength at Bayonet Lake

Since the earth's magnetic field is inclined at 80° at Bayonet Lake, it is well within the limits of observational accuracy to approximate this field to the vertical. The vertical component of the earth's magnetic field at Bayonet Lake in 1959 was 60,000 γ and thus to obtain the vertical component of induced magnetization, $H = 0.6$ can be substituted in the above equation.

Similarly, to obtain the vertical component of the remanent magnetic intensity of each sample it is necessary to multiply the remanent intensity by the sine of the angle of dip of the remanent magnetic vector, which has been determined and given in Table (xv).

The vertical components of the induced and remanent magnetic fields are included in Table (xviii).

TABLE (xviii)

THE VERTICAL COMPONENTS OF THE INDUCED AND REMANENT
MAGNETIC INTENSITIES IN THE BAYONET LAKE AREA

Sample Number	Mean Vert. Induced Intensity $I_i = 0.6k \times 10^{-6}$ c. g. s.	Mean Vert. Remanent Intensity $I_r = \sin D \cdot I_r \times 10^{-6}$ c. g. s.	Mean Total Vert. Magnetic Intensity $\times 10^{-6}$ c. g. s.	Q_v Factor
1	1710.0	1095.0	2805.0	0.640
2	83.0	2.35	85.35	0.028
3	50.0	6.7	56.7	0.013
4	30.6	13.8	44.4	0.450
5	531.0	25.3	556.3	0.047
6	16.6	1.9	18.5	0.114
7	9.22	1.25	10.47	0.135
8	21.8	1.0	22.8	0.046
9	127.0	13.6	113.4	0.107
10	166.0	18.6	184.6	0.112
11	43.8	0.5	44.3	0.011
12	20.4	9.1	29.5	0.446
13	21.8	1.4	23.2	0.064
14	22.7	1.0	23.7	0.044
15	34.4	6.28	40.68	0.182
16	47.0	3.66	50.66	0.078
17	42.0	365.0	407.0	8.7
18	284.0	375.0	3215.0	0.132
19	1119.0	2110.0	3229.0	1.89
20	45.6	10.5	56.1	0.230
21	103.0	34.2	69.8	0.332
22	41.0	5.2	46.2	0.127
23	12.1	1.0	13.1	0.083

The susceptibility (k) is given in Table (xv). The mean values of k for samples with more than one specimen are simply the average values. $\sin D$ and I_r , which are the sine of the angle of dip of the remanent magnetic vector and the intensity of magnetization of the remanent vector, are given in Table (xvii).

Samples numbers 8, 14 and 23 exhibited an intensity of magnetization which was too small to be measured on the astatic magnetometer. For the purposes of the comparison of the remanent and induced magnetic intensities, the immeasurable samples were assigned the value of 1.0×10^{-6} c.g.s. for their vertical remanent magnetic component. This figure is probably too high, but this fact will not detract from the object of the study.

The Q_v factor is here defined as

$$Q_v = \frac{\text{Vertical Component of Remanent Intensity}}{\text{Vertical Component of Induced Intensity}}$$

The Q factor, or the ratio of remanent to induced intensity of the material was first used by Koenigsberger (1938), who related the figure to the magnetic stability. The nearer the Q factor was to unity, the more magnetically stable was the material.

In only two cases out of the twenty-three samples examined were the remanent intensities greater than the induced intensities, and one of these samples has anomalous petrological properties, while the other has anomalous magnetic intensity. The median Q_v factor is about 0.1.

Since it is seldom possible to obtain a basement depth to an accuracy of greater than 15%, it appears valid to use an assumption of dominant induced magnetic field in this area, and hence utilise one of the

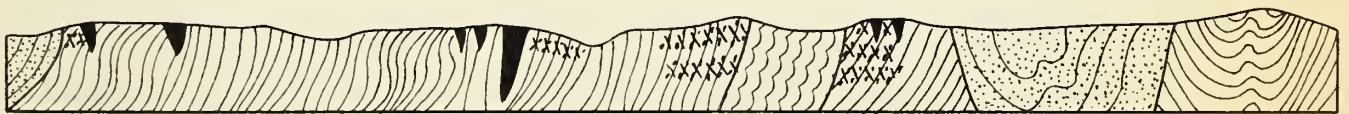
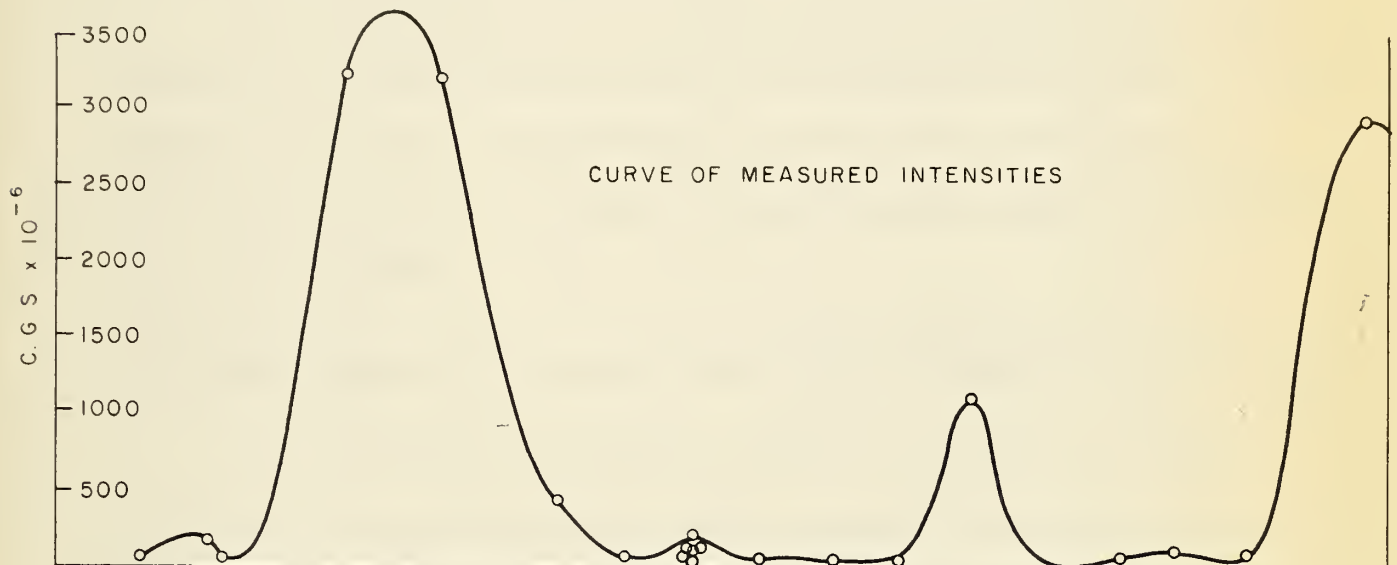
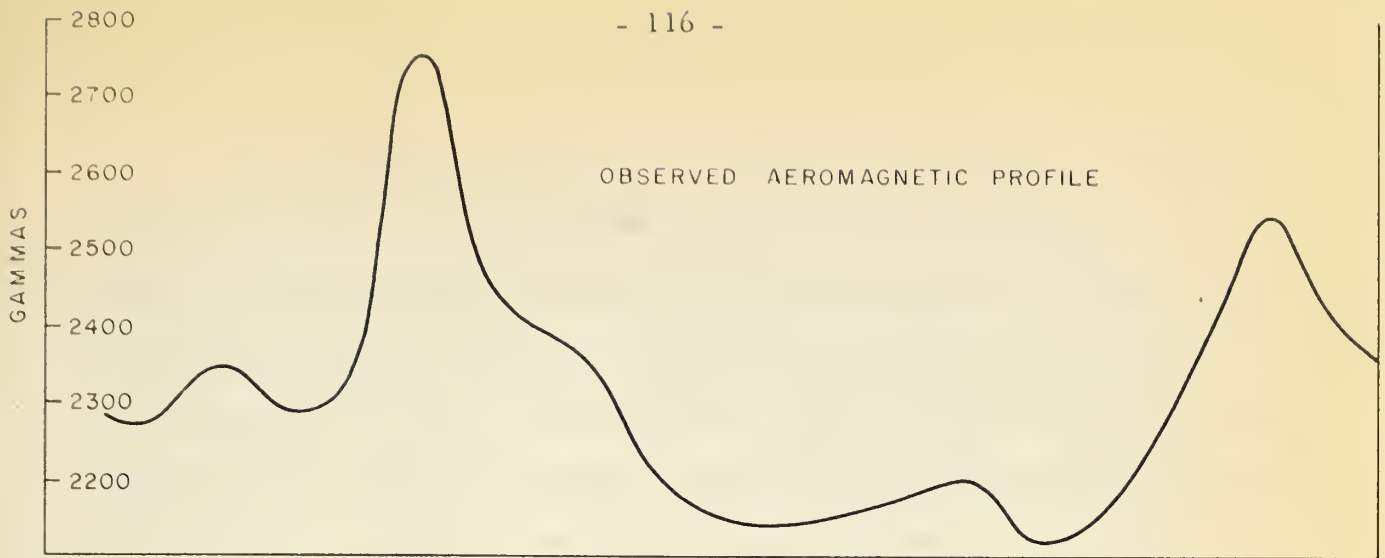
many rapid interpretation techniques based on that assumption. It could be possible, then, that the application of the Vacquier et al. (1951) interpretation method is successful in western Canada because the buried Precambrian Shield has negligible remanent magnetism.

It is of interest to note that two of the samples (Nos. 9 and 21) have reverse remanent vectors. The foliation planes are generally very steep, and thus these reverse vectors could represent overturned units.

Figure 13 shows the profile of observed total magnetic intensity, taken from the aeromagnetic map included in Figure 10, and the curve of measured total magnetic intensity. The near-surface geological cross-section is also given. The close correlation of observed and measured intensities indicates that the measurements are representative of the intensities existing in the metamorphic rocks. The flight level of the magnetometer (500 feet above ground level) agrees with the "depths" calculated using the Vacquier et al. (1951) system over this exposed surface. This gives some evidence of the vertical nature of the geological interfaces, since the interpretation method used assures, among other things, that the rock prisms have vertical sides.

The low mean remanent intensities measured agree with the statements by Hospers (1954) and others, that the mean intensity of magnetization apparently decreases with age. The low Q_v values substantiate Nagata's (1953) observations for older rocks.

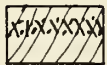
It can be concluded that the geological age of the strata and the accuracy required should be equated when choosing the interpretation method to be used.



- LEGEND -



GRANITE
GNEISS



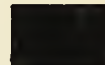
MYLONITIC
GRANITE
GNEISS



ULTRA-
MYLONITE



METASEDIMENT



AMPHIBOLITE

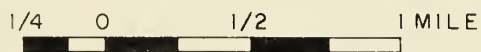


FIGURE 13
GEOLOGICAL CROSS SECTION, WITH OBSERVED
AEROMAGNETIC PROFILE AND CURVE OF MEASURED
VERTICAL MAGNETIC INTENSITY

Other significant aspects of this study can be seen by comparing the aeromagnetic contours and the geological map in Figure 10. The value of the aeromagnetic maps for integration into the resolving of the mapping problems is obvious. Determination of the magnetic properties of the samples serves to confirm the correlation between the aeromagnetic anomalies and distinct lithological units and, as has been mentioned, the attitude of the geological interfaces can be suggested.

The measured intensities have shown that a gradation from granite gneiss to mylonitic granite gneiss to ultramylonite is synonymous with decrease in intensity of magnetization, which serves to emphasize the associated magnetic low, and the increase in quartz content to a maximum in the ultramylonite.

7.5 Relationship of the Foliation Planes and the Remanent Magnetic Vector

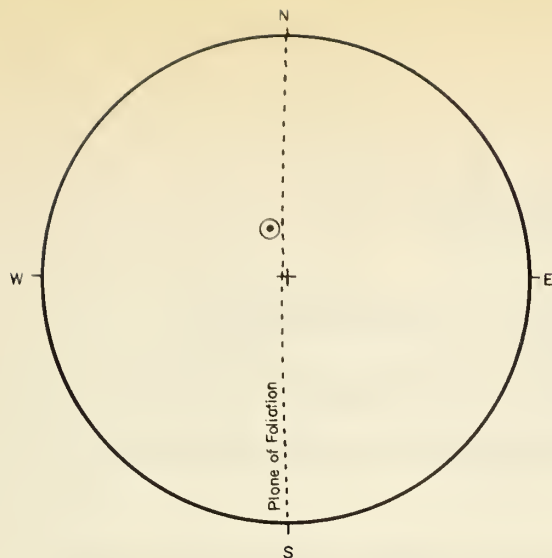
Howell, Martinez and Statham (1958) have studied the magnetic properties of some metamorphic rocks in detail. One of their observations was that there appears to be a relationship between the direction of remanent magnetization and planar elements in such rocks. Martinez et al. (1960) showed that the plane of foliation in the Packsaddle Schist and in the Valley Spring Gneiss of Texas, is also the plane in which the remanent vector lies.

Colville and Mead (1960) have demonstrated that Precambrian amphibolites in the north Tobacco Root Mountains of Montana show a remanent magnetization that is parallel to the planes of schistosity, despite later deformation.

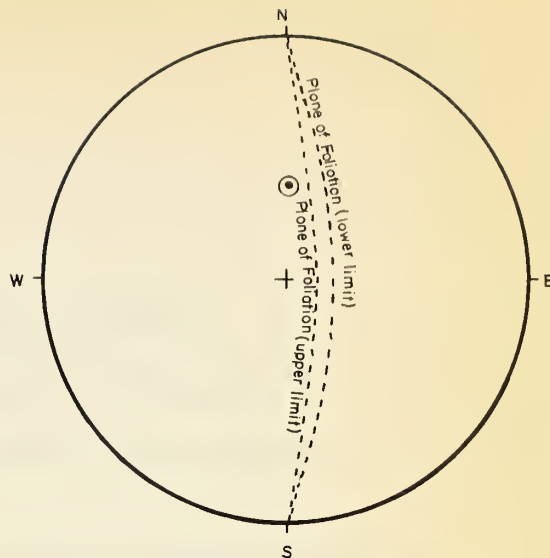
In Figure 14, the relationship of the foliation plane and the remanent magnetic vector for four samples are illustrated in the form of stereographic projections. Only one remanent vector direction is given for each sample, since only one specimen was used for the magnetic measurements in each case.

In each case the remanent vectors lies close to, but not exactly in, the plane of foliation. Of the twenty-three samples examined, these four samples best exhibit the relationship under discussion. Most of the samples do not show any tendency to exhibit the magnetic vector in the foliation plane.

A statistical analysis of the magnetic vector from many specimens in a single sample might render possible a more conclusive statement concerning the magnetic vector to foliation plane relationship, in this area. At the moment, however, the relationship between the two parameters which has been observed elsewhere, does not seem to be definitely applicable in the Bayonet Lake Area.



Sample No.: 1



Sample 22

● Remanent Magnetic Vector
(upper hemisphere)

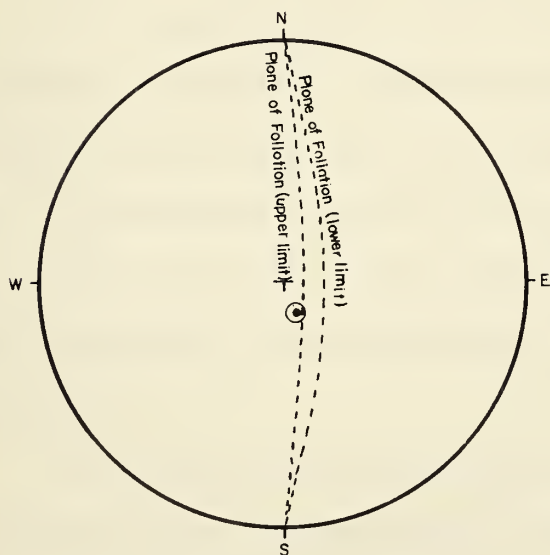
Foliation Plane :
Az. N 0° E
Dip 88° E

Remanent Vector :
Az 340°
Dip + 67°

● Remanent Magnetic Vector
(upper hemisphere)

Foliation Plane :
Az. N 2° E
Dip 65 to 75° W

Remanent Vector :
Az. 4°
Dip + 45°

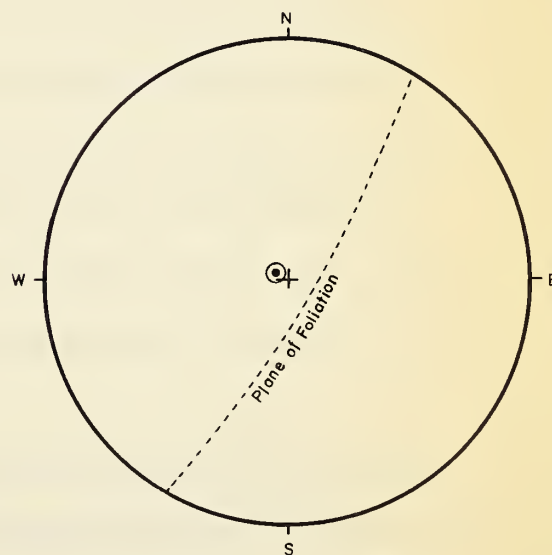


Sample 19

● Remanent Magnetic Vector
(upper hemisphere)

Foliation Plane :
Az. N 2° E
Dip 70 to 80° W

Remanent Vector :
Az 156°
Dip + 75°



Sample 17

● Remanent Magnetic Vector
(upper hemisphere)

Foliation Plane :
Az N 32° E
Dip 75° W

Remanent Vector :
Az. 302°
Dip + 85°

Fig.: 14

STEREOGRAPHIC PROJECTIONS SHOWING RELATIONSHIP BETWEEN
DIRECTION OF REMANENT MAGNETISM AND PLANE OF FOLIATION

CHAPTER 8

UNSUCCESSFUL ATTEMPTS TO UTILISE THE PALEOMAGNETIC PROPERTIES OF ROCKS IN THE SOLUTION OF SOME GEOLOGICAL PROBLEMS

One of the great disadvantages of the study of paleomagnetism is that the examination of the magnetic vector will frequently reveal a negative result. That is, the scatter of the magnetic vectors within a single horizon may be so great that no sensible result can be obtained, whether the object of the study is to correlate, date, obtain a paleomagnetic pole, or to resolve a structural problem. Common to every successful paleomagnetic study is the need for the examined formation to possess a reasonably consistent magnetic vector.

The most important requirement in a rock suitable for paleomagnetic investigation, is that the intensity of magnetization is strong enough to be measurable. This factor is also one of the great disadvantages in paleomagnetic work; for frequently field work, reorientation of the sample in the laboratory, coring and measurement will reveal simply that the material is magnetically too weak to be of use in the study of rock magnetism.

In addition to the work on the Siberian and Bayonet Lake samples, two other studies were attempted, but the magnetic properties of the rocks concerned produced negative results.

8.1 The Lewis Overthrust

The Lewis Overthrust of Southern Alberta and Northern Montana is one of the major tectonic features of the western cordillera.

It is possible that the thrust sheet may have suffered differential movement along minor thrusts and faults. Mr. G. Hunt of the University of Alberta Geology Department has included study of this problem in order to fulfil Ph.D requirements.

Since this particular study was unsuccessful and is, in any case, only an incidental part of this thesis, it is sufficient to mention that the stratigraphic and petrological details are dealt with in Hunt's thesis. The purpose of the study of the magnetic properties of a lava in the east, and a sill to the west within the Lewis Overthrust sheet, was an attempt to correlate the two units, and thus aid in the resolving of the relationships of the east and west parts of the overthrust.

Obviously, if the magnetic vector within two local igneous bodies features the same attitude relative to a determinable original horizontal, this is some evidence of contemporaneity. The relative attitudes of the vectors from the respective igneous bodies could also be of use in postulating any relative rotational movement within the tectonic units along minor thrusts or faults, always assuming that the lava and the sill are themselves relatable to the attitude of the sediments in the thrust sheet.

(i) The Cameron Lake Lava:

The lava is within the Lewis Overthrust sheet, and is one mile north of Cameron Lake, which is on the international border. The lava

lies within the Purcell Group of the Proterozoic (Daly, 1912). At the time of sampling it was thought that the lava represented a single volcanic outburst. Subsequent detailed geological study by Hunt has revealed that the flow is in fact complex, several successive outpourings having contributed to the lava's present dimensions. If this fact had been known at the time of obtaining orientated samples, careful vertical control of the samples could have been carried out. Instead, the usual random selection of samples was made. The magnetic vector for each specimen is given below. These results are uncorrected for the geological dip of the lava.

TABLE (xix)

THE MAGNETIC VECTORS OF SPECIMENS
FROM THE CAMERON LAKE AREA

Sample, Core and Specimen	Azimuth ^o of Magnetic Vector	Dip ^o of Magnetic Vector
11A	15	-35
11B	6	-36
12A	48	-47
21A	314	+64
21B	7	+43
22A	346	+30
23A	1	+29
23B	359	-11
31A	356	- 3
32A	350	+ 3
32B	350	+12
33A	343	+27
41A	345	+12
41B	341	0
42A	357	-11
42B	351	+10
51A	358	- 4
51B	42	+34
52A	353	+62
52B	353	+41
61A	358	-43
62A	351	-61

TABLE (xix)--Continued

Sample, Core and Specimen	Azimuth ^o of Magnetic Vector	Dip ^o of Magnetic Vector
71A	32	-18
71B	34	-17
81A	351	- 5
81B	355	- 3
82A	5	-28
82B	358	-20
91A	343	- 6
91B	355	+ 4
92A	350	+ 5
92B	350	-14
93A	316	+21
93B	333	+ 1
101A	10	+80
101B	335	+80
101C	278	+78
102A	305	+57
102B	346	+69
103A	310	+62
103B	305	+34
111A	356	+ 8
112A	345	+17
121A	6	+14
122A	315	+20
123A	4	+ 8

First figure refers to sample.

Second figure refers to the core.

The letter refers to specimen cut from the core.

Azimuth is with respect to present magnetic north.

Dip is positive downwards, negative upwards.

It can be seen from the above results that the azimuths of the specimens are grouped around magnetic north. The mean azimuth is 351° relative to magnetic north. The standard deviation is $\pm 15^{\circ}$. This encouraging fact was invalidated upon measurement of the magnetic dips which vary from steep downward directions to steep upward directions.

The great scatter of the measured vectors about a reasonably consistent azimuthal direction is suggestive of magnetic instability, particularly since the azimuth is close to that of present magnetic north. Cox (1957) and Creer (1958) have stated that the magnetic vector in early Paleozoic and older lavas frequently exhibits wide scatter about an azimuth close to the magnetic north at the time of sampling. In a recent study, Irving and Banks (1961) have shown that the lavas of the Newark Group of the Upper Triassic of Massachusetts possess a consistent northerly direction, but highly variable inclination in the magnetic vector. This suggests an unstable component is aligning itself close to the earth's present horizontal component. Why the unstable component, if any, does not align preferentially with the total magnetic field of the earth is, at present, inexplicable. It is possible that the in-situ magnetic vector might have rotated in the plane of the azimuth of the magnetic vector as the lava moved at a temperature below the Curie Point, but while still viscous.

It is by no means impossible that an attempt to demagnetize the unstable component by limited alternating fields might result in a closing together of the magnetic vectors into a more limited direction, as has been shown by Irving and Banks (1961), but the instrumentation for this operation is unavailable at present.

Since there is some consistency in the azimuth and dip of the magnetic vector within individual samples, there exists the possibility that careful vertical sampling of the compound lava flow might reveal a systematic variation of the lava with change of age, similar to that observed by Hospers (1954) in the Tertiary lava flows of Iceland. This systematic variation is assumed to be due to the relatively rapid variations of the non-dipole component of the earth's magnetic field, which Hospers (1954) and others have shown will average out if a large vertical extent of a given formation is sampled.

Since only one igneous body was sampled for the purpose of this study, there exists little point in determining a paleomagnetic pole position for this Proterozoic material, even if there were a consistency of direction of the magnetic vectors to warrant such an operation.

Late information has rendered the study of the magnetic properties of the Cameron Lake lava almost completely useless for correlation purposes. Hunt has indicated that there may have been more than one phase of tectonics during the existence of the sill, and that some of those phases may have involved dynamic or mild thermal metamorphism. To determine the original in-situ magnetic vector for such a material is likely to be very difficult.

(ii) The Irishman Creek Sill:

The igneous body chosen in the western part of the Lewis Overthrust for the attempted magnetic correlation to the Cameron Lake lava in the eastern part of the thrust sheet, is situated one quarter of a

mile northeast of Irishman Creek, which is about eight miles northeast of Kingsgate on the international boundary. The structural, stratigraphic, and petrological details are given in Hunt's thesis. The East Half of the Nelson Map Area, by Rice (1941) is another source of the geological detail of the area. The diabase sill is in the Aldridge Formation of the Lower Purcell of the Proterozoic.

Orientated samples were obtained from this sill prior to the completion of the measurements of the magnetic properties of the Cameron Lake lava.

The samples were reorientated in the laboratory, cored, and sliced into specimens.

The specimens were found to be almost completely non-magnetic. The astatic magnetometer was at this time operating at a sensitivity whereby a cylinder of material of magnetic intensity 10^{-7} c. g. s. could create a measurable deflection, and the Irishman Creek sill specimens did not cause any observable deflection.

The attempt to correlate the western and eastern parts of the Lewis Overthrust by examining the magnetic vector in chosen igneous bodies thus resulted in a completely negative result on four counts:

- (a) The Cameron Lake lava appears to be magnetically unstable,
- (b) The Cameron Lake lava is a compound flow, and must be sampled, therefore, with careful vertical control.
- (c) The Cameron Lake lava may have suffered many phases of mild metamorphism, thus possibly destroying the original magnetic directions.

(d) The Irishman Creek Diabase Sill is so magnetically weak that the magnetic vector is completely unmeasurable using the available apparatus.

(iii) Other Work on Magnetism in the Lewis Overthrust:

It is of interest to note the other work carried out on the lavas of the Lewis Overthrust.

D. K. Norris (1960) has stated: "Remanent magnetism studies indicate tentatively that the orientation of the horizontal component of magnetic vectors within two formations is the same within the Flathead and Clarke ranges of the Lewis Overthrust. Thus the rocks of the Lewis thrust plate in this region suffered little, if any, differential rotation in the horizontal plane during thrust faulting."

Norris confirms this conclusion in a 1961 report. "Additional data on remanent magnetism from samples collected during 1960 sustain the preliminary conclusion that orientation of the horizontal component of magnetic vectors is the same at common stratigraphic levels in the Lewis thrust plate in the Flathead and Clarke ranges, and hence the rocks of the plate near the North Kootenay Pass underwent little, if any, differential rotation in a horizontal plane during thrust faulting." (The author has underlined horizontal.)

This unprecedented utilization of just one of the components of the magnetic vector (the azimuth) for local structural deductions points directly to what may render the deductions to be invalid. Unless Norris utilised a horizontal component of the magnetic vector which was

substantially different from the direction of the earth's present field, it seems unlikely that his statement concerning the differential rotation within a horizontal plane of the Lewis plate is a reasonable one. For as was shown for the Cameron Lake lava, the horizontal component was fairly consistent in direction, but its grouping about the present magnetic north indicates an unstable component; and thus other unstable igneous materials of similar age in the area will probably exhibit similar azimuth. (It should be noted that the Proterozoic pole position, despite its poor experimentally defined position, would not have given an azimuth close to the present magnetic north.) The fact that Norris neglected to use the dip of the magnetic vector in his analysis is some evidence of the wide scatter of the dip of the magnetic vector, and hence it would be surprising if his obviously reasonably consistent, horizontal component (the azimuth) of the vector were anything but close to the present magnetic north direction.

8.2 The Proterozoic Pole Position from Dykes in Northern British Columbia

The geology of northeastern British Columbia is well documented in Memoir 259 of the Geological Survey of Canada, by Mclearn and Kindle (1950).

In "The Geological Investigation Along the Alaska Highway from Fort Nelson, B. C., to Watson Lake, Yukon" by Williams (1944), some detail of the Proterozoic stratigraphy is included.

At Mile 441, near the Toad River bridge, highly folded, light-coloured

quartzite and porcellanous argillite and slaty rocks are unconformably overlain by nearly flat grey limestone containing Middle Silurian chain corals. Six local vertical dykes are also truncated by this pre-Silurian unconformity. Dr. J. Lipson (personal communication) using the mass spectrometer of the Physics Department at the University of Alberta, has dated a sample of one of these dykes at about 600 million years, or late Proterozoic in age. Mclearn and Kindle (1950) have also assigned these dykes to the Proterozoic.

The dykes have been examined in thin section by J. Deleen, and his findings are documented in Williams' report. In general, the dykes are quartz gabbros, moderately altered to chlorite and carbonate. The thin sections from the centre of the dykes indicate the development of hornblende at the expense of augite "that leads some authorities to apply the name hornblende gabbro or gabbrodionte."

Late Precambrian diabase dykes from the Canadian Shield have had their magnetic properties determined by Strangway (1960). The magnetic vector was shown to have a random direction. Following demagnetization in an alternating field of 100 oersteds, the stable component of magnetization was seen to be parallel to the dyke, whatever the strike of the body.

During the summer of 1959, the author was a member of a surface geological mapping party in the Toad River Area of northern British Columbia. Several orientated samples of the dykes were taken, with the main objective being to determine a magnetic pole position for the Proterozoic. A subsidiary motive was the examination of the relationship

of the magnetic vector to the sides of the dyke; for unlike the case of Stangways' samples, it is always possible that no unstable component exists, and the initially observable component is, as in Stangway's observations, parallel to the dyke.

The samples were prepared for measurement of the magnetic vector, but the intensity of magnetization is so low that, unfortunately, no deflection could be detected with the astatic magnetometer. This means that the intensity of magnetization of the dykes are probably less than 10^{-7} c. g. s. ; or less magnetic than many sediments.

The unsuccessful studies do not necessarily mean that no future studies can be carried out on the igneous materials concerned.

In the case of the Cameron Lake lava, demagnetizing apparatus might be used to some profit. The intensity of magnetization of the lava is certainly high enough for accurate measurements to be made easily.

Both the Irishman Creek Sill and the Toad River Dykes would require a magnetometer of a sensitivity which would be capable of measuring an intensity of 10^{-9} c. g. s. before reasonable deflections could be obtained. This is just possible, but only with a highly astatized apparatus.

CONCLUSIONS

The studies made for the purpose of completing this thesis support the following conclusions:

1. The Triassic magnetic pole position for Siberia is at 65.3° North, 155.7° East. The radius of the circle of 95% confidence is 8.5° . The pole position agrees within the limits of error to previously determined magnetic pole positions for the Triassic period based on European data. This agreement indicates that no differential movement of northern Asia relative to Europe seems to have taken place during movement between North America and Europe, which has been inferred by other paleomagnetic studies.

2. In the Bayonet Lake area of northeastern Alberta, the remanent magnetism is a negligible part of the observed magnetic field. This indicates that methods based on the assumption that induced magnetism is solely responsible for the observed magnetic field can be utilised for interpreting local magnetic anomalies.

3. Correlation of measured and observed magnetic intensities in the Bayonet Lake area confirm that the measured intensities are representative of the intensities existing in the rock units.

4. The obvious relationship of the surface geology and the aeromagnetic map in the Bayonet Lake area demonstrates the value of integrating the aeromagnetic map into surface mapping of exposed metamorphic rocks.

5. A gradation from granite gneiss to mylonite to ultramylonite in the Bayonet Lake area is synonymous with decreasing magnetic intensity, which confirms the increase of quartz to a maximum in the ultramylonite.

6. The remanent magnetic vector in the rocks of the Bayonet Lake area does not seem to lie consistently in the foliation plane, as has been observed in other areas.

7. There exists an unstable component in the magnetic vector of a lava in the Lewis Overthrust. A sill in the western part of the Lewis Overthrust is magnetically too weak to be studied using the available apparatus. Thus the magnetic properties of the igneous bodies within critical sections of the tectonic units could not be readily used to aid in the resolving of structural problems.

8. The nature of the suggested magnetic instability in the lava in the Lewis Overthrust is such that demagnetizing by limited alternating fields might result in the removal of the unstable component.

9. The magnetic properties of Proterozoic dykes from northern British Columbia are immeasurable with available apparatus, since the magnetic intensities of the dykes are unusually low.

BIBLIOGRAPHY

- Beck, A. E., 1961. Energy Requirements of an expanding Earth : Journ. Geophys. Research; Vol. 66, pp. 1485-89.
- Bitter, F., 1931. Ref. p. 1070, Physics (Starling and Woodall), Longams; London, 1950.
- Belshé, J. C.; 1957. Palaeomagnetic Investigations of Carboniferous Rocks in England and Wales : Advances in Physics; Vol. 6, pp. 187-191.
- Blackett, P.M.S.; 1952. A Negative Experiment Relating Magnetism to the Earth's Rotation : Royal Sec. London Philos. Trans.; Ser. A; Vol. 245, pp. 303-370.
- Brynjólfsson, A; 1957. Studies of Permanent Magnetism and Viscous Magnetism in the Basalts of Iceland : Advances in Physics; Vol. 6, pp. 247-54.
- Bullard, E. C.; 1949. The Magnetic Field Within the Earth : Proc. Royal Soc.; Vol. 4, pp. 5-162.
- Carey, S.W.; 1958. The Tectonic Approach to Continental Drift : Continental Drift Symposium; Univ. Tasmania, Hobart.
- Chapman S. and Bartels, J.; 1940. Geomagnetism : Oxford, Clarendon Press.
- Clegg, J. A.; Deutsch, E.R.; Everitt, C.W.F. and Stubbs, P.H.S.; 1957 : Some Recent Palaeomagnetic measurements made at Imperial College, London : Advances in Physics; Vol. 6, pp. 219-231.
- Clegg, J.A.; Radakrishnamurty, C. and Sahasrabudhe, P.W.; 1958 : Remanent magnetism of the Rajmahal Traps of Northeastern India : Nature; Vol. 181, pp. 830-31.
- Collinson, D. W. and Runcorn, D.K.; 1960. Paleomagnetic Observations in the United States; New Evidence for Polar Wandering and Continental Drift : Bull. Geol. Surv. America; Vol. 71, No. 7, pp. 915-58.

- Colville, A. A., and Mead, J.; 1960. Structural Implications of a Paleomagnetic Investigation, North Tobacco Root Mountains, Montana : U.S.G.S. Meeting; Denver.
- Cox, A.; 1957. Remanent Magnetization of Lower to Middle Eocene Basalt Flows from Oregon : *Nature*; Vol. 179, pp. 685-86.
- Cox, A.; and Doell, R. R.; 1960. Paleomagnetic Evidence Relevant to a Change in the Earth's Radius : *Nature*, Vol. 189, pp. 45-47.
- Creer, K.M.; 1958. Preliminary Palaeomagnetic Measurements from South Africa : *Annales Geophysique*; Vol. 14, pp. 373-90.
- Creer, K.M.; Irving, E. and Runcorn, S.K.; 1957. Palaeomagnetic Investigations in Great Britain, VI; Geophysical Interpretation of Palaeomagnetic Directions from Great Britain : *Royal Soc. London Philos. Trans.*; Ser. A, Vol. 250, pp. 144-56.
- Daly, R.A.; 1912. North America Cordillera. Forty-Ninth Parallel : *Geol. Survey. Dept. of Mines*; Ottawa, Memoir No. 38.
- Deutsch, E.R.; 1956. The Magnetic Hysteresis of Rocks and Minerals at High Temperatures : *Journ. Geomag. Geoelec.*; Vol. 8, pp. 118-128.
- Deutsch, E.R.; Radakrishnamurty, C. and Sahasrabudhe, P.W.; 1959. Palaeomagnetism of the Deccan Traps : *Annales Geophysique*; Vol. 15, pp. 39-59.
- Deutsch, E.R.; Unpublished Manuscripts : Some Notes Regarding Design of a Simple Astatic Magnetometer; Further Notes on a Small Magnetometer; and Large Magnetometer : Data and Procedures for Measurements.
- Doell, R. R.; 1956. Remanent Magnetization of the Upper Miocene "blue" Sandstones of California : *Am. Geophys. Union Trans.*; Vol. 37, pp. 156-67.
- Dubois, P.M.; Irving, E.; Opdyke, N. D.; Runcorn, S.K.; and Banks, M. R.; 1957. The geomagnetic Field in Upper Triassic Times in the United States : *Nature*; Vol. 180, pp. 1186-87.
- Dubois, P.M.; 1959. Correlation of Keweenawan Rocks of Lake Superior District by Paleomagnetic Methods : *Proc. Geol. Assoc. Canada*; Vol. 11, pp. 115-128.
- Eaton, G. P.; 1960. Ground Distribution of Windborne Volcanic Ash as a Possible Index to Polar Wandering : U.S.G.S. Meeting; Denver.

- Egyed, L. ; 1956. The Change of the Earth's Dimensions Determined from Palaeogeographical Data : *Geofisica Pura e Applicata*; Vol. 33, pp. 42-48.
- Egyed, L. ; 1960. Some Remarks on Continental Drift : *Geofisica Pura e Applicata*; Vol. 45, pp. 115-16.
- Elsasser, W.M. ; 1955. Hydromagnetism; I. A Review : *Am. Journ. Phys.*; Vol. 23, pp. 590-609.
- Fineberg, F.S. ; and Dashkevitch, N.N. ; 1959. Report, Third Palaeomagnetic Conference; Univ. of Leningrad.
- Fisher, R.A. ; 1953. Dispersion on a Sphere : *Royal Soc. London Proc.*; Ser. A; Vol. 217, pp. 295-305.
- Girdler, R.W. and Peter, G. ; 1960. An Example of the Importance of Natural Remanent Magnetization in the Interpretation of Magnetic Anomalies : *Geophys. Prosp.*; Vol. 8, No. 3.
- Godfrey, J.D. ; 1961. Geology of the Andrew Lake, North District : *Res. Coun. of Alberta*; Prelim. Report No. 58-3.
- Gottschalk, V.H. ; 1935. The Coercive Force of Magnetite Powders : *Journ. of Phys.*; Vol. 6, pp. 127-32.
- Graham, J.W. ; 1949. The Stability and Significance of Magnetism in Sedimentary Rocks : *Journ. Geophys. Research*; Vol. 54, pp. 131-67.
- Graham, J.W. ; 1953. Changes of Ferromagnetic Minerals and Their Bearing on Magnetic Properties of Rocks : *Journ. Geophys. Research*; Vol. 58, pp. 243-60.
- Graham, J.W. ; 1955. Evidence of Polar Shift Since Triassic Time : *Journ. Geophys. Research*; Vol. 60, pp. 329-47.
- Griffiths, D.H. ; 1955. The Remanent Magnetism of Varved Clays from Sweden : *Royal Astron. Soc. Monthly Notices, Geophys. Supp.*; Vol. 7, pp. 103-114.
- Green, R. ; 1960. Remanent Magnetization and the Interpretation of Magnetic Anomalies : *Geophys. Prosp.*; Vol. 8, No. 1.
- Gusev, B.V. ; 1959. Age of Alkaline-Ultrabasic Rocks of Maymecha-Kotuy Region According to Palaeomagnetic Data : *Informatsionnyy Byulleten Instituta Geologii Arkтики*; Leningrad, No. 4, pp. 30-33.
- Haigh, G. ; 1958. The Process of Magnetization by Chemical Change : *Philos. Mag.*; Vol. 3, pp. 267-86.

- Heezen, B. C. ; 1959. Paleomagnetism, Continental Displacements, and the Origin of Submarine Topography : Internat. Oceanog. Cong. : Preprints Edit. by Sears, M. ; pp. 26-28.
- Hood, P. J. ; 1961. Paleomagnetic Study of the Sudbury Basin : Journ. Geophys. Research; Vol. 66, pp. 1235-41.
- Hospers, J. ; 1954. Magnetic Correlation in Volcanic Districts : Geol. Mag. Vol. 91, No. 5.
- Hospers, J. ; 1955. Rock Magnetism and Polar Wandering : Journ. Geol. ; Vol. 63, pp. 59-73.
- Howell, L. G. ; Martinez, J. D. and Statham, E. H. ; 1958. Some Observations on Rock Magnetism : Geophysics; Vol. 23, pp. 285-98.
- Irving, E. ; 1956. Palaeomagnetic and Palaeoclimatological Aspects of Polar Wandering : Geofisica Pura e Applicata; Vol. 33, pp. 23-41.
- Irving, E. ; and Green, R. ; 1958. Polar Movement Relative to Australia : Royal Astron. Soc. Geophys. Journ. ; Vol. i, pp. 64-72.
- Irvings, E. ; 1959. Palaeomagnetic Pole Positions : A Survey and Analysis : Royal Astron. Soc. ; Geophys. Journ. ; Vol. 2, pp. 51-79.
- Irving, E. ; and Tarling, D. H. ; 1961. The Paleomagnetism of the Aden Volcanics : Journ. of Geophys. Research; Vol. 66, pp. 549-56.
- Irving, E. ; and Banks, M. R. ; 1961. Paleomagnetic Results from the Upper Triassic Lavas of Massachusetts : Journ. of Geophys. Research; Vol. 66, pp. 1935-41.
- Khramov, A. N. ; 1958. The Paleomagnetic Correlation of Sedimentary Strata : Gostoptekhizdat, Leningrad, p. 218.
- King, R. F. ; 1955. The Remanent Magnetism of Artificially Deposited Sediments : Royal Astron. Soc. Monthly Notices; Geophys. Supp. ; Vol. 7; pp. 115-134.
- Kobayashi, K. ; 1959. Chemical Remanent Magnetization of Ferromagnetic Minerals and its Application to Rock Magnetism : Journ. Geomag. and Geoelec. ; (Kyoto), Vol. 10, pp. 99-117.
- Koenigsberger, J. G. ; 1938. Stabilität der Magnetischen Thermoremanenz in Tongegenständen und Gesteinen bei Bestimmungen des Magnetischen Erdfeldes in der Vergangenheit; Gerl. Beitr. z. Geophys. ; Vol. 53, pp. 344-51.
- Koenigsberger, J. G. ; 1947. Ferromagnetic Parameter and Grain Size : Phil. Mag. Vol. 38, pp. 640-57.

- Makerova, Z.V.; 1959. Bull. Acad. Sci. U.S.S.R.; Geophys. Ser. 1959; p. 1520; and Trans. Am. Geophys. Union; 1960; p. 1081.
- Martinez, J.D.; and Howell, L.G.; 1956. Palaeomagnetism of Chemical Sediments : Nature ; Vol. 178, pp. 204-05.
- Martinez, J.D.; Statham, E.H.; and Howell, L.G.; 1960. A Review of Paleomagnetic Studies of Some Texas Rocks : Aspects of Geol. of Texas Symp. : Bureau of Econ. Geol., Univ. of Texas.
- McLearn, F.H.; and Kindle, E.D.; 1950. Geology of Northeastern British Columbia : Geol. Surv. Canada; Memoir 259.
- Nagata, T.; 1953. Rock Magnetism : Tokyo, Japan, Maruzen Co. Ltd.
- Nagata, T.; Akimoto, S.; Shimizu, Y.; Kobayashi, K.; and Kuno, H.; 1959. Paleomagnetic Studies on Tertiary and Cretaceous Rocks in Japan : Japan Acad. Proc.; Vol. 35, pp. 378-83.
- Nairn, A.E.M.; 1956. Relevance of Palaeomagnetic Studies of Jurassic Rocks to Continental Drift : Nature; Vol. 178, pp. 935-36.
- Nairn, A.E.M.; 1957. A Palaeomagnetic Study of Jurassic and Cretaceous Sediments : Royal Astron. Soc. Monthly Notices, Geophys. Supp.; Vol. 7, pp. 308-313.
- Nairn, A.E.M.; 1960. Paleomagnetic Results from Europe : Journ. of Geol.; Vol. 68, pp. 285-306.
- Néel, L.; 1951. L'Inversion de L'Aimantation Permanente des Roches : Annales Geophysique, Vol. 7, pp. 90-102.
- Néel, L.; 1955. Some Theoretical Aspects of Rock Magnetism : Advances in Physics; Vol. 4, pp. 191-243.
- Norris, D.K.; 1960. Field Work, 1959 : Geol. Surv. Canada. Inform. Circ. No. 3; Dept. of Mines and Tech. Surveys, Ottawa.
- Norris, D.K.; 1961. Field Work, 1960 : Geol. Surv. Canada. Inform. Circ. No. 4; Dept. of Mines and Techn. Surveys, Ottawa.
- Opdyke, N.D., and Runcorn, S.K.; 1960. Wind Direction in the Western United States in the Late Paleozoic : Bull. Geol. Surv. America; Vol. 71, pp. 959-72.
- Rice, H.M.A.; 1941. Nelson Map Area, East Half, British Columbia : Geol. Surv. Canada; Memoir 228.
- Rimbert, F.; 1956. Sur la Desaimantation par Action de Champs Magnetique Alternatifs, de la Magnetite et da Sesquioxyde de Ferr α : Acad. Sci. (Paris); Comptes Rendus; Vol. 242, pp. 890-93.

- Runcorn, S.K.; 1956 (a). Paleomagnetic Survey in Arizona and Utah, Preliminary Results : Bull. Geol. Soc. America; Vol. 67, pp. 301-16.
- Runcorn, S.K.; 1956 (b). Paleomagnetic Comparisons Between Europe and North America : Geol. Assoc. Canada Proc.; Vol. 8, pp. 77-85.
- Sachs, V.N.; and Strelkov, S.A.; 1960. Mesozoic and Cenozoic of the Soviet Arctic : Report for the First International Symposium on Arctic Geology, Calgary, Canada.
- Snider, A., 1858. La Creation et ses Mysteres dévoiles, Paris.
- Shotten, F.W.; 1937. The Lower Bunter Sandstones of North Worcester-shire and East Shropshire : Geol. Mag.; Vol. 74, p. 5.
- Strangway, D. W.; 1960. Magnetic Studies of Some Diabase Dykes : Unpublished Ph.D. thesis; University of Toronto.
- Taylor, F.B.; 1908. The Lateral Migration of Land Masses : Proc. Wash. Acad. Sci.; Vol. 13, pp. 445-97.
- Thellier, E., 1951. Proprietes Magnetiques des terres Cuites et de Roches : Jour. Phys. et Radium; Vol. 12, pp. 205-218.
- Thellier, E.; and Rimbart, F., 1954. Sur l'analyse D'Aimantations Fossiles par Action de Champs Magnetiques Alternatifs : Acad. Sci. (Paris); Comptes Rendus; Vol. 239, pp. 1399-1401.
- Vacquier, V.; Steenland, N.C.; Henderson, R.G.; and Zietz, I., 1951. Interpretation of Aeromagnetic Maps : Geol. Surv. America; Memoir No. 47.
- Weiss, K.; Ref. p. 1070, Physics (Starling and Woodall), Longams; London, 1950.
- Wegener, A.; 1915. Die Entschelung der Kontinente und Ozeane : Petermann. Mitt; pp. 235-36, 185-195, and 305-309. The origin of Continents and Oceans : Methuen; London, 1924. Translation by Skerl, J.G.A.
- Williams, R. L.; 1944. Geological Investigations Along the Alaska Highway from Fort Nelson, British Columbia, to Watson Lake, Yukon : Geol. Surv. Canada; paper 44-28, Ottawa.
- Wilson, R.L.; 1959. Remanent Magnetism of Late Secondary and Early Tertiary British Rocks : Phil Mag.; Vol. 14, pp. 750-55.
- Zietz, I.; 1960. Remanent Magnetization and Aeromagnetic Interpretation : Thirteenth Annual Internat. Meeting of Society Expl. Geophys.

APPENDIX

Details of all the measurements of the magnetic vector, and the processing of those measurements are too voluminous to be included in this thesis.

The original notes, readings and detailed calculations are kept on file in the Department of Geophysics at The University of Alberta.

B29795